FUNCTIONALITY OF A DAMAGED STEEL TRUSS BRIDGE STRENGTHENED WITH POST-TENSIONED CFRP TENDONS

A Thesis
Submitted to the Graduate Faculty
of the
North Dakota State University
of Agriculture and Applied Science

By

Garrett Floyd Brunell

In Partial Fulfillment
for the Degree of
MASTER OF SCIENCE

Major Department: Civil Engineering

March 2012

Fargo, North Dakota

North Dakota State University
Graduate School

Title

Functionality of a Damaged Steel Truss Bridge Strengthened with

Post-tensioned CFRP Tendons

By

Garrett Floyd Brunell

The Supervisory Committee certifies that this ***disquisition*** complies with North Dakota State University's regulations and meets the accepted standards for the degree of

MASTER OF SCIENCE

SUPERVISORY COMMITTEE:

Dr. Jimmy Kim
Chair

Dr. Frank Yazdani

Dr. Jerry Gao

Dr. Sivaplan Gajan

Approved:

4/5/2012 — Date

Dr. Eakalak Khan — Department Chair

ABSTRACT

This research program investigates the performance of a steel truss bridge when subjected to both localized web damage and a subsequent post-tensioned strengthening approach. The investigation utilizes a combined approach involving an experimental scale model bridge and a numerical computer model generated using the commercial finite element software RISA 3-D. The numerical model is validated using test data and further extended to parametric studies in order to investigate the theoretical load rating, strain energy, load redistribution, mode shapes and frequency of the bridge for control, damaged and strengthened states. The presence and severity of damage are found to significantly influence the global safety and reliability of the bridge. Also, higher order modes are more susceptible to changes in shape and frequency in the presence of damage. A recovery of truss deflection and a reduction of member forces are achieved by the proposed strengthening method.

ACKNOWLEDGEMENTS

I would like to acknowledge several people who assisted me in the process of designing experiments, performing experiments, determining appropriate numerical modeling procedures and writing the manuscripts which resulted from that work. A fellow graduate student, Amer Hmidan, provided insight into experimental testing procedures and the use of test monitoring equipment. His regular presence in the laboratory significantly influenced the quality of the test results. Also, Dr. Majura Selekwa of the Mechanical Engineering department at North Dakota State University was kind enough to provide monitoring equipment which aided in electronically gathering data during the experimental testing process of the research. My advisor, Dr. Jimmy Kim, was instrumental in providing guidance which directed the path of this work. His experience working on projects which investigate theoretical methods for strengthening bridges and methods used for evaluating the performance of constructed bridges aided in determining the most appropriate process for evaluating the effects of damage on steel truss bridges and the subsequent results from strengthening the bridge.

A special thanks to the Department of Civil Engineering at North Dakota State University for their financial support of the requirements for experimental tests and the software required for numerical modeling.

There were many others who provided thoughtful discussions pertaining to this work and other works which contributed to my understanding of the research process and writing scholarly articles. Thank you to all who I have worked with during my graduate career.

DEDICATION

My interest in pursuing a graduate degree was strengthened by the work that I performed while an undergraduate student participating in the McNair Scholars Program. It was the director of this program at North Dakota State University who really pushed me to find my passion and pursue further education in that field. Because of the McNair Scholars program and its director, Mrs. Kay Modin, I explored the option of enrolling in a master's program and attaining a Master of Science Degree in Civil Engineering. In addition to the support and influence that the McNair Scholars program provided I received significant support from my parents through my academic career. Their consistent encouragement to "find my passion" and "give my best at whatever I do" was a driving force in completing this thesis.

PREFACE

The purpose and function of bridges has always intrigued me, especially truss bridges. What I find most interesting about truss bridges in comparison to others types of bridges is their capacity to "bridge" relatively large spans with a minimal ratio of dead load to live load capacity. The relatively simple and efficient application of material that truss bridges exhibit provides interesting design challenges from initial conception of new bridge designs to rehabilitation schemes for existing bridges. In addition, the ability of steel truss bridges to support heavy loads with an appropriate arrangement of tension and compression members provides relatively challenging design considerations which when analyzed properly can provide the engineer with rewarding results. For this reason I have always been interested in designing and working with steel truss bridges. The opportunity for me to become involved in the AISC/ASCE Student Steel Bridge Competition as an undergraduate student at North Dakota State University (NDSU) initially spurred on my interest in this area of civil/structural engineering. After partaking in the competition one year I decided to try my hand at designing the bridge the next year. The first year that I was in charge of the steel bridge team at NDSU we produced a very competitive bridge and ended up taking 2nd place in the National Competition. The second year that I was in charge of the steel bridge team we ended up winning the National Student Steel Bridge Competition. After having experienced this level of involvement with scale model steel bridges I felt overwhelmingly interested in researching the effects that damage has on the performance of a steel truss bridge. Some preliminary reviews of literature suggested that little experimental work had been done pertaining to the effects of damage on steel truss bridges, and there was even less literature pertaining to applications for state of the art techniques for rehabilitating steel truss bridges. With the guidance of Dr. Jimmy Kim I was able to focus the path for this research

and formulate a better understanding for the effects that damage and subsequent strengthening have on the performance of steel truss bridges.

TABLE OF CONTENTS

LIST OF TABLES

LIST OF FIGURES

LIST OF ABBREVIATIONS

ASCE: American Society of Civil Engineers

AASHTO: American Association of State Highway and Transportation Officials

APC: Advanced Polymer Composite

CFRP: Carbon Fiber Reinforced Polymer

DI: Damage Index

FRP: Fiber Reinforced Polymer

GIS: Geographic Information System

LRFD: Load and Resistance Factor Design

NBI: National Bridge Inventory

NDSU: North Dakota State University

NTSB: National Transportation Safety Board

RF: Rating Factor

U.C.: Unity Capacity

US: United States

LIST OF SYMBOLS

A: member cross sectional area

A_1: dead load rating factor

A_2: live load rating factor

C: capacity

D: dead load

E: elastic modulus

f: frequency

I: impact factor

k: control truss stiffness

k'*:* damaged/strengthened truss stiffness

k_e: equivalent stiffness

kN: kilonewton

L: live load

m: meter

m: mass

mm: millimeter

P: member force

U_n: normalized strain energy

U_i: strain energy of the truss

Z: global safety index

Z_e: element safety in service

δ_{ult}: ultimate deflection

δ_{serv}: service deflection

σ_y: yield stress

ε_y: yield strain

$\sigma_{(\delta serv)}$: standard deviation of service deflection

$\sigma_{(\delta ult)}$: standard deviation of ultimate deflection

$\sigma_{(Pserv)}$: standard deviation of member service load force

$\sigma_{(Pult)}$: standard deviation of member ultimate load force

υ: poisons ratio

LIST OF APPENDIX FIGURES

CHAPTER 1. INTRODUCTION

1.1 GENERAL

The civil infrastructure which supports the daily activities sustaining our modern way of life has been quietly aging beneath our feet. In December 2008 the most recent bridge inventory estimated that of the 600,905 active bridges in America, 12.1% were considered structurally deficient and 14.8% were considered functionally obsolete. A structurally deficient bridge is considered to lack the structural integrity required to support the loads that are demanded by the traffic which uses the bridge, where as a functionally obsolete bridge lacks the geometry required by vehicle traffic and it does not accommodate the vehicle sizes and weight or traffic volume. Bridges are a critical component of the transportation network which is the backbone of America's economy. As of 2009, the ASCE estimated that the transportation network of surface roads experiences nearly 3 trillion vehicle miles each year of which nearly 223 billion miles are truck traffic. Since the early 1990's truck traffic has nearly doubled and the average truck weight has increased significantly (ASCE 2009). These increasing vehicle loads and volumes have played a significant role in the deterioration of bridges at a much more rapid rate than what they had been designed for. Considering that most bridges are designed with a 50 year lifespan in mind and the average age of bridges in America is currently 43 years old (ASCE 2009) it is clear why existing brides are not meeting the demand being placed on them.

In order to fix the issues with currently deficient bridges AASHTO estimated in 2009 that it would cost $140 billion of which approximately $48 billion would be spent on structurally deficient bridges and $91 billion would be spent on upgrading functionally obsolete bridges. However, this expense was estimated as a requirement to update currently deficient bridges, not to update the additional bridges that would require repairs in the upcoming years. In order to get

ahead of the issues associated with aging bridges the ASCE (2009) estimated that it would require a total of $650 billion over the next 50 years from both Federal and State associations combined which works out to an annual average investment of $13 billion.

When considering repairing or replacing a deficient bridge many factors influence the decision. Ultimately, the deciding factor is generally the annual cost to operate the bridge at the required capacity. For the case of a functionally obsolete bridge, making repairs to the existing structure often times will not provide the desired operating results. However, when a bridge is considered structurally deficient there are existing and state-of-the art techniques that are cost effective which can be employed to rehabilitate the structure so that is will operate at the required capacity.

This paper focuses on using a state-of-the art construction material, referred to as a fiber reinforced polymer (FRP), for a specific strengthening application. The name FRP refers to several variations of fiber types and polymer compounds which are used in combination to achieve a required strength characteristic. Typical fiber types include glass, aramid, and carbon fibers. These fibers are combined with either epoxy, polyester or vinylesters polymer compounds to create the fiber reinforced polymer. The combination of fibers and polymer compounds is achieved in one of two ways. Either the two are combined in a factory through a pultrusion process which impregnates the fibers with the polymer and presses the compound into a desired structural shape or the fibers are woven into uni-directional or bi-directional sheets and impregnated with the desired polymer during field application through a process referred to as a “wet layup”. The uses for FRP’s have experienced many applications because of their unique properties. In civil engineering applications to date they have been used in strengthening both concrete and steel structures. For concrete strengthening applications FRP materials are used to

provide the structural reinforcement that steel typically would provide. In concrete beams, FRP materials are used for flexural and shear strengthening. Either pultruded shapes or post-impregnated sheets are applied to the tensile side of the beam for flexural strengthening and both the tensile side and vertical sides of the beam for shear strengthening. Concrete columns have experienced the use of FRP sheets wrapped around the column in an effort to create a confining pressure and increase the load capacity. In an effort to increase the strength of degraded steel beams applications similar to those for concrete have been researched.

These previously mentioned strengthening methods focus on the stability of local members within the structural system as opposed to globally strengthening the structure. When considering a retrofit for a steel truss bridge local stability of truss elements is an important consideration, however a global strengthening system which provides redundancy to the entire structural system while increasing local member performance is a much more desirable objective.

1.2 OBJECTIVES

Previous research on steel truss systems has taken a mathematical approach to computing the effects that damage has on the performance of the system. Little to no previous research work has been found pertaining to experimental testing of steel trusses for the effect of simulated damage on their overall performance. A minimal amount of previous research has been found to have investigated the theoretical effects that various orientations of post-tensioning systems have on the overall load capacity of trusses and member stress distribution in the presence of local damage. In an effort to extend upon the previous work in this field, this research focuses on several ojectives;

1) To determine the effects that local damage has on the global performance of a truss system by characterizing the distribution of element forces.
2) To develop methods for detecting damage in truss bridges.
3) To experiment with a state of the art technique for rehabilitating a damaged steel truss bridge using post-tensioned carbon fiber reinforced polymer tendons.

The performance of the bridge is characterized by monitoring changes in member strain and truss deflection when damage is present at various locations within the truss system. The changes in performance are used to evaluate the reliability of the truss at varying levels of damage. Understanding the relationship between the location of damage and the severity of its impact on the capacity of the truss is of prime importance. Also, an evaluation is performed to examine the post-tensioning systems ability to modify the performance of the damaged truss so that acceptable levels of member force and truss deflection are achieved.

1.3 SCOPE

The work presented within this thesis considers a scale model steel truss bridge which is used to experimentally gather data and then verify the data against a computers numerical model prediction. Two types of bridge conditions were evaluated in this work. First, a damaged bridge was examined for the effects that local damage has on the overall performance of the truss system. Then, a strengthening system was employed using a post-tensioned carbon fiber polymer tendon which was monotonically harped beneath the truss between the ends of the bottom truss chord.

In order to compare the behavior of the bridge between undamaged and damaged conditions several damage scenarios were designed for the truss bridge and then experimentally tested and numerically verified using RISA 3D, a commercially available structural analysis

software. Each damage scenario included damage at a specific location within the truss system. For each location that damage was considered, 4 adjacent web elements were removed from the truss. In total 16 damage scenarios were generated. The variation in member strain and truss deflection was identified for each damage scenario and an evaluation of the structural effect was determined.

Prior to strengthening the damaged bridge, the post-tensioning system was load tested using a SATEC 22 EMF tensile test machine to determine the failure mechanism of the system. This test was performed to determine if the CFRP failure load could be achieved with the designed anchorage system. Once the anchorage system for the CFRP tendon was determined to be adequate to fail the tendon the post-tensioning system was fabricated and attached to the scale model bridge.

Testing the strengthened bridge utilized the same 16 damage scenarios as for the damaged bridge. However with the addition of the strengthening scheme a total of 48 strengthened scenarios were experimentally tested and modeled using RISA 3D. This increased number of testing scenarios was attributed to the fact that for each damage scenario, three levels of post-tensioning were applied to the bridge. The three post-tensioning levels included 2 kN, 4 kN and 6 kN of post-tensioning. Modeling the effect of post-tensioning was performed using theoretically equivalent nodal forces as experienced from the harped post-tensioned tendon. This method was selected as it reasonably equated the static conditions imposed on the bride by the strengthening system.

Each scenario, both damaged and strengthened was load tested 5 times to ensure accuracy of the experimental results. The stiffness of the bridge for each load test was examined and compared to the other 4 load tests for that particular scenario. Upon verification that the 5 load

tests produced reasonably similar results one test was selected to represent the results for that scenario.

Upon completion of the experimental and computer modeling the data was analyzed to determine the effects that local damage and subsequent strengthening have on the overall performance of the truss system.

1.4 OUTLINE OF THESIS

This thesis consists of five chapters and several supporting appendices which include; Chapter 1 –introduction and need for research, Chapter 2 - a review of literature relevant to the present research program, Chapter 3 - a paper considering the effects of local damage on the behavior of a steel truss bridge, Chapter 4 - a paper considering the functionality of a damaged steel truss bridge strengthened with post-tensioned CFRP tendons, and Chapter 5 - a summary of all technical findings and future research needs.

Chapter 2 focuses on literature pertaining to issues associated with steel trusses, truss classification, dynamic analysis processes, post-tensioning applications, applications for FRP's and design considerations for FRP applications. Chapter 3 details the experimental and numerical analysis that was conducted on a scaled steel truss bridge. It looks at the behavior of the truss system when undamaged compared to when damage is present. Then an evaluation of the level of damage and the effects on the performance of the truss is conducted. Chapter 4 presents a novel approach to strengthening a damaged steel truss bridge. The effects that post-tensioning have on the performance of the truss are evaluated and an analysis is performed to determine the efficiency of the proposed strengthening method. Chapter 5 provides a summary of the findings in chapters 3 and 4 and offers concluding remarks with regard to the effects of damage on truss systems and the ability of the proposed strengthening system to repair a

damaged steel truss system. Finally, the several appendices provide additional data with regard to experimental and numerical analysis that was not included in either Chapters 3 or 4. The supplemental data includes member strains, truss deflections and dynamic analysis mode shapes.

CHAPTER 2. LITERATURE REVIEW

2.1 ISSUES ASSOCIATED WITH BRIDGES

There are many potential issues that bridges are faced with when exposed to harsh environmental factors and demanding vehicle loads. Often times issues arise after years of continued wear and tear from environmental degradation such as freeze thaw cycles, application of de-icing agents, harsh saline atmospheric conditions, excessive vehicle loads and additional traffic volumes all of which deviate from what the initial designs considered. Other times issues arise suddenly and without warning when un-anticipated impacts occur or earthquakes happen. Yet still there are other areas for potential issues such as shortfalls in the initial design that did not meet the requirements of the anticipated loads, issues with construction not being performed properly so that the design requirements are met or materials do not meet design requirements. For these and additional reasons bridges can experience unexpectedly shortened life spans. Several examples of inadequate design issues follow.

2.1.1 Design Issues

After the collapse of the I-35W bridge in Minneapolis, MN on August 1, 2007, Hao (2010) performed an analysis on the original design. Using construction drawings a 3 dimensional finite-element model was developed to evaluate the magnitude of stress in all of the truss elements at the time of collapse. The analysis showed that the gusset plate thickness at several locations where floor members connected to the main truss were inadequately designed and that the anticipated service load level alone was enough to nearly initiate yielding of the gusset plates. He also explained that the NTSB had disclosed that the original method of a “one-dimensional model” used to analyze the truss didn’t consider the effect of the forces from the diagonal truss members which lead to the insufficient gusset plate design.

2.1.2 Environmental Issues

Of other concerns are deterioration issues that arise in cold weather regions. In 2010 Kim and Yoon discussed the performance of bridges that currently are in use throughout the state of North Dakota. In their study they employed the use of GIS, geographic information systems, along with multiple regressions to determine the main reasons that the 5,289 bridges in North Dakota were deteriorating. Their study utilized data from the NBI, National Bridge Inventory, database of bridges that were inspected from 2006 to 2007and it evaluated the physical, environmental and material factors which could be associated with the bridges. Their results highlighted that routine maintenance and rapid repairs to damage, along with the volume of traffic and year built significantly influenced the degree at which structural deterioration occurs. Of primary concern from their work was the note that truss bridges may have inherent down falls for applications in cold weather regions.

2.2 TRUSS CLASSIFICATION

An important metric in evaluating the capacity of truss bridges is the classification of the truss. The two main truss classifications which have been agreed upon include either light or heavy class trusses. The distinction between a light and heavy class truss is defined by the type of members that comprise the truss and the style of connection that is used to secure members to one another. Nagavi and Aktan (2003) identified light class trusses being comprised of pin-ended solid bar tension members and small rolled shapes for compression members. Where as in heavy class trusses the compression and tension members are both constructed using rolled shapes and all the connections are made using riveted gusset plates. Nagavi and Aktan used the heavy truss classification to identify the type of truss used for their analysis of nonlinear behavior. In this work they used a decommissioned heavy class steel truss bridge to load to failure. The bridge

was modeled using a nonlinear modeling procedure and then evaluated using a sensitivity analysis from which the best representation of the bridge was compared to the experimental results. Their results concluded that heavy class trusses have the ability to maintain redundancy even after the occurrence of initial yielding in multiple truss members.

Similarly, Frangopol and Curley (1987) identified types of bridges with respect to the level of redundancy of the truss, citing Csagoly and Jaeger (1979) who stated that bridges have various alternative load paths which are often difficult to identify. Here Frangopol and Curley made the connection that "weakest-link" structures have a single load path before failure where as "fail-safe" structures have the ability to redistribute loads to alternative load paths thereby effectively increasing the level of system redundancy. Their approach focused on using an analytical method to examine the effect that both damage and system redundancies have on the overall reliability of the trusses structural system.

2.3 APPLICATIONS FOR FRP

The use of fiber reinforced polymers (FRP's) has experienced significant growth since the early 1980's with new applications for FRP's researched annually. This fact results in more opportunities for the material to be commercially produced which decreases the material costs and increases the cost-effectiveness of using the material for large scale projects. Several reviews of the current applications for FRP's follow.

Bakis et al (2002) provided a summarized review of the uses for FRP's in construction applications. The current list of civil applications includes internal and external reinforcement, structural shapes, types of bridge decks, and proposed standards/codes. A review of these sections included consideration for the history, current state of the art, and challenges that were yet to overcome. They noted that even though this material has been in existence since the

1940's its use in civil structures was previously limited. This was due to the fact that the construction industry is fairly conservative with its application of emerging materials along with the previously higher price tag that was associated with its production. The acceptance of FRP materials for civil construction projects is increasing now that many new applications have emerged for FRP's along with a documented history of extensive material testing and a defined knowledge base of the materials properties.

Teng et al (2003) reviewed the current state of strengthening reinforced concrete structures using FRP materials. They examined the effects that flexural, and shear strengthening have on beams and slabs. For these cases the failure modes were examined and the strength of the system was considered. Similarly they investigated the effects of strengthening concrete columns based on the modes of failure, the axial stress-strain behavior and the seismic response of the structure. The primary focus of their work was based on developing rational models which national and international organizations could use to develop codes and guidelines for the application of FRP's in concrete construction projects. In addition to the research that Ten et al used to identify the current state of FRP applications, work by Kim and Heffernan (2008) investigated the fatigue characteristics of fiber reinforced polymer sheets externally bonded to concrete beams. Included in their research were the effects on fatigue life as related to the applied load range, bond behavior at the FRP and concrete interface, effects from damage accumulation, the propagation of cracks, effects from size, residual strength of the member and the failure modes of the beam. They also focused on summarizing the current literature such as codes and design guides available for this type of FRP application.

Hollaway and Cadei (2002) summarized the current state of rehabilitation techniques for metallic structures using advanced polymer composites (APC's). Of primary concern are the

issues surrounding bonding of the APC's to a metallic surface. The same principles apply when bonding plates to metallic structures as when bonding plates to concrete structures. However, the adhesives used for metallic structures create more difficult problems to overcome. The most common uses for bonding APC's include short-term retrofits and long-term rehabilitations of bridge beams and structural buildings. A few years later, in 2006, Zhao and Zhang reviewed the current state of the art for FRP strengthening of steel structures. They express that the option for retrofitting steel structures with fiber reinforced polymers has experienced significant growth and is becoming a fairly attractive method for rehabilitation of existing steel structures. The primary focus of their work was on the bond behavior of the FRP to steel, methods for strengthening hollow steel sections, and crack propagation within the FRP-steel based on fatigue loading. They also identified that future needs for research include the relationship between bond-slip, the stability of members strengthened using CFRP and modeling of fatigue cracks.

Kim and Harries (2012) investigated the application of CFRP strips for repairing notched steel beams. They analyzed the flexural behavior of the notched beams as well as the bond slip behavior at the interface of the CFRP-steel and the local plasticity around the area of the notch. Their conclusion was that application of the CFRP strip reduced stress and plasticity around the notch while the stiffness of the adhesive influenced local bond behavior but didn't affect the overall behavior of the member. In similar work by Kim and Harries (2010) they investigated the effect that CFRP composites have on flexural strengthening of timber beams. The research utilized experimental data to validate a 3 dimensional finite-element model. Using the validated model a parametric study was expanded to consider the orthotropic characteristics of the most common timber species used in engineering practice. From the results they determined that the strengthened beams could carry a greater load and had an increased capacity for energy

absorption over their unstrengthened counterparts. However, the failure of the beams was not governed by the CFRP material properties, but instead by the properties of the timber species.

Kim et al (2008) performed a full scale retrofit of a prestressed concrete bridge girder which was 56 meters long and comprised of 4 equal continuous 14 meter spans. The girder had been previously damaged by frequent impacts from heavy truck traffic, so for this case the selected retrofit of the girder utilized prestressed CFRP sheets. In order to analyze the effects that the various phases of structural integrity had on the flexural behavior of the girder a finite element model was created. The several phases that were considered consisted of the undamaged bridge, the damaged and the repaired bridge. An assessment utilized existing bridge codes from the American Association of State Highway and Transportation Officials LRFD code and the Canadian Highway Bridge Design Code. Based on these codes a good prediction of the live load effect on the exterior girder was made. However the effects on the interior girders were underestimated by the design codes resulting in the recommendation that refined analysis be required for retrofits of that type of bridge.

MacDougall et al (2010) applied the use of carbon fiber reinforced polymer (CFRP) tendons for a retrofit of post-tensioned unbonded tendons in a concrete parking structure. The existing steel tendons had corroded and lost the required strength for the structure to operate at the required capacity. By engineering the installation of the CFRP tendons to replace the existing tendons the capacity of the parking structure was recovered. Since the steel tendons were replaced with the state-of-the-art FRP material the retrofit was not susceptible to electrochemical corrosion, it experienced less relaxation than steel and provided similar strength to steel. To the best of the authors knowledge, this was the first retro-fit of its kind. Although this case resulted in anchorage losses up to 60% it was determined that by changing the anchorage design the

losses could be reduced to an acceptable 1-9%.

2.4 POST-TENSIONING

Methods used for increasing the strength of truss systems can pose inherently different challenges than those required for strengthening beams and columns. In addition to requirements for strengthening the components of truss systems there is often times a need to increase the level of system redundancy, especially in older structures which have degraded to a point where there serviceability level is less than that which is required. From this need, the application of a post-tensioning system has been brought to attention. Research work in this area has been limited thus far, experiencing mostly theoretical investigations for applications with documented experimental testing even more limited.

Ayyub et al (1990) focused on using an analytical approach to investigate the theoretical application of either an internal or external post-tensioning tendon. Their work examined the effects of various tendon drape configurations within a truss profile. The purpose was to find a cost-effective process for both strengthening individual truss members and increasing the redundancy, ergo reliability, of the structure to meet the requirements of increasing traffic loads and volumes. Considerations were made as to the effects that post-tensioning had on either a statically determinate truss versus a statically indeterminate truss. What they found was that use of an internal tendon on a determinate truss reduced stress in only the tension members when the tendon coincides with individual members and when the tendon does not coincide with members the method is not very effective. Whereas for an indeterminate truss use of the internal layout results in a reduction of stress for tension members only and with an external layout compression and tension members are strengthened. From their results they concluded that the post-tensioning method was effective for increasing the fatigue resistance, elastic range, redundancy

and reliability of the truss system. All the while it effectively decreased the member strains and overall truss deflection. This result was what they had hoped to achieve as it provided an extended service life for the bridge by way of a relatively cost-efficient retrofit.

Expanding on the work performed by Ayyub et al (1990), Han and Park (2005) performed a parametric study of various types of post-tensioned tendon orientations for strengthening a truss bridge. They focused on the use of either a straight or draped tendon profile and examined the effects that truss type, tendon profile, tendon eccentricity, and tendon force have on the capacity of the truss. They determined that the allowable load for a truss is directly related to the level of post-tensioning force and eccentricity of the tendon. Similar to Ayyub et al (1990), it was their conclusion that the elastic range and redundancy of the truss are increased while the truss deflection and member strains are decreased resulting in an increased load capacity for the bridge.

Further investigation as to design criteria for post-tensioning tendons concentric with members in steel truss bridges was performed by Albrecht and Lenwari (2008). Their discussion considered design criteria for tendon cross-sectional area and post-tensioning force required to prevent tendon yielding, member buckling, member fracture and member yielding. Their design considered two proposed strengthening methods. The first utilized the post-tensioned tendons to reduce member strains and control fatigue crack propagation. The second method provided the tendons as an available backup in the case of overloading the existing member.

CHAPTER 3. EFFECTS OF LOCAL DAMAGE ON THE BEHAVIOR OF A STEEL TRUSS BRIDGE

*Note: Contents of this chapter have been submitted to the Journal of Bridge Engineering, ASCE, for possible publication.

3.1 ABSTRACT

This chapter presents an investigation into the performance of a steel truss bridge subjected to local damage. An experimental program with sixteen damage scenarios is conducted to study the behavior of damaged truss systems. A three-dimensional numerical model is developed to predict test results. Static and dynamic responses of the damaged trusses are compared with those of the control. Foci of the study are damage quantification using a damage index, load rating, variation of strain energy, modal analysis, and structural safety based on a simple reliability theory. Service performance of the truss bridges is significantly influenced by local damage and their load-carrying capacity is exponentially reduced with an increasing damage index. A high mode shape such as the 4^{th} mode is of use to diagnose local damage in the truss systems. The global safety index derived using deflection characteristics is an indicator to indirectly detect the presence of local damage in the system. Stress redistribution among the constituent truss members is found to be insignificant, except for those adjacent to the damage. The need for developing a repair method that can address the global redundancy of a damaged truss bridge is highlighted.

3.2 INTRODUCTION

Deterioration of bridge infrastructure is a critical concern over the world. According to the American Society of Civil Engineers (ASCE 2010), the average age of bridges in the US is 43 years old as of 2010 and an overall grade of C was given to these bridges. Correspondingly,

over 25% of bridges in the nation are classified as structurally deficient or functionally obsolete. Bridges classified by one of these two categories do not operate at their required capacity and require restrictions which impede the public's use of the bridge. Government agencies spend significant expenditures for timely maintenance and rehabilitation to address these issues. In many cases, bridge insufficiencies can be attributed to aging, environmental damage, higher levels of demand and load being realized by bridges than what they were initially designed for, greater amounts of deicing agents in use, and shortfalls in the initial design. In addition to many bridges not meeting current standards, catastrophic bridge failure events such as the I-35 collapse in Minneapolis, MN, have generated an increased level of attention on the issues associated with existing bridges. Hao (2010) reported that the I-35W bridge had collapsed because of excessive stresses accumulated in local members: inadequate gusset plate design thickness and member side wall thickness which were insufficient to support service loads.

Efforts have been made to study the behavior of constructed truss bridges. Lenett et al. (2001) conducted an inspection project on a three-span truss bridge between Ironton, Ohio and Rusell, Kentucky. The states of existing and repaired truss members were visually examined. Strain responses of selected members were monitored when subjected to known truck loads. Inspection data provided crucial information to the rating and posting of the bridge. Azizinamini (2002) performed a full-scale load test using a decommissioned truss bridge. Load-carrying capacity of the bridge was experimentally determined and failure mode was observed. Local failure of a diagonal tension member initiated abrupt failure of the truss system. It was highlighted that attention should be paid to the local behavior of tension members in aged truss bridges. Alampalli and Kunin (2003) examined the interaction between the deck and truss system of a rehabilitated 50-year old bridge. A couple of load combinations with heavy trucks were used

to measure the response of the bridge. Test results indicated that the response of the bridge deck was affected by the local behavior of truss members. Hickey et al. (2009) tested a 260 m truss bridge situated between Pulaski and Hillsville, Virginia using two 25 ton trucks. Deflections and strains were measured. A numerical model was developed to predict test data. Findings included that the bridge's response was characterized by floor beams and stringers, and that local failure of truss members was a critical consideration.

More specific to truss bridges from a structural redundancy perspective, Frangopol and Curley (1987) identified that truss bridges were often classified as either multiple load path (*fail-safe* structures) or single load path (*weakest-link* structures). The type of classification depends on the structure's ability to find suitable alternative load paths when damage is present. Structures that are classified as *weakest-link* lack system redundancy and therefore when subject to damage become increasingly more susceptible to failure. Ghosn and Moses (1998) proposed methodologies to examine the level of redundancy in existing truss bridges. Several limit states were defined based on ultimate, service, and damage configurations. System factors were suggested to evaluate structural redundancy and preliminary design provisions were discussed. Nagavi and Aktan (2003) categorized trusses as either a *light* or *heavy* classification. A truss system categorized into the *light* class was composed of pin-ended, solid bar, tension members, and small rolled shapes for compression members, while a system classified as the *heavy* class was assembled from members of only hot rolled shapes and connected by riveted gusset plates. Differences in performance between these two classes were predominantly due to the pin-ended connection in the *light* class truss where a lack of redundancy created a greater failure potential. Kim and Yoon (2010) stated that a lack of redundancy in steel truss bridges could cause susceptibility to premature failure. This is because truss bridges are generally considered to be a

non-redundant system as the failure of a single component often leads to the successive failure of multiple components and ultimately the failure of the entire system.

As discussed above, the global response of a truss bridge is significantly influenced by the local behavior of constituent members. Most of existing research is concerned with non-destructive load tests on truss bridges and corresponding responses. Limited information is available regarding the effect of local damage on the behavior of a truss system. This paper presents an experimental study to examine the response of a scaled truss bridge having various damage scenarios. A three-dimensional numerical model was developed and validated with test data. The model was further used to expand laboratory findings. A simple reliability analysis was carried out to evaluate the performance of damaged truss bridges.

3.3 RESEARCH SIGNIFICANCE

Truss bridges intrinsically lack structural redundancy when compared to slab-on-girder bridges. Reliability of such a system is significantly influenced by local damage due to the alteration of load path. A catastrophic event may take place if increased distress exceeds the capacity of a damaged system. The effect of local damage on the behavior of a truss bridge needs further research. Current design and practice of truss bridges do not explicitly take into consideration the interaction between constitutive members and global response. These facts create the need to study the effects that damage has on steel truss bridges. Although a few numerical investigations have been conducted to examine the behavior of damaged truss bridges (Ghosn and Moses 1998; Hao 2010), experimental efforts have been limitedly reported. Of primary concern of this laboratory investigation combined with a modeling approach is the change in response of steel truss bridges from intact to damaged conditions, including static and dynamic behavior.

3.4 EXPERIMENTAL PROGRAM

3.4.1 Material and Truss System

A scaled truss bridge (L = 6.2 m) was fabricated using several different sizes of steel tubes (Grade A36), as shown in Fig. 3.1. The material and bridge dimensions are displayed in Fig. 3.1(a). The truss system consisted of two main trusses (Trusses 1 and 2), lateral stiffening frames welded along the top chord of each truss to provide a stable test environment, cross braces, and leg members [Fig. 3.1(b)]. The number of cross braces was minimized during design by addition of the lateral frame that would prevent buckling of the top chord on each truss. Steel

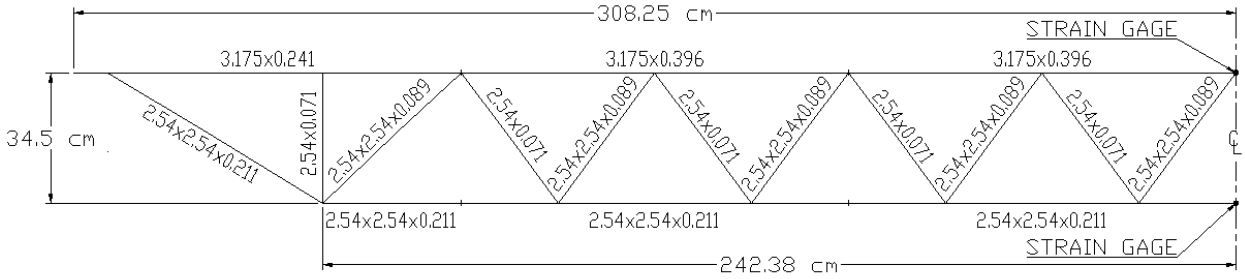

(a)

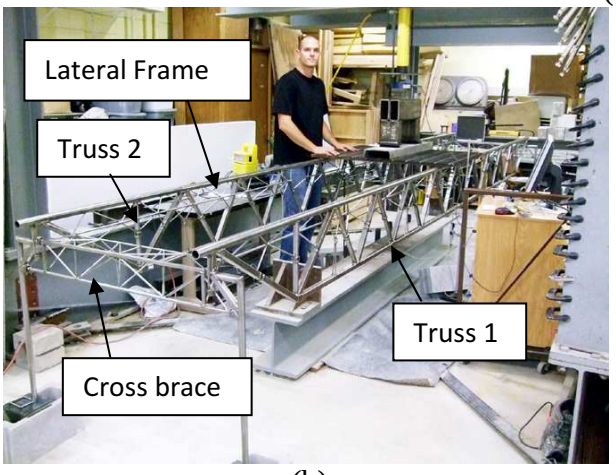

(b)

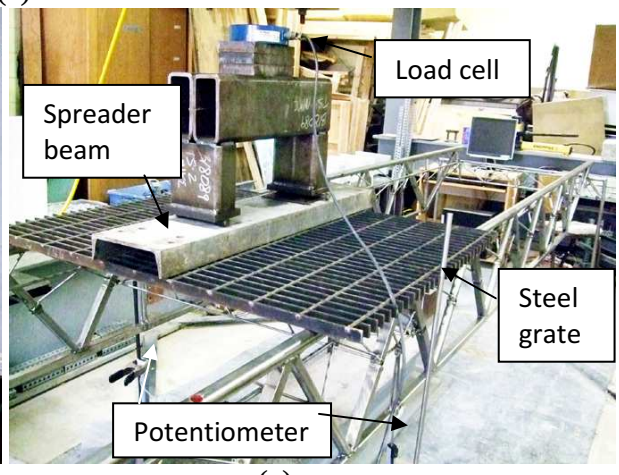

(c)

Fig. 3.1 Truss details: (a) truss members; (b) fabricated truss system; (c) loading and instrumentation

components included the following nominal properties: yield stress (σ_y) = 290 MPa, elastic modulus (E) = 200 GPa, and Poissons ratio (υ) = 0.3.

3.4.2 Damage Simulation

Damage simulations were generated by removing web elements from the truss. Figure 3.2(a) provides a schematic view of damage configurations. To represent significant damage in constructed truss bridges, a set of four adjacent elements was removed per damage scenario, as typically shown in Fig. 3.2(b). A total of 16 damage combinations were designed, depending upon the location of damaged elements (Table 3.1). Identification code of each damage scenario indicated the location of damage in Trusses 1 and 2, and the position of the damage within the truss [positions 1, 2, 3, and 4, as shown in Fig. 3.2(a)]. For example, Specimen 1_1 denotes that the location of damage was in Truss 1 with position 1, while Specimen 1_2 & 2_3 calls out Truss 1 with damage position 2 and Truss 2 with damage position 3.

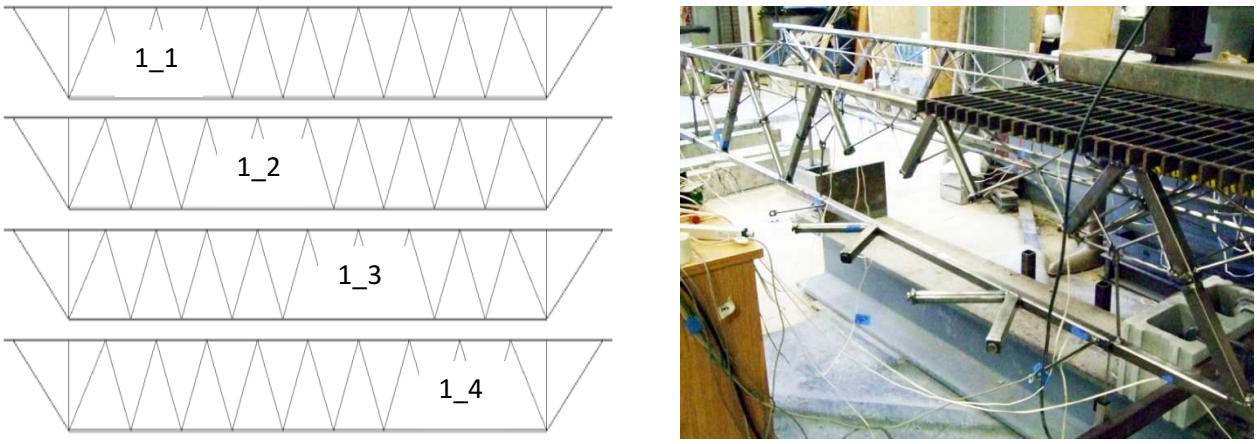

(a) (b)

Fig. 3.2 Damage scenario: (a) identification of damage position; (b) simulated damage (Specimen 2 with damage position 1_2)

3.4.3 Loading and Instrumentation

The truss system was monotonically loaded at a typical service load of 4.5 kN (i.e., 25% of the predicted capacity of the control truss). Each test category was loaded five times to ensure the reproducibility of experimental results. A 25 mm thick by 919 mm square steel grate was used near midspan of the truss, as shown in Fig. 3.1(c). To achieve a uniform distribution of load

from the hydraulic actuator along the length of the grate, a steel channel was centered at the middle of the grate and spanned the length of the grate. Deflection of the test truss was recorded by linear potentiometers located at midspan of the truss. Strain gages were bonded to selected members [Fig. 3.1(a)]. Structural responses of the control truss and each damage scenario were recorded using a data acquisition system.

3.5 NUMERICAL MODELING

Modeling the truss bridge was performed using RISA 3-D structural analysis software. A complete three-dimensional model of the bridge was used for analysis, including two single span trusses, three cross braces, and four piers, as shown in Fig. 3.3. The respective element cross section geometries were input into the software's material database where the cross sectional

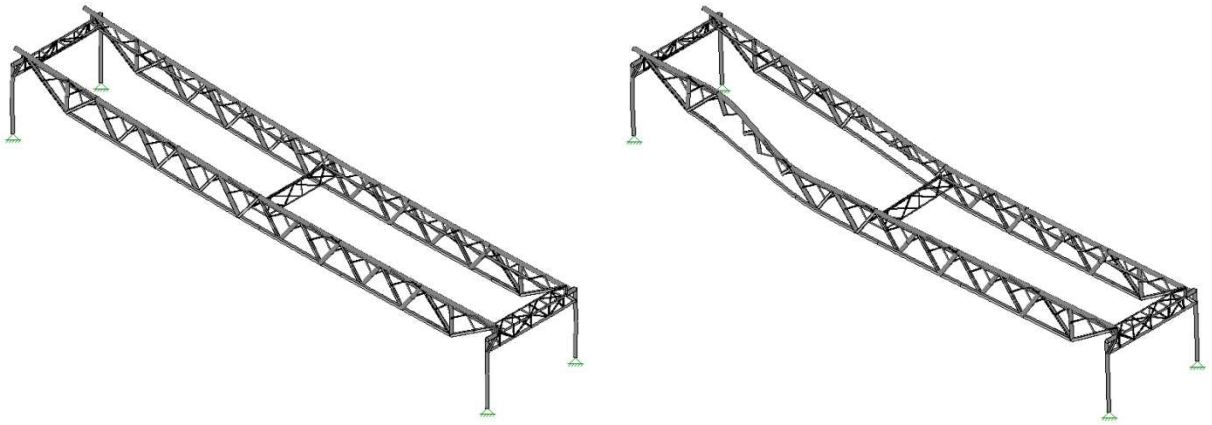

(a) (b)

Fig. 3.3 Numerical model showing deflection at 20 times magnification for the service load of 4.5 kN: (a) control truss; (b) damaged truss (Specimen 7)

properties were calculated. Boundary conditions were established at the base of each pier. The degrees of freedom that were restrained at each pier included translation in the longitudinal, lateral, and vertical directions. Upon generation of members in RISA 3-D, finite elements were automatically sub-meshed. In total, 404 line elements and 250 nodes were used to generate the control truss. Fixed connectivity was achieved at all the element connections in the truss model.

Material properties were input based on the values mentioned in the “Experimental Program” section.

3.6 TEST RESULTS AND MODEL PREDICTION

3.6.1 Static Behavior

3.6.1.1 Damage index

To quantify the behavior of the damaged truss systems, a damage index (DI) was used:

$$DI = 1 - \frac{k'}{k} \tag{3.1}$$

where k and k’ are the stiffness of the control and damaged trusses, respectively. The stiffness of each truss was obtained from the ratio of applied load to corresponding deflection at midspan. It should be noted that use of a damage index is more relevant than a comparison employing a load versus deflection response because the applied load to the truss specimens was in an elastic range. Table 3.1 presents the measured and predicted damage indices. Reasonable agreement was made between these damage indices with average margins of 16.1% and 28.1% for Trusses 1 and 2, respectively. Substantially high margins were noticed for Truss 2 when the primary damage was present in Truss 1 (Specimens 1 to 5 as shown in Table 3.1). Such an observation illustrates that the load distribution between experimental Trusses 1 and 2 was not even when one of these trusses was damaged, which was different from the ideal load distribution in numerical counterparts. This is confirmed by the reduced margins of Specimens 12 through 16 (3.9% on average) where damage occurred in both trusses.

Figure 3.4(a) shows the relationship between the damage index and the normalized deflection at midspan (i.e., deflection of a damaged truss divided by that of the control at a load of 25% of the control capacity). A gradual increase in the normalized deflection was observed when the damage index increased. Predicted results exhibited good agreement with the test data,

including an average error of 19% for Truss 1 and 5% for Truss 2. These results indicate that local damage in a truss system considerably influenced the serviceability of the system, particularly critical when a damage index was greater than 0.5. Similarly, the relationship between the damage index and predicted failure load was developed in Fig. 3.4(b). The load at failure was defined by the load causing the first truss member to reach its yield capacity (Hickey

Table 3.1 Details of test specimens and corresponding damage indices

Specimen ID	Damage Scenario	Damage index					
		Truss 1			Truss 2		
		Exp[1] (a)	Model (b)	Margin[2] (%)	Exp[1] (a)	Model (b)	Margin[2] (%)
Control	None	N/A	N/A	N/A	N/A	N/A	N/A
1	1_1	0.52	0.62	19.2	0.09	0.01	88.9
2	1_2	0.39	0.49	25.6	0.12	0.01	91.7
3	1_3	0.41	0.49	19.5	0.04	0.01	75.0
4	1_1 & 1_3	0.60	0.72	20.0	0.01	0.02	100.0
5	1_1 & 1_4	0.65	0.76	16.9	0.05	0.03	40.0
6	1_1 & 2_1	0.58	0.63	8.6	0.60	0.63	5.0
7	1_1 & 2_2	0.51	0.63	23.5	0.50	0.49	2.0
8	1_1 & 2_3	0.52	0.62	19.2	0.53	0.49	7.5
9	1_1 & 2_4	0.56	0.63	12.5	0.65	0.63	3.1
10	1_2 & 2_2	0.38	0.49	28.9	0.41	0.49	19.5
11	1_2 & 2_3	0.37	0.49	32.4	0.45	0.49	8.9
12	1_1, 2_1 & 2_3	0.59	0.63	6.8	0.73	0.72	1.4
13	1_1, 2_1 & 2_4	0.62	0.63	1.6	0.76	0.77	1.3
14	1_2, 2_1 & 2_3	0.45	0.49	8.9	0.69	0.72	4.3
15	1_2, 2_1 & 2_4	0.57	0.49	14.0	0.77	0.77	0.0
16	1_3, 2_1 & 2_3	0.49	0.49	0.0	0.71	0.72	1.4

[1]: Average value of measured test data
[2]: margin (%) = absolute value of (a-b)/a $\times$100

et al. 2009). Figure 3.4(b) shows that the predicted ultimate load exponentially decreased with an increasing damage index. For example, the control truss experienced a failure load of 18.7 kN, while at a damage index of 0.76 a failure load of 6.3 kN (i.e., 33.7% of the control capacity) was observed. These results imply that the degree of damage severity abruptly influences the response of a truss system. Such a trend explains why truss systems collapse in a sudden manner

without a warning of impending failure.

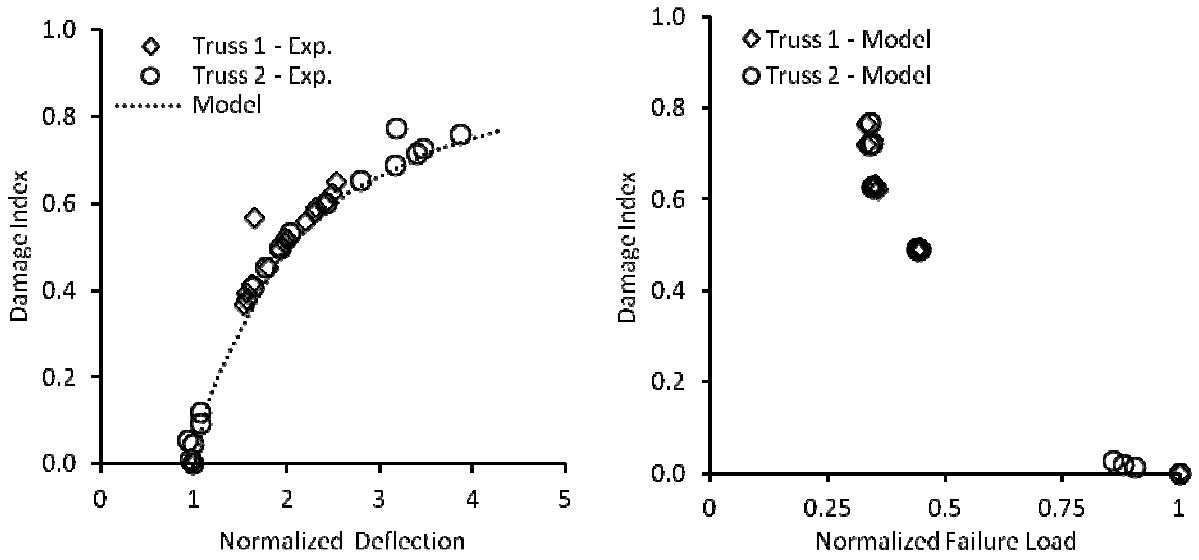

(a) (b)

Fig. 3.4 Effect of damage level on performance of truss: (a) normalized deflection; (b) normalized failure load

3.6.1.2 Strain response

Figure 3.5 compares the measured and predicted member strains at midspan (presented here for brevity are the top and bottom chords for the control and damaged trusses 1 and 7). Strain response of all experimental specimens was basically linear and the recorded strain values were considerably lower than the yield strain of A36 steel ($\varepsilon_y = 0.0015$). These observations ensured that multiple damage scenarios using a single truss system (Table 3.1) were adequately conducted without the presence of plastic damage in the system. The experimental strains tended to be stiffer than those predicted. This can be explained by the initial incomplete engagement of all connections; in other words, load transfer from the actuator to the members was delayed because the piecewise members needed to be engaged together when loaded.

3.6.1.3 Rating of a damaged truss system

Load rating of the damaged truss systems was conducted using the method shown in the

Manual for Condition Evaluation of Bridges (AASHTO 2003):

$$RF = \frac{C - A_1 D}{A_2 L(1+I)} \tag{3.2}$$

where RF is the rating factor consisting of Operating and Inventory ratings; C is the predicted capacity of the truss system; D and L are the dead and live load effects, respectively; A_1 and A_2 are the factors for the dead and live loads, respectively; and I is the impact factor. For Operating rating, A_1 and A_2 are 1.3 and 1.3, respectively, while for Inventory rating these are 1.3 and 2.17, respectively. The impact factor for the present truss systems was set to 0.1 by assuming smooth approach and deck conditions (AASHTO 1989). It should be noted that use of the impact factor can generate a more realistic rating for constructed truss bridges even though such an impact factor has not been presented in the test trusses. The truss capacity for each scenario was taken as the load that initiated first yielding of a member; the dead load was taken as the self weight of the bridge, 0.77 kN; and the live load was the service load of 4.5 kN. Figure 3.6 compares the rating factors of each damaged truss using the Operating and Inventory ratings [Fig. 3.6(a) and (b), respectively]. Relatively constant rating factors were observed for Truss 1 because it was primarily damaged in all damage scenarios, as shown in Table 3.1 and Fig. 3.2(a). The rating of Truss 2 was, however, fluctuating due to their inconsistent damage location. The rating factors of Truss 2 in Specimens 1 to 5 were 63% and 63% higher than those of Truss 1, on average, for the Operating and Inventory, respectively. These results illustrate that load transfer between these two trusses was not significant when only one truss was damaged because a concrete deck slab connecting these two members was not included in this study. Figure 3.7(a) shows the relationship between the rating factors and the ratio of service deflection to ultimate (failure) deflection. The predicted relationship exhibits that as the rating factor decreases the service

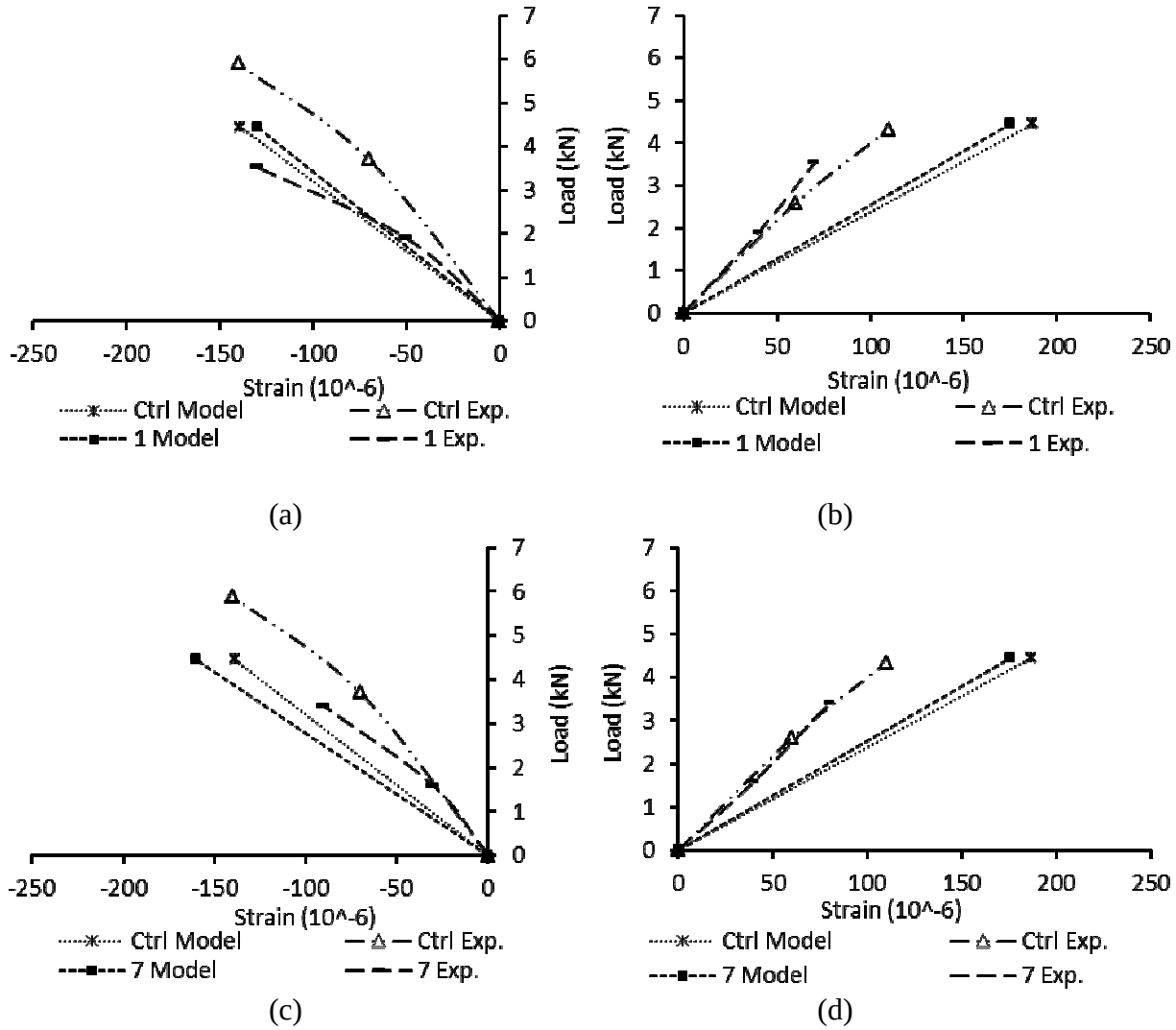

Fig. 3.5 Strain response: (a) Specimen 1- Truss 1 top chord; (b) Specimen 1- Truss 1 bottom chord; (c) Specimen 7- Truss 1 top chord; (d) Specimen 7- Truss 1 bottom chord

normalized deflection for Operating and Inventory was similar to each other. For instance, the changes in the Operating and Inventory ratings for Truss 1 were 57.1% and 58.8%, respectively, when the normalized deflection increased from 0.26 to 0.55, as shown in Fig. 3.7(a). Figure 3.7(b) compares the damage index with the failure load of the damaged trusses normalized to that of the control. The damage index of the truss systems was found to be less than 0.4 to maintain an Inventory rating factor (representing vehicle loads being safely operated for an indefinite period of time) equal to or greater than 1.5 that were associated with a normalized

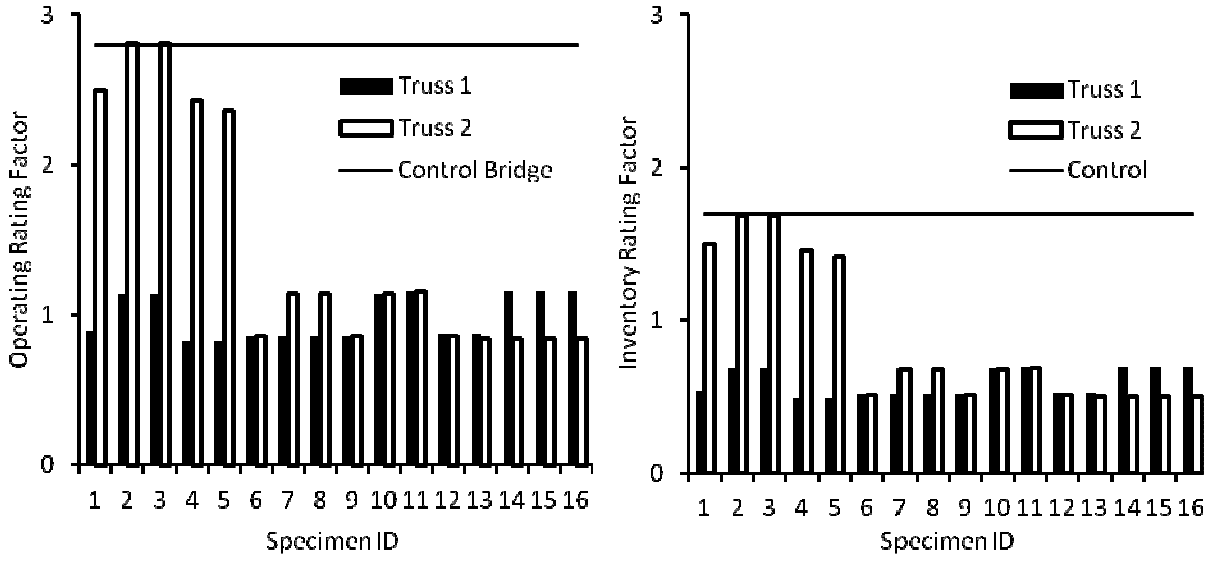

(a) (b)

Fig. 3.6 Load rating of damaged truss systems for Trusses 1 and 2: (a) Operating rating; (b) Inventory rating

failure load of 0.9.

3.6.1.4 Strain energy

To analyze force redistribution resulting from local truss damage, the element strain energy of a damaged truss was normalized against the strain energy of the control by the following.

$$U_n = \frac{U_{i-damaged}}{U_{i-control}} \text{ in which } U_i = \frac{P^2 L}{2AE} \tag{3.3}$$

where U_n is the normalized element strain energy; U_i is the strain energy of the truss; A and L are the cross-sectional area and length of the members, respectively; P is the member force; and E is the elastic modulus of the member. Figure 3.8 depicts that member proximity to damage is a key factor on the performance of truss components. For example, the strain energy of Member M1_6 increased roughly 3.5 times more than that of other members (i.e., M1BCA_1 and M1_17) because M1_6 was directly adjacent to damage for the majority of the damage scenarios (except

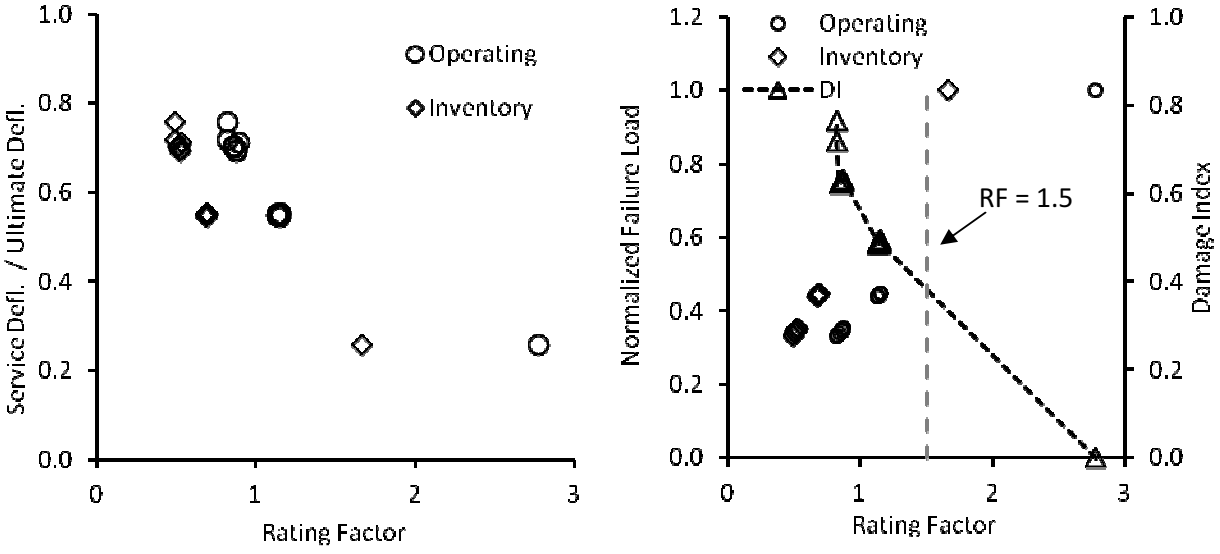

(a) (b)

Fig. 3.7 Load rating versus predicted performance of damaged truss systems (Truss 1): (a) deflection; (b) failure load

when M1_6 was removed or when scenario 1_3 or 1_4 was tested). Such an observation indicates that the stress of a damaged truss member may not be effectively redistributed to other members except for those located near the damage. A catastrophic failure event of a truss system can thus initiate at the critical region. This conclusion highlights the need for improving the redundancy of a damaged truss system, rather than localized element-level repair, so that the overall performance of the truss can be enhanced.

3.7 DYNAMIC BEHAVIOR

Dynamic analysis of a predictive model may be reasonably performed once the modeling has been validated with static conditions (Zein and Gassman 2010). The following discusses the predicted dynamic behavior of the truss systems subjected to the same live load criteria used for the static investigations.

3.7.1 Mode Shape

Mode shapes of the control and damaged trusses were generated and the equivalent mode

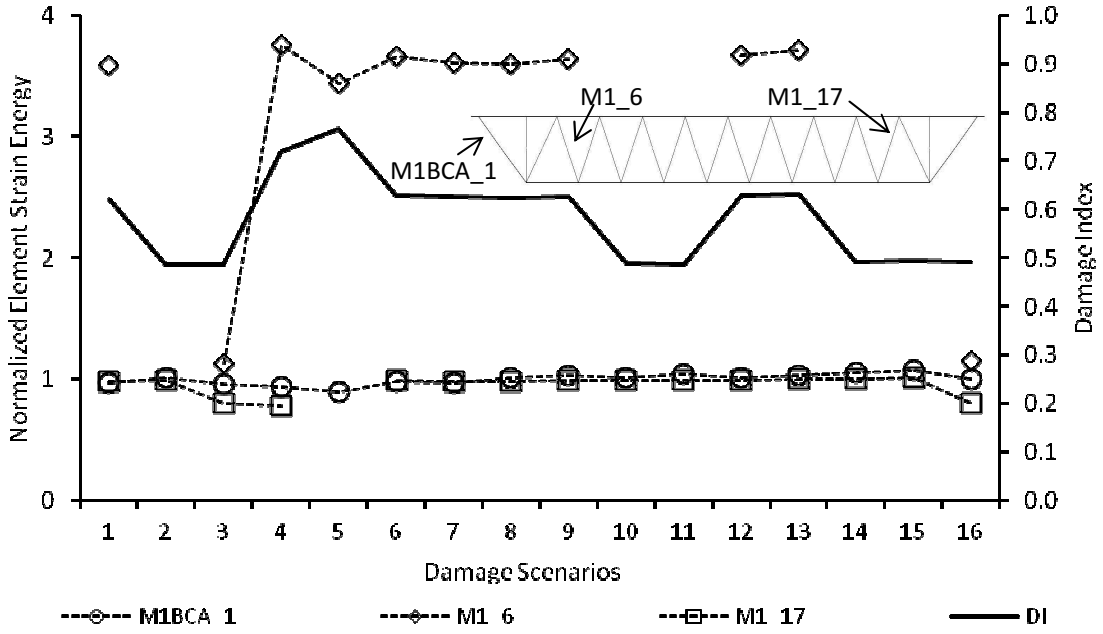

Fig. 3.8 Comparison of the normalized strain energy for three tension members

shapes were compared to one another. Figures 3.9 and 3.10 show the first four modes for the control truss and Specimen 9 that represents a typical damaged truss system studied here. The shape of modes 1 and 2 was observed to be independent of the level of damage; however, variance between the control and damaged trusses was present at higher modes. For the control truss, modes 1 and 2 displayed lateral sway [Fig. 3.9(a)] and longitudinal shift [Fig. 3.9(b)], respectively, while modes 3 and 4 demonstrated twist about the center of the truss [Fig. 3.9(c)] and camber [Fig. 3.9(d)], respectively. Mode shapes 1 and 2 of the damaged truss (Specimen 9) were the same as those of the control [Fig. 3.10 (a) and (b)], whereas modes 3 and 4 lacked the symmetry and direction of deformation that the control mode shape exhibited, as respectively shown in Fig. 3.10(c) and (d). Such distinct changes in mode shapes of the damaged truss are attributed to the reduced stiffness in the direction of displacement. The sensitivity of higher modes was confirmed by the changes in frequency discussed in the following section.

3.7.2 Frequency

Damage detection by changes to resonant frequencies may be useful because they are reliable and quickly obtainable. This method of damage detection is based on the principle that structural frequency (f) is directly related to the equivalent stiffness of the structural system (k_e)

Table 3.2 Truss specimen modal frequencies

Specimen ID	Mode and frequency							
	1		2		3		4	
	Hz	Δ^a	Hz	Δ^a	Hz	Δ^a	Hz	Δ^a
Control	0.94	-	1.41	-	5.28	-	8.17	-
1	0.94	0.4%	1.41	0.1%	5.29	-0.1%	5.09	37.7%
2	0.94	0.4%	1.41	0.1%	5.21	1.3%	5.81	28.9%
3	0.94	0.4%	1.41	0.1%	5.21	1.3%	5.81	28.9%
4[b]	0.94	0.7%	1.41	0.1%	5.22	1.2%	4.38	46.4%
5[b]	0.94	0.7%	1.41	0.1%	5.29	-0.1%	4.06	50.3%
6[b]	0.94	0.7%	1.41	0.1%	5.18	2.0%	4.99	38.9%
7[b]	0.94	0.7%	1.41	0.1%	5.22	1.2%	5.08	37.8%
8[b]	0.94	0.7%	1.41	0.1%	5.22	1.1%	5.07	37.9%
9[b]	0.94	0.7%	1.41	0.1%	5.29	-0.2%	4.99	38.9%
10	0.94	0.7%	1.41	0.1%	5.13	3.0%	5.74	29.7%
11	0.94	0.7%	1.41	0.1%	5.13	2.9%	5.72	30.0%
12[c]	0.93	1.1%	1.41	0.1%	5.23	0.9%	4.36	46.6%
13[c]	0.93	1.1%	1.41	0.1%	5.29	-0.2%	4.05	50.4%
14[b]	0.93	1.1%	1.41	0.1%	5.13	2.9%	4.37	46.5%
15[b]	0.93	1.1%	1.41	0.1%	5.22	1.2%	4.05	50.4%
16[b]	0.93	1.1%	1.41	0.1%	5.13	2.8%	4.37	46.5%

*Note: frequencies shown in table for damage scenarios are frequencies of modes corresponding to the first four modes of the control bridge. The changes in mode are noted by; b or c.
a: difference between control and damaged truss
b: mode 3 switches with mode 4
c: mode 3 is mode 4 and mode 5 is mode 3

and inversely related to the mass (m):

$$f = 2\pi\sqrt{\frac{k_e}{m}} \tag{3.4}$$

A decrease in resonant frequency signifies a loss of stiffness and therefore damage to the system. However, changes in frequency greater than 5% are the only way to be sure that damage is present as long as these measurements are not subject to changes in ambient conditions (Salawu 1997). Table 3.2 summarizes the frequencies of the damage scenario modes corresponding to the first four modes of the control bridge. It is important to note that mode shapes that demonstrate similar deformation should be compared so that an accurate measure for the change in modal frequency is achieved. From a comparison of the control truss to the damaged counterparts, modes 1, 2, and 3 showed negligible change in frequency (less than 3.0%) with changes to the amount of damage present. Mode 4, on the other hand, demonstrated much greater changes to frequency from the control to damaged cases. Mode 4 readily detected changes in frequency from 28.9% (Specimens 2 and 3) to 50.4% (Specimens 13 and 15), indicating that this is a recommended mode to diagnose the presence of damage in the truss systems studied here. Figure 3.11 shows the change in natural frequency of the system for modes 1 through 4 with respect to the worst-case damage index of Trusses 1 and 2. As discussed above, modes 1 through 3 had little to no effect on the natural frequency; however, the frequency of mode 4 remarkably decreased with an increasing damage index. This implies that the use of natural frequency associated with a higher order mode shape (i.e., 4^{th} mode in this study) is a quantifiable indicator of damage; thereby a meaningful tool for damage inspection of constructed truss bridges.

3.8 RELIABILITY ANALYSIS

3.8.1 Safety Index

A deflection-based safety index was used to quantify the performance of the damaged truss systems:

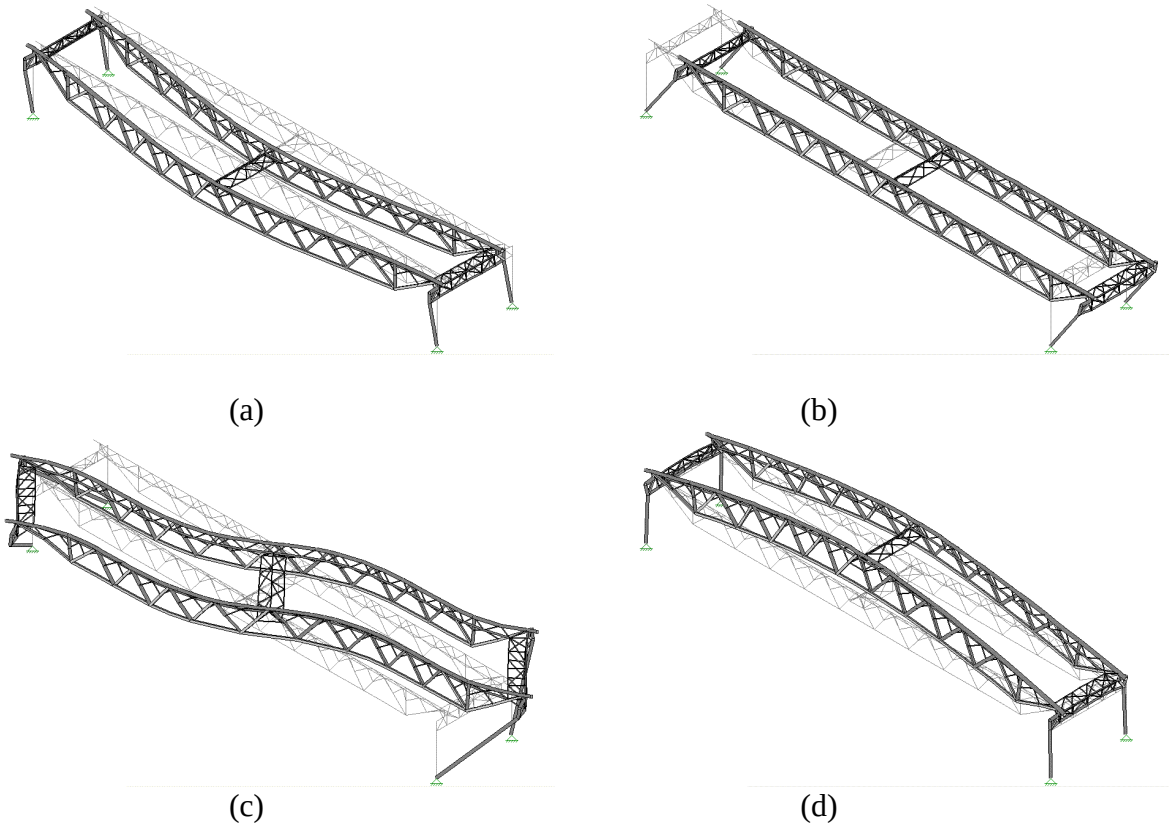

Fig. 3.9 Mode shape of control truss during service load level of 4.5 kN: (a) mode 1 (b) mode 2 (c) mode 3 (d) mode 4

$$Z = \frac{\delta_{ult} - \delta_{serv}}{\sqrt{[\sigma(\delta_{ult})]^2 + [\sigma(\delta_{serv})]^2}} \tag{3.5}$$

where Z is the global safety index; and δ_{ult} and δ_{serv} are the ultimate and service deflections, respectively; and $\sigma(\delta_{ult})$ and $\sigma(\delta_{serv})$ are their standard deviations. As discussed previously, the ultimate and service deflections were respectively obtained when the first truss member reached its yield capacity and when a service load of 4.5 kN was applied (25% of the control bridge's ultimate capacity). The proposed safety index is fundamentally aligned with the classical concept of a reliability index based on the ultimate and service loads (Frangopol and Curley 1987). The coefficient of variation was taken from previous research (Nowak 1993,1995): 0.12 and 0.18 for the ultimate state that is related to strength and the service state that is associated with a live load

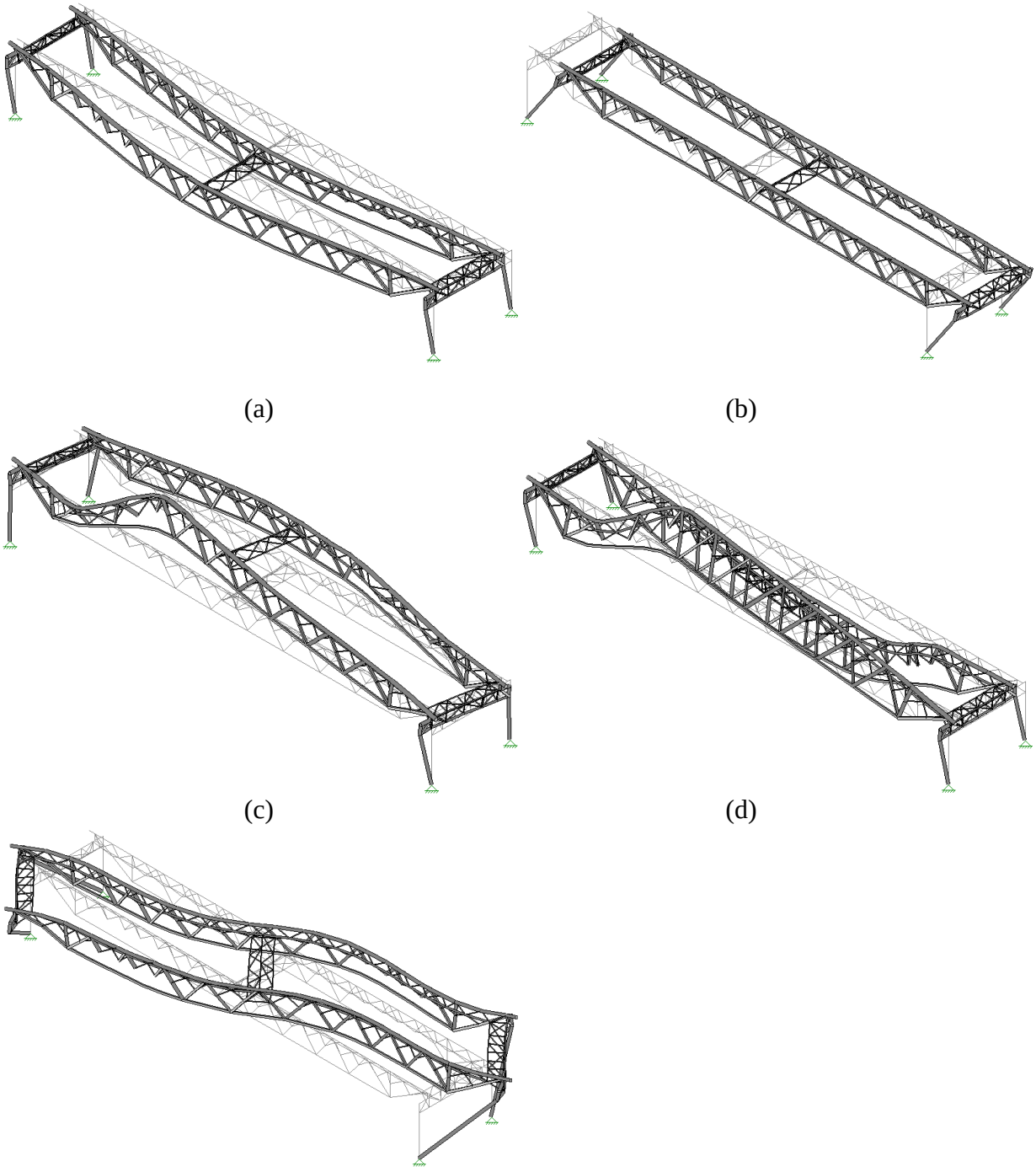

(a) (b)

(c) (d)

(e)

Fig. 3.10 Mode shapes of Specimen 9 during service load level of 4.5 kN: (a) mode 1 (b) mode 2 (c) mode 3 (d) mode 4 (e) mode 5

effect, respectively. It should be noted that the measured coefficients of variation in the laboratory were much less than those used here because the measured values were obtained in a

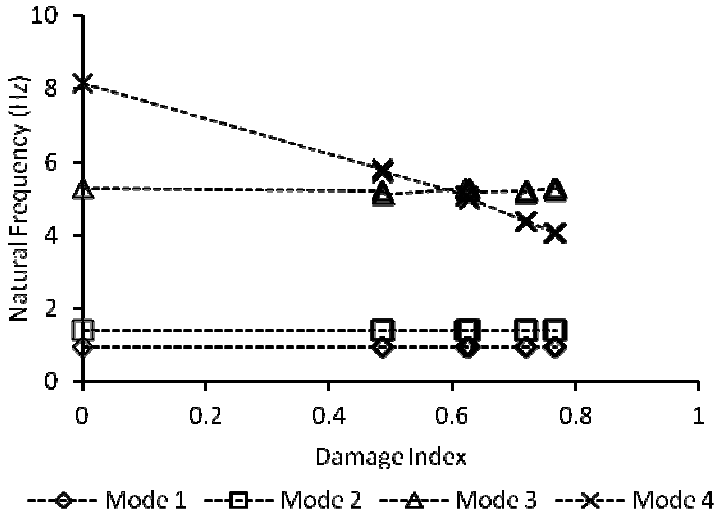

Fig. 3.11 Natural frequency response with the worst case damage index

controlled environment that might not represent in-situ conditions. Relationships between the global safety index and the deflection characteristics of the damaged truss systems are shown in Fig. 3.12, including the normalized deflection of a damaged system to that of the control [Fig. 3.12(a)] and the service deflection normalized to the *L*/800 limit of AASHTO [Fig. 3.12(b)]. The service deflection of the damaged trusses significantly increased when the safety index decreased, whereas their ultimate deflection was relatively constant, as shown in Fig. 3.12(a). There was no difference between the service and ultimate deflections of the damaged trusses having a safety index of greater than 4 when compared to those of the control. A global safety index of 2.5 was found to be the lowest bound to satisfy the AASHTO deflection limit, as shown in Fig. 3.12(b). It is, thus, recommended that the reliability calibration of constructed truss bridges in service be conducted with a safety index of 2.5.

Using the same approach as for the global safety index, both the average and minimum safety indices were determined based on the capacity of individual truss elements governing the failure of the entire system. For this method, the unity capacity (U.C.) of the truss members was

employed: the ultimate capacity of a critical member was represented by unity and thus any value less than one meant that the member had not failed yet, as shown in Eq. 3.6:

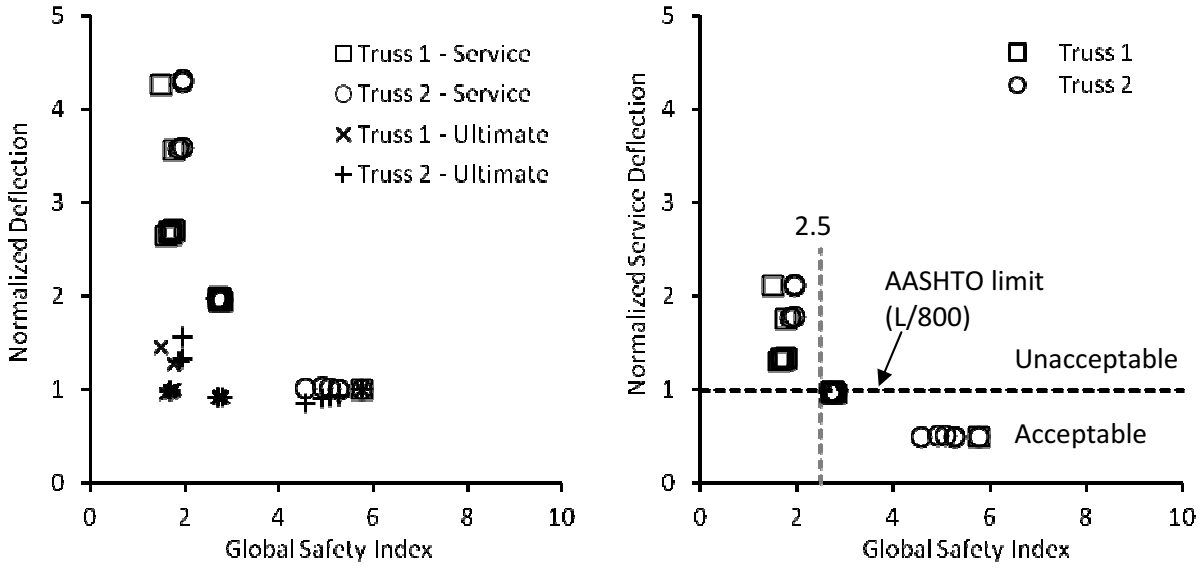

(a) (b)

Fig. 3.12 Relationship between global safety index and normalized deflection: (a) to control deflection; (b) to AASHTO deflection limit

$$Z_e = \frac{1 - U.C.}{\sqrt{[\sigma(p_{ult})]^2 + [\sigma(p_{serv})]^2}} \tag{3.6}$$

where Z_e is the element safety in service (i.e., 25% of the control capacity was applied here), and $\sigma(p_{ult})$ and $\sigma(p_{serv})$ are the standard deviations for the ultimate and service forces in the truss element, respectively. The standard deviations for the member's ultimate and service capacities were evaluated using the same coefficients of variation as for the global safety index. Figure 3.13 presents the element safety index of each damage scenario. In this figure, the Control-Avg and Damage-Ave are defined as the average element safety indices of the entire truss elements for the control and damaged trusses, respectively, while Control-Min and Damage-Min denote the minimum indices of the critical member of those trusses. The average change in element safety indices between the control and the damaged cases were not significant: 12.6% and 11.7 % for

Trusses 1 and 2, respectively, on average. The minimum indices for the damaged truss systems were, however, remarkably lower than those of the control: 64.3% and 51.0% for Trusses 1 and

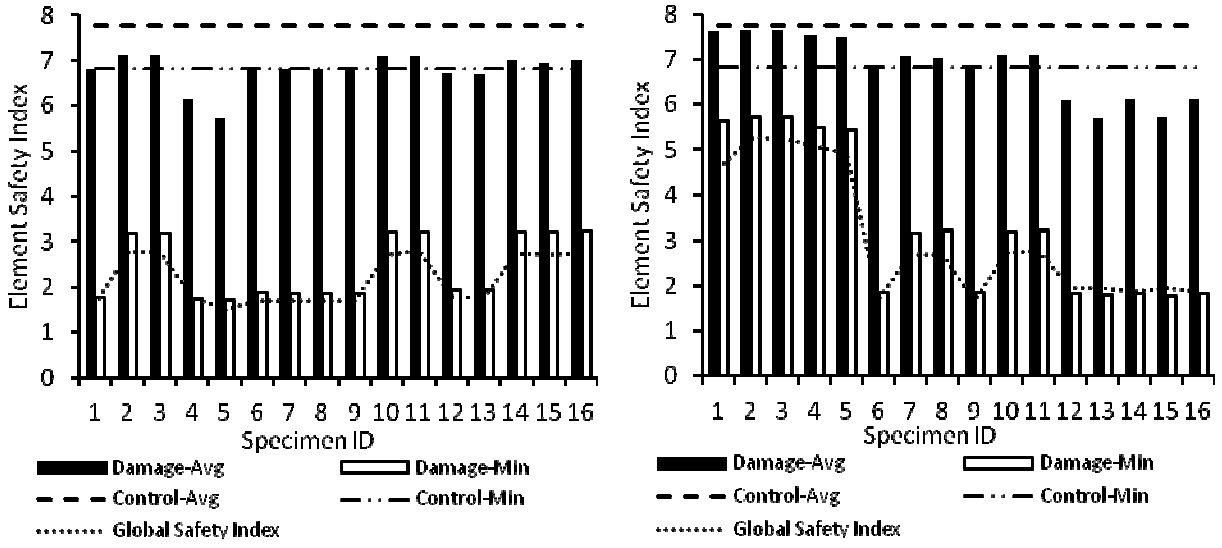

Fig. 3.13 Truss safety based on element safety index: (a) Truss 1; (b) Truss 2

2, respectively, on average. These observations confirm that damage distribution (or stress redistribution among truss members due to local damage) in a truss system was not significant and damage localization was a critical factor leading to the safety of the system. It is interesting to note that the global safety index based on the deflection of a damaged truss system (Eq. 3.5) was aligned with the minimum element safety index derived from member force, as shown in Fig. 3.13. This correlation implies that as load is transferred to critical elements due to the presence of damage the capacity of the element with respect to safety against failure follows the same trend as the deflection of the system. Regular monitoring of the deflection of an existing truss bridge is thus an important task, unless a refined health monitoring method is utilized, to indirectly estimate the progression of the minimum element safety index that represents the current state of a critical region in the bridge. This approach could be an inexpensive and practical method to determine the safety of the bridge against impending member failure.

3.9 SUMMARY AND CONCLUSIONS

An investigation has been performed as to the effects that local damage in steel trusses has on the overall behavior of the bridge. The investigation utilized an experimental program to test a scaled model bridge, which was validated with a numerical model. The numerical modeling was then extended to investigate the relationship between damage and bridge failure. The behavior of sixteen damage scenarios was compared to that of the control truss. A static analysis was carried out which utilized a damage index to quantify the level of damage present in the bridge, to examine the load transfer relationship between truss members, and to quantify the failure load for various scenarios. In addition, a dynamic analysis investigated the effect of damage on mode frequency and changes in mode shape. A simple reliability analysis was conducted to assess the safety of the truss systems. The following is concluded:

- The presence of local damage in the truss system significantly influence the serviceability of the system (i.e., deflection), particularly noticeable for those with a damage index of greater than 0.5. The load-carrying capacity of the damaged truss systems exponentially decreased with an increasing damage index.
- The current AASHTO load rating method was reasonably applicable to the truss bridge systems, while the rate of change in the normalized deflection for the Operating and Inventory ratings was almost identical. It was recommended that the Inventory rating factor be greater than 1.5 for the safe operation of existing truss bridges.
- From a dynamic analysis perspective, a higher mode shape and corresponding frequency were useful to detect the presence of local damage in the truss systems. The natural frequency associated with the 4^{th} mode remarkably decreased when the damage index increased, implying that the equivalent stiffness of the system was reduced in a specific

direction of displacement.

- The stress of the damaged truss member was not effectively redistributed to other members, except for those adjacent to the damage. The average safety index of the constituent members was not sensitive to the local damage, whereas the safety index of the critical members was. The global safety index of the system based on deflection characteristics was a good indicator to indirectly diagnose the presence of local damage. A repair method that can improve the redundancy of a damaged truss bridge, rather than localized repair, is required to enhance the overall performance of such a bridge.

CHAPTER 4. FUNCTIONALITY OF A DAMAGED STEEL TRUSS BRIDGE STRENGTHENED WITH POST-TENSIONED CFRP TENDONS

4.1 ABSTRACT

Since the catastrophic collapse of the I-35W bridge the performance of steel truss bridges has come under question. Research shows that the presence of damage in a steel truss bridge has a significant impact on the serviceability and load capacity of the structure. Due to this fact it becomes imperative to design a strengthening method that will increase the redundancy, serviceability and load capacity of the steel truss bridge when damage is present. In this work an externally draped post-tensioned carbon fiber tendon is used to rehabilitate a damaged steel truss bridge. The method uses a scale model bridge from the ASCE's Student Steel Bridge Competition which is load tested for a control scenario, 16 damage scenarios and three levels of post-tensioning for each damage scenario. A 3-D model was generated using RISA 3-D structural analysis software and then used to verify the experimental results. Methods used to compare the numerical models results to the experimental results include member strain, deflection and camber. Upon verification of the experimental results, the numerical model was extended to further develop the relationship between strengthening and the performance of the bridge.

4.2 INTRODUCTION

As of 2010 the American Society of Civil Engineers "Report Card for Americas Infrastructure" evaluated the national bridge inventory with a grade of "C". This evaluation was in response to 25% of bridges being classified as either structurally deficient or functionally obsolete. With the current state of constructed steel truss bridges in the US new materials and methods for repairing and rehabilitating damaged bridges is required. Most recently, the use of

fiber reinforced polymer's (FRP's) have received investigation for their application in structural strengthening schemes. Bakis et al. (2002) reviewed the current state of fiber-reinforced polymer composites used in construction. The review considered civil engineering applications for carbon fiber reinforced polymer's (CFRP's) in bridge decks, internal and external reinforcements, and codes. In a majority of previous works most FRP applications focused on strengthening concrete structures. Kim et al. (2008) examined the use of prestressed carbon fiber reinforced polymer (CFRP) sheets to repair damaged concrete bridge girders. The strengthening scheme was designed in accordance with AASHTO LRFD and the Canadian Highway Bridge Design Code. The work evaluated the flexural behavior of the bridge during undamaged, damaged and repaired conditions. A full-scale FEA model was used to compare the results to those predicted by AASHTO LRFD and determined that the AASHTO LRFD code provided conservative results compared to the FEA model.

In addition, applications for steel strengthening with CFRP's have been gaining interest in the civil engineering industry. Hollaway and Cadei (2002) summarized some recent applications for advanced polymer composite (APC) materials. The review identified issues related to service conditions which focused on the problems associated with the adhesives used for bonding the APC material to the structure and some concerns regarding the durability of both the APC and the bonding agent. In other work the strengthening material was attached directly to the deteriorated members. Still, other methods have added members to the structural system in order to strengthen steel trusses. The method of using post-tensioned tendons strung using various profiles within a truss system is one that adds structural members to the system and to date has experienced only nominal theoretical investigations. Albrecht and Lewan (2008) proposed using post-tensioned tendons that were concentric with members to strengthen a steel

truss. By using standard truss analysis methods it was possible to determine both the geometric design and the required post-tension levels for the truss system. Han and Park (2005) studied the effects that straight and draped post-tensioned tendons have on strengthening steel trusses. They examined the effect that tendon profile, truss type, post-tension force, and tendon eccentricity have on the trusses load capacity and deflection. From their work they determined that the load capacity of a steel truss increases linearly with post-tension level and tendon eccentricity. Additionally they concluded that the trusses elastic range, working load and load capacity were increased while the truss deflection was reduced with increasing post-tension levels.

This paper presents an experimental study to examine the response of a scaled truss bridge having various damage scenarios subjected to a post-tensioned externally draped CFRP tendon. Experimental test data was validated using a three-dimensional numerical model. Upon verification of the experimental results by the numerical model, the numerical model was extended to include a simple reliability analysis in order to evaluate the performance of damaged truss bridge when subject to strengthening using a post-tensioned system.

4.3 RESEARCH SIGNIFICANCE

Traditional methods for strengthening bridges have focused on repairing or replacing damaged elements using the same materials as the originally constructed bridge. In most cases the need for strengthening was a result of either deterioration in the original material caused by environmental factors or damage caused by vehicle use. To reduce the need for future reconstruction due to environmental factors the application of an alternative construction material is required. The use of CFRP (carbon fiber reinforced polymer) tendons provides strong resistance against environmental factors which lead to degradation of the structure. In addition, a suitable alternative to element level strengthening is desirable. With the addition of a post-

tensioned tendon, which is draped outside of the truss profile, the redundancy of the truss is increased and through the post-tensioning method truss element forces are reduced. By effectively increasing system redundancy and reducing element level stress the performance of the system will increase providing a longer service life with decreased failure probability.

4.4 EXPERIMENTAL PROGRAM

4.4.1 Materials

A steel truss bridge was designed and fabricated to 1:20 scale. The bridge is approximately 6.2 meters in length and fabricated from round and square tubes of grade A36 steel shown in Fig. 4.1(a). The bridge was designed using a system of two main trusses designated truss 1 and truss 2 as shown in Fig. 4.1(b). A secondary frame was designed to support the truss's top chord and prevent lateral buckling, cross braces were utilized at both ends

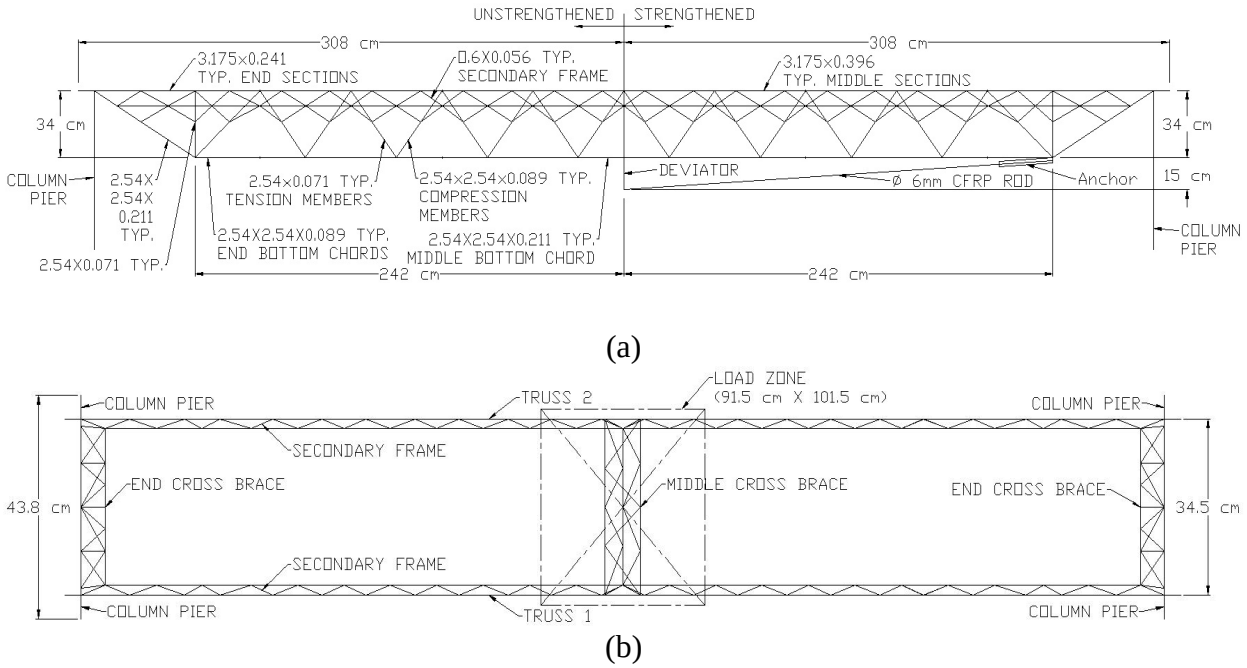

Fig. 4.1 Schematic of truss systems: (a) Side view; (b) Top view

of the trusses and at midspan, along with four column piers at each corner of the bridge [Fig. 4.1(b)]. The steel used consisted of the following properties: elastic modulus (E) = 200 GPa,

yield stress (σ_y) = 290 MPa, and Poisson's ratio (υ) = 0.3. The strengthening system utilized steel

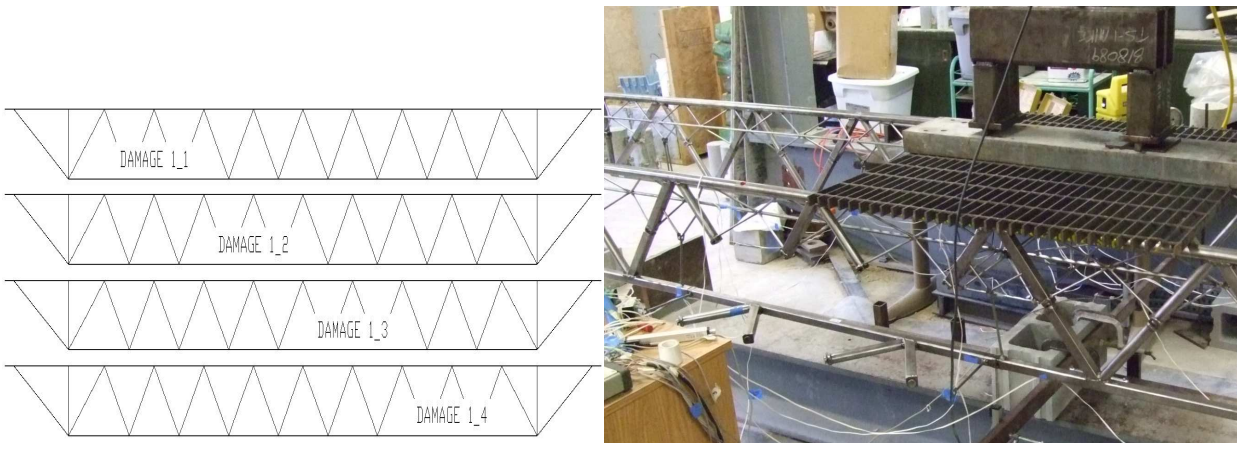

(a) (b)

Fig. 4.2 Damage simulation: (a) position of damage; (b) Specimen 2, damage location 1_2

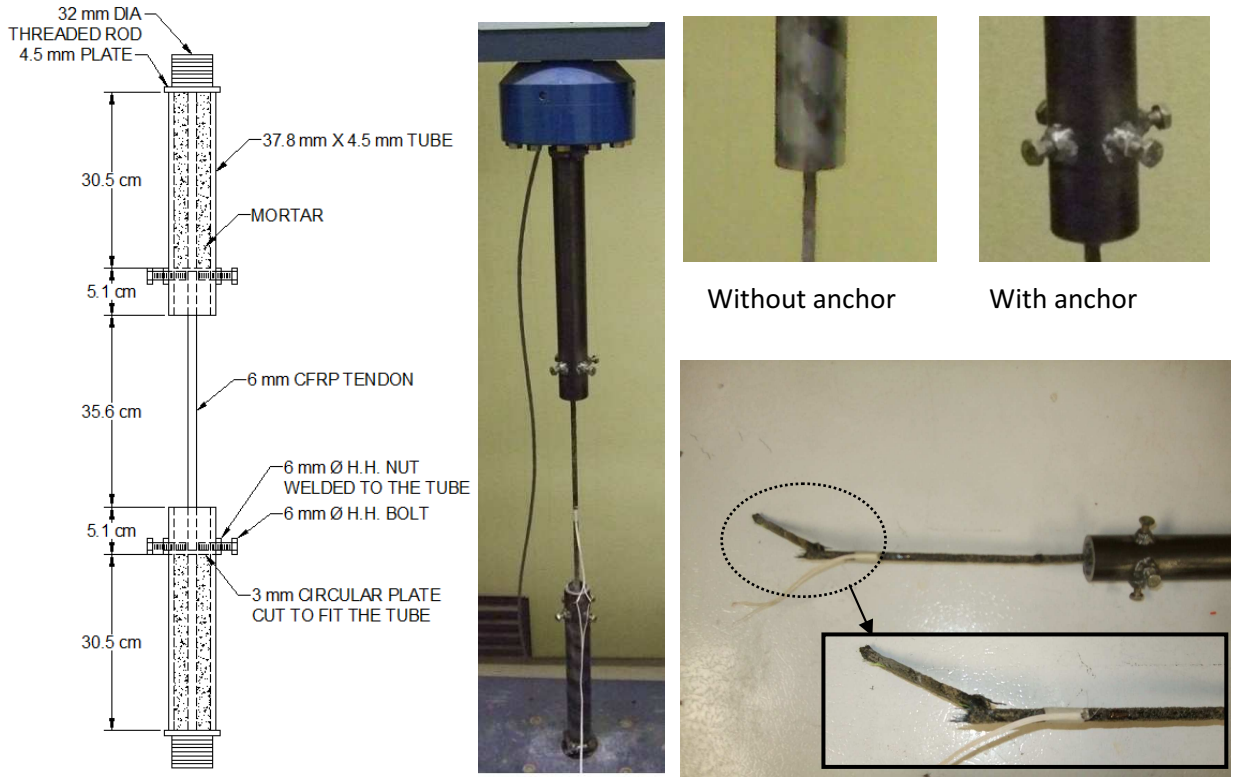

(a) (b)

Fig. 4.3 Tension test for anchorage: (a) specimen dimension; (b) test details

tubing and plates of the same properties as that used for the bridge. High strength steel bolts and extended length coupler nuts were used to tension the CFRP rod, as shown in Fig. 3(a), non-shrink mortar anchored the CFRP rod in the steel tubes and carbon fiber reinforced polymer rods of tensile strength (σ_r) = 2068 MPa, and elastic modulus (E) = 124 GPa were the main strengthening component [Fig. 3(b)].

4.4.2 Fabrication Of Test Truss

The experimental steel bridge was fabricated by hand for use in the ASCE Student Steel Bridge Competition. Fabrication was performed using jigs, which consisted of steel plates and bars, and drawings printed to scale for assistance with dimensioning and layout of the truss. Truss connections were fabricated by use of a CNC (computer numeric controlled) lathe and mill. Several trials were required with the lathe and mill to achieve an acceptable tolerance in the connections. A tight tolerance was required to reduce the probability of having disengaged connections while still allowing for assembly of the bridge while competing.

4.4.3 Design Of Anchorage

In order to tension the CFRP rod an anchor system was required. The anchorage system employed a mortared steel tube which secured each end of the CFRP rod. The steel tubes were secured to anchor blocks using threaded rod which was welded to a backer plate on the end of the steel tube and extended from the ends of the mortared steel tubes through the anchor blocks. An extended length coupler nut was used to tension the CFRP rod against the anchor blocks which were welded to the bottom of the truss on the exterior truss diagonals. This system resulted in a relatively simple installation process and allowed the CFRP to be tensioned from both ends of the truss. In this scale model application the anchor block was designed using 3/16” plate from which a partially enclosed box was welded together. The threaded rod that was used

to anchor the CFRP to the anchor block was a 3/8” high strength alloy rod.

4.4.4 Preparation For Anchorage System Testing

Tensile tests were performed in order to determine the mode of failure for the CFRP rod bonded with non-shrink mortar in the steel tube. The test specimens were prepared based on reviewed literature and manufacturer specifications. The test machine used for tensile testing was a SATEC 22 EMF which has a load capacity of 100 kN. The specimen preparation procedure consisted of cutting two 30.5 cm long tubes from 3.8 cm outside diameter by 4.5 mm wall thickness stock tube. The steel grade of the tube was A500 Gr. 50. The inside of the tubes were roughened with a round file to remove undesirable debris from the sidewalls and add grooves to assist with adhesion between the mortar and steel. The inside of the tube was then wiped clean with acetone to remove any remaining debris from the tube. A square backer plate, 7.8 cm x 7.8 cm x 4.5 mm, was cut and polished on both of its wide faces using a wire wheel in order to remove corrosion and oil from the steel in preparation for welding. Once clean, the plate was welded to one end of the 30.5 cm long tube. The entire perimeter of the tube was welded to the plate. A Miller 135 wire feed welder was used for all welding operations. Next, a 3.2 cm long section of threaded rod was cut. The rod was 1 ¼ -12 standard threads per inch (UNF, Class 1A) as per requirement to attach the specimen to the tensile test machine used for this experiment. The threaded rod was then aligned with the center of the tube using a jig. Having an alignment that was centered along the longitudinal axis of the tube was necessary in order to achieve alignment between both the upper and lower steel tubes in the testing machine. The threaded rod was then welded to the backer plate. This procedure was used in order to ensure alignment between the tube and threaded rod so that the tube would rest perpendicular to the load cell and base in the testing machine. Two specimens were prepared in this fashion for a total of four tubes

with threaded rods welded to them. Of the four tubes, two were prepared so that bolts could be threaded from the outside into the tube. To do this, four holes were drilled in the tube at 90° to one another about the longitudinal axis of the tube. The holes were drilled with a 4.5 mm bit at a distance of 4.3 cm from the open end of the steel tube. Then, a 6 mm nut was centered on the hole and welded to the outside of the tube. Four 6 mm dia. bolts were then threaded into the nuts. Next, a three foot section of Aslan 200 CFRP rebar was aligned with the center of the steel tube using a jig. Then, a mix of Quickrete non-shrink precision grout was prepared in accordance with the manufactures recommendations for a mix with "fluid" consistency. This mix required 3 days of curing to attain full strength per manufactures recommendation. Based on the dimensions of the steel tube, a grout mix was chosen which consisted of 350 g of mortar and 80 g of water per tube. The mix was prepared on a small scale because only one pullout test could be performed at a time, and only one of the two tubes for each specimen could be filled and cured at a time. For the specimen with 4 shear bolts at each end, a 3 mm circular plate with a 4.5 mm hole in the center was prepared to be inserted into the tube around the CFRP rod. Once the tube was filled with mortar the circular plate was slid down the CFRP rod and inserted into the steel tube. The plate was pressed into the mortar until it was at the appropriate position to allow for the bolts to be threaded into the tube. The bolts were threaded into the tube until they were approximately 1.5 mm from the CFRP rod. After the first tube which was filled with mortar had cured for 7 days, the specimen was removed from the jig. This end of the specimen was then threaded into the top arm of the testing machine. The second tube was then threaded into the bottom plate of the testing machine and the upper arm of the testing machine was lowered until the CFRP rod was touching the backer plate on the inside of the lower steel tube. No compression force was allowed to be exerted on the CFRP rod. The alignment of the CFRP rod within the lower steel

tube was checked by measuring with a tape measure to ensure that the rod was in the center of the tube. The mortar mix was then prepared and placed in the lower steel tube. For the specimen

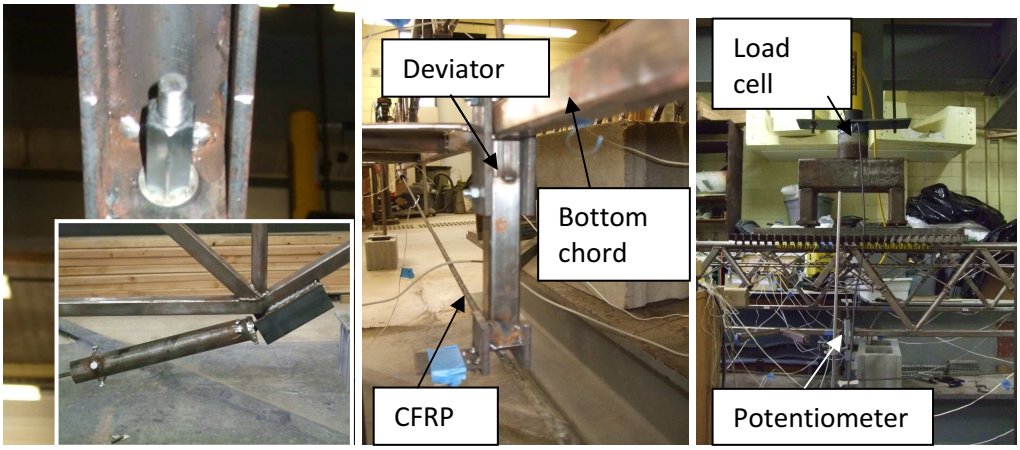

(a) (b) (c)

Fig. 4.4 Test details: (a) CFRP anchorage system; (b) deviator and CFRP rod; (c) loading and instrumentation

with shear bolts at each end the same procedure was used for the second tube as was used for the first when inserting the circular plate into the steel tube. The completed specimen is shown in Fig. 4.4(a) and 4.4(b). At this point the entire specimen had been inserted into the testing machine and the alignment of the rod was verified before allowing the mix to cure. This two part process was required in order to align the CFRP rod within the tube and to allow the mortar to cure. This process was also necessary because the threaded rod which was required to properly fix the specimen to the machine needed to be welded to the specimen. This situation made it impossible to thread the specimen into or out of the testing machine once both ends of the CFRP rod were bonded in the mortared tube.

4.4.5 Damage Scenario

In order to simulate damage scenarios, web elements were removed from the truss system. In order to represent high levels of damage in truss bridges four adjacent web elements were removed at each specified damage location. Figure 4.2(a) depicts the web element labeling

convention for the damage scenarios that were used to generate 16 combinations of damage locations. The 16 combinations of damage locations are detailed in Tables 4.1, 4.2 and 4.3 where

Table 4.1 Damage Index – 2kN

Specimen ID	Damage Scenario	Damage index – 2 kN					
		Truss 1 - Strengthened			Truss 2 - Unstrengthened		
		Exp[1] (a)	Model (b)	Margin[2] (%)	Exp[1] (a)	Model (b)	Margin[2] (%)
Control	None	N/A	N/A	N/A	N/A	N/A	N/A
1	1_1	0.26	0.55	111%	0.23	-0.10	143%
2	1_2	-0.25	0.35	244%	0.15	0.00	103%
3	1_3	0.00	0.36	425790%	0.01	-0.01	157%
4	1_1 & 1_3	0.39	0.67	73%	0.09	0.01	91%
5	1_1 & 1_4	0.46	0.73	57%	0.12	0.01	88%
6	1_1 & 2_1	0.45	0.56	26%	0.63	0.62	0%
7	1_1 & 2_2	0.36	0.56	56%	0.52	0.49	6%
8	1_1 & 2_3	0.35	0.56	58%	0.55	0.49	12%
9	1_1 & 2_4	0.45	0.56	23%	0.66	0.62	6%
10	1_2 & 2_2	-0.09	0.36	481%	0.37	0.48	29%
11	1_2 & 2_3	0.21	0.36	67%	0.49	0.48	1%
12	1_1, 2_1 & 2_3	0.56	0.56	0%	0.75	0.72	4%
13	1_1, 2_1 & 2_4	0.54	0.57	6%	0.77	0.77	1%
14	1_2, 2_1 & 2_3	0.20	0.36	84%	0.71	0.72	1%
15	1_2, 2_1 & 2_4	0.11	0.37	234%	0.78	0.76	2%
16	1_3, 2_1 & 2_3	0.20	0.36	83%	0.73	0.72	1%

a Specimen ID code was used to differentiate the combinations of damage locations. Damage locations were identified based on the truss that was damaged, either truss 1 or truss 2 and the position of damage present [positions 1, 2, 3 and 4]. Several examples of the identification code follow; Specimen ID 2 calls out damage scenario 1_2 which denotes that damage is located in truss 1 position 2 whereas Specimen ID 6 calls out damage scenario 1_1 & 2_1 indicating that damage is present in truss 1 position 1 and truss 2 position 1.

4.4.6 Strengthening Scheme

An externally attached post-tensioning system was chosen to strengthen the steel truss by increasing the redundancy of the system and reducing element forces when damage was present.

The strengthening system utilized a singly harped CFRP (carbon fiber reinforced polymer) tendon attached to the bottom chord of the damaged truss. The tendon was anchored at each end

Table 4.2 Damage Index – 4kN

Specimen ID	Damage Scenario	Damage index – 4 kN					
		Truss 1 - Strengthened			Truss 2 - Unstrengthened		
		Exp[1] (a)	Model (b)	Margin[2] (%)	Exp[1] (a)	Model (b)	Margin[2] (%)
Control	None	N/A	N/A	N/A	N/A	N/A	N/A
1	1_1	0.17	0.46	175%	0.21	-0.11	151%
2	1_2	-1.10	0.14	113%	0.10	-0.01	109%
3	1_3	-0.73	0.14	119%	-0.02	-0.01	51%
4	1_1 & 1_3	0.03	0.60	1643%	0.14	0.00	98%
5	1_1 & 1_4	0.242	0.68	183%	0.18	0.01	95%
6	1_1 & 2_1	0.274	0.47	71%	0.63	0.62	0%
7	1_1 & 2_2	0.050	0.46	830%	0.48	0.48	1%
8	1_1 & 2_3	0.050	0.46	829%	0.54	0.48	10%
9	1_1 & 2_4	0.283	0.47	66%	0.67	0.622	7%
10	1_2 & 2_2	-0.759	0.14	119%	0.38	0.482	28%
11	1_2 & 2_3	-0.152	0.14	193%	0.51	0.482	5%
12	1_1, 2_1 & 2_3	0.469	0.47	1%	0.74	0.718	3%
13	1_1, 2_1 & 2_4	0.488	0.48	2%	0.77	0.765	1%
14	1_2, 2_1 & 2_3	-0.333	0.16	147%	0.72	0.717	0%
15	1_2, 2_1 & 2_4	-1.036	0.17	116%	0.78	0.764	2%
16	1_3, 2_1 & 2_3	-0.098	0.16	261%	0.72	0.717	0%

of the bottom chord of the truss [Fig. 4.3(a) inset]. A threaded rod was used to tension the CFRP rod against the anchor blocks at each end of the bottom of the truss. A steel deviator at mid-span [Fig. 4.3(b)] was used to harp the tendon to the desired eccentricity and direct an upward load onto the trusses bottom chord. When the tendon was tensioned it induced an uplift force at mid-span of the truss which counteracted the forces in the truss elements from the applied live load on top of the bridge. By adjusting either the length of the deviator or the level of post-tension it was possible to control the amount of vertical force applied to the truss and optimize the strengthening system based on the live load requirements and geometric design constraints.

4.5 TEST SETUP AND INSTRUMENTATION

Experimental testing of the steel truss bridge utilized a manually operated hydraulic actuator. The load was typically applied to 25% of the theoretical load capacity of the control

Table 4.3 Damage Index – 6kN

Specimen ID	Damage Scenario	Damage index – 6 kN					
		Truss 1 - Strengthened			Truss 2 - Unstrengthened		
		Exp[1] (a)	Model (b)	Margin[2] (%)	Exp[1] (a)	Model (b)	Margin[2] (%)
Control	None	N/A	N/A	N/A	N/A	N/A	N/A
1	1_1	-0.29	0.31	205%	0.24	-0.11	147%
2	1_2	-6.86	-0.31	95%	0.17	-0.01	108%
3	1_3	14.45	-0.31	102%	-0.04	-0.01	61%
4	1_1 & 1_3	-0.86	0.48	156%	0.16	0.00	102%
5	1_1 & 1_4	-0.30	0.62	306%	0.20	0.00	99%
6	1_1 & 2_1	-0.19	0.32	272%	0.64	0.62	2%
7	1_1 & 2_2	-0.77	0.31	141%	0.46	0.48	5%
8	1_1 & 2_3	-0.81	0.31	139%	0.53	0.48	10%
9	1_1 & 2_4	-0.11	0.32	381%	0.67	0.620	7%
10	1_2 & 2_2	-10.90	-0.30	97%	0.40	0.481	21%
11	1_2 & 2_3	-2.46	-0.31	88%	0.53	0.481	9%
12	1_1, 2_1 & 2_3	0.34	0.33	4%	0.77	0.717	7%
13	1_1, 2_1 & 2_4	0.34	0.34	2%	0.77	0.764	1%
14	1_2, 2_1 & 2_3	-4.73	-0.27	94%	0.72	0.716	1%
15	1_2, 2_1 & 2_4	6.97	-0.25	104%	0.80	0.763	5%
16	1_3, 2_1 & 2_3	-1.11	-0.27	76%	0.72	0.717	0%

[1]: Average value of measured test data
[2]: margin (%) = absolute value of (a-b)/a $\times$100

truss, which was dependent on the level of damage. This load level equates to a typical service load of 4.5 kN. In order to transfer load from the hydraulic actuator to the two trusses a steel channel was centered on the middle of a steel grate with dimensions, 2.5 cm thick by 91.5 cm square, located at the trusses midspan. Truss deflection was monitored and electronically recorded at midspan of each truss by way of linear potentiometers [Fig. 4.3(c)]. Individual member strain was recorded for selected members by using flexible foil strain gages. The response of the structural truss system for damaged and strengthened scenarios was attained by

electronically recording response data by way of a data acquisition system.

4.6 FINITE ELEMENT MODELING

A three dimensional model of the steel truss bridge was generated using RISA 3-D structural analysis software. The model used for analysis included two simple span trusses, one crossbrace at each end of the trusses and one at midspan of the trusses, a three dimensional frame attached to the top chord of each truss, and four cantilevered column piers as depicted in Fig. 4.5.

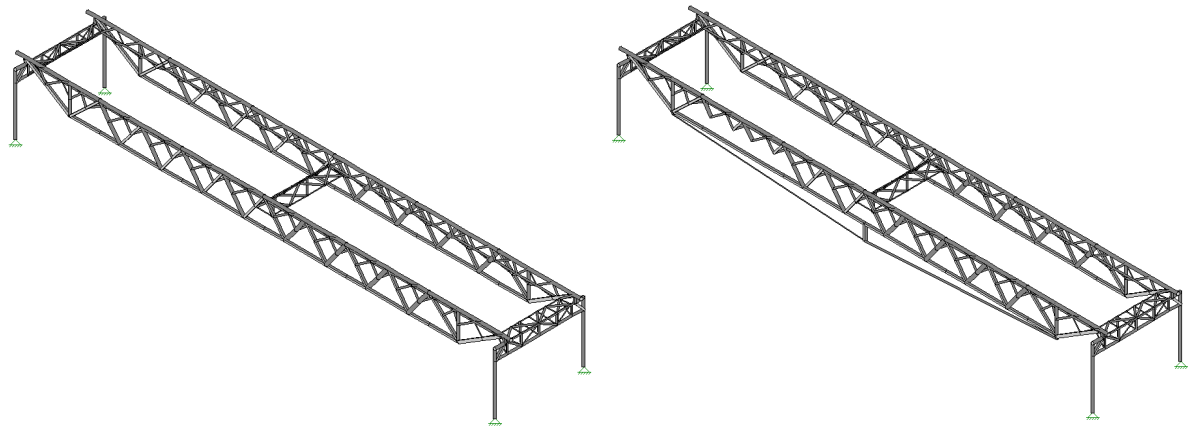

(a) (b)

Fig. 4.5 Developed FE model: (a) control; (b) CFRP strengthened (Scenario 1, damage location 1_1)

The truss element properties were selected based on the material available from Central Steel & Wire as of 2010 and they were entered into the material database of RISA 3-D then applied to appropriate members. The control bridge was composed of 250 nodes and 404 line elements. Appropriate truss members were removed from the model in accordance with the damage simulation requirements. Removal of web elements consisted of only the lower portion of the truss web below the secondary frame. All truss elements were assumed to have a rigidly fixed connection to one another. The truss was restrained by boundary conditions at the base of each pier. The columns were assumed to support reactions in the X, Y, and Z directions but were allowed to rotate at the base because bending moment was not restrained by the experimental

model. For the purpose of analyzing truss deflection and member strains, special considerations were made for the application of loads imposed by the post-tensioning method. Since RISA 3-D does not allow for consideration of initial strain in the CFRP elements a method to simulate the load effects that the post-tensioning system imposed on the truss was required.

4.6.1 Modeling Post-Tensioning Effects

In order to model the effects from the post-tensioning system equivalent forces were applied to the locations where force was transferred from the post-tension system to the truss system. This approach was used for the static analysis. The equivalent forces from post-tensioning were simplified so that a vertical component of force was applied from the deviator at midspan of the truss and the horizontal component of force was applied at the anchor blocks to the bottom chord of the truss. Since the vertical component of force at the anchor blocks was negligible it was ignored in order to simplify the modeling process. These forces were applied to the node at the midspan of the bottom chord and the nodes at the outside ends of the bottom chord for consideration of truss deflection and member strain. For the purpose of dynamic analysis the CFRP tendon was included in the numerical model. For this case the same equivalent forces used for modeling deflection and strain were applied to the same locations except the vertical force at midspan was applied to the point of attachment between the CFRP and the deviator as opposed to the bottom truss chord.

4.7 TEST RESULTS AND ANALYSIS

4.7.1 Anchor Test

In order to verify the tensile strength of the anchorage system a tensile test of each specimen was performed. A displacement rate of 1 mm/minute was used with measurements automatically recorded at a rate of 10 per second. An automatic shut off load of 75 kN was

specified for the machine. During the loading process for the first test specimen, “mortar only” specimen, minor slipping between the steel tube and mortar interface occurred several times at regular intervals but each time the slipping was immediately recovered. A slip was identified by a decrease in load accompanied by a proportionally large displacement relative to the previous displacement. At 10.7 kN the single largest slip occurred resulting in 0.033 mm of displacement before permanent failure occurred at 11.1 kN. At this point the load rapidly decreased as there was bond failure between the steel tube and the mortar. The accumulated slip prior to failure was 0.274 mm. The bond failure resulted in a decrease of load capacity to approximately 9.6 kN or a decrease of 13.5% while maintaining the displacement rate of 1 mm/minute. Once bond failure was achieved, the ultimate load capacity of the CFRP anchorage system was observed to slowly decrease with time as shown in Fig. 4.6. A second test was conducted on the CFRP anchor with

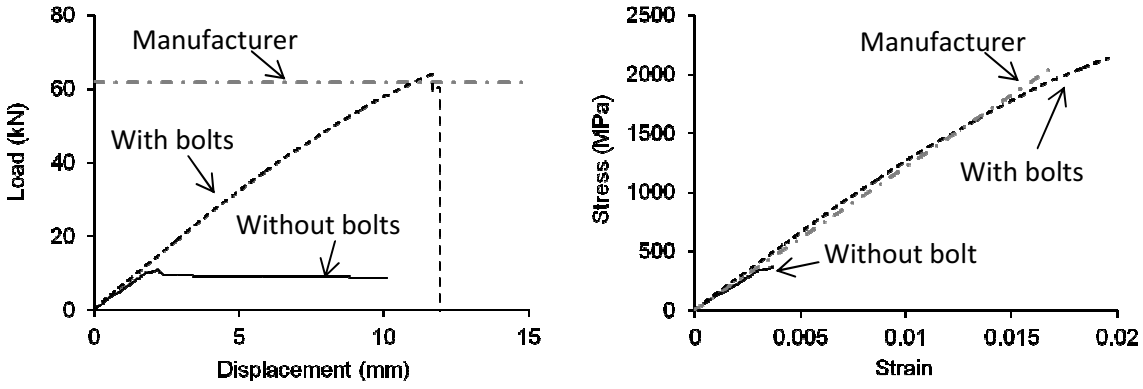

(a) (b)

Fig. 4.6 Response of tested anchor systems: (a) load-displacement; (b) stress-strain of CFRP

modifications to the anchorage system. The modification utilized a steel plate to cover the mortar with the plate held in place using 4 bolts in shear. The second anchorage test specimen was prepared in the same fashion as the first test except as previously outlined in the *Specimen Preparation Procedure*. The plate and shear bolts were used to prevent the mortar from slipping and eventually pulling out of the steel tube under ultimate load. Using this method, the

experimental results provided reasonable agreement with the manufacturers maximum load specification [Fig. 4.6(a)]. The stiffness of the experimental results was slightly less than the manufacturer's specifications [Fig. 4.6(b)]. This fact is attributed to the bond slip which occurs at both the CFRP/mortar interface and the mortar/steel tube interface. The 2nd anchor test specimen experienced minor slipping prior to failure which accumulated to 0.103 mm of additional displacement. For the 2nd anchor test failure occurred suddenly at 64.0 kN, which was in excess of the manufacturers failure specification of 61.8 kN. The accumulated slip for test 2 represented 37.6% of the slip observed during test 1 while the ultimate load of test 2 was found to be 576.6% of that during test 1. The results of the second anchor test provided sufficient evidence to indicate that the 2nd anchorage system would mobilize the load capacity required to fail the CFRP rod. This result allows the designer of the post-tensioning system to perform their design with the ultimate capacity of the CFRP as the limiting design consideration for failure.

4.7.2 Static Behavior

Experimental and numerical analysis were used to evaluate the static performance of the steel truss bridge. Using the method described in the previous section, *Strengthening Scheme,* a static analysis examined the behavior of the bridge's deflection and member's strains at three different levels of post-tension load. Comparisons were made between the behavior of the un-strengthened control bridge and the strengthened damaged bridge for the experimental and numerical model results. An evaluation of the models ability to predict the behavior of the steel bridge was performed to determine the usefulness of the model for simulating probable damage conditions and the subsequent response of the bridge.

4.7.2.1 Deflection response

Experimental tests were conducted 5 times in sequence in order to verify that the bridges

response was unchanged during subsequent application and removal of load. Figure 4.7(a) shows the experimental deflection results for Specimen 1, which was typical for most damage scenarios with the applied post-tension loads. These results indicate that consistent deformation was

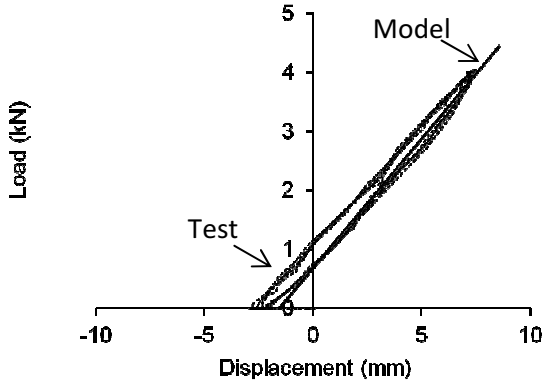

Fig. 4.7 Comparison between model and test for truss 1 of Damage scenario 1_1 at a post-tensioning force of 2 kN

experienced during experimental testing during various load applications. From a comparison of the experimental results to the numerical model for various levels of post-tensioning it is observed in Figure 4.8(a) and 4.8(c) that with increasing post-tension levels the deflection curve shifts to the left compared to the un-strengthened bridge deflection curves which results in a decreased ultimate deflection with increasing levels of post-tension. From a comparison of the experimental stiffness to the theoretical stiffness it was identified that the experimental stiffness of the strengthened bridge is slightly less than what the model predicted. Additionally, the experimental deflection curve experienced more camber than what the model predicted. This result was to be expected due to the difference in stiffness of the truss system from the experimental to the numerical model. With application of the post tension load an increased magnitude of camber is to be expected with the experimental results when compared to the numerical model. These results show that the truss deflection can be effectively controlled by the level of applied post-tension; however the stiffness of the bridge will be relatively unchanged

with increasing levels of post-tension.

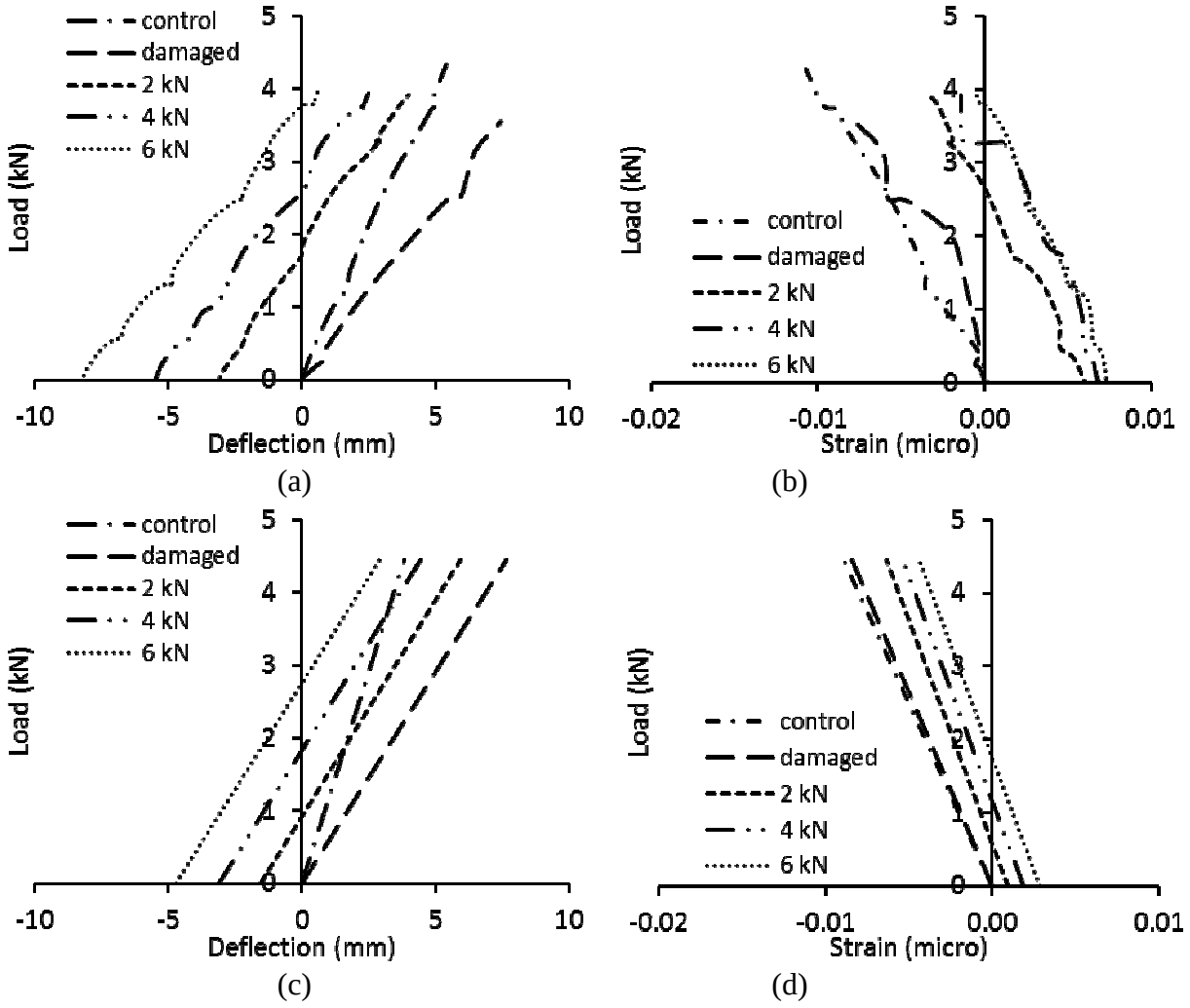

Fig. 4.8 Effect of post-tensioning for Specimen 2 (damage scenario 1_2): (a) Experimental load-deflection Truss 1; (b) Experimental load-strain Truss 1 member 3; (c) Model load-deflection Truss 1; (d) Model load-strain Truss 1 member 3

4.7.2.2 Strain response

When damage is present in truss bridges the distribution of load between members changes as the stiffness of the system is altered. By examining member strain it is possible to determine the presence of damage within the system. When damage is present the distribution of applied load amongst members is altered which causes the undamaged members to take on additional load and therefore their level of strain increases. The experimental and numerical

strain results of member C3 for Specimen 2 are shown in Fig. 4.8(b) and Fig. 4.8(c) for post-

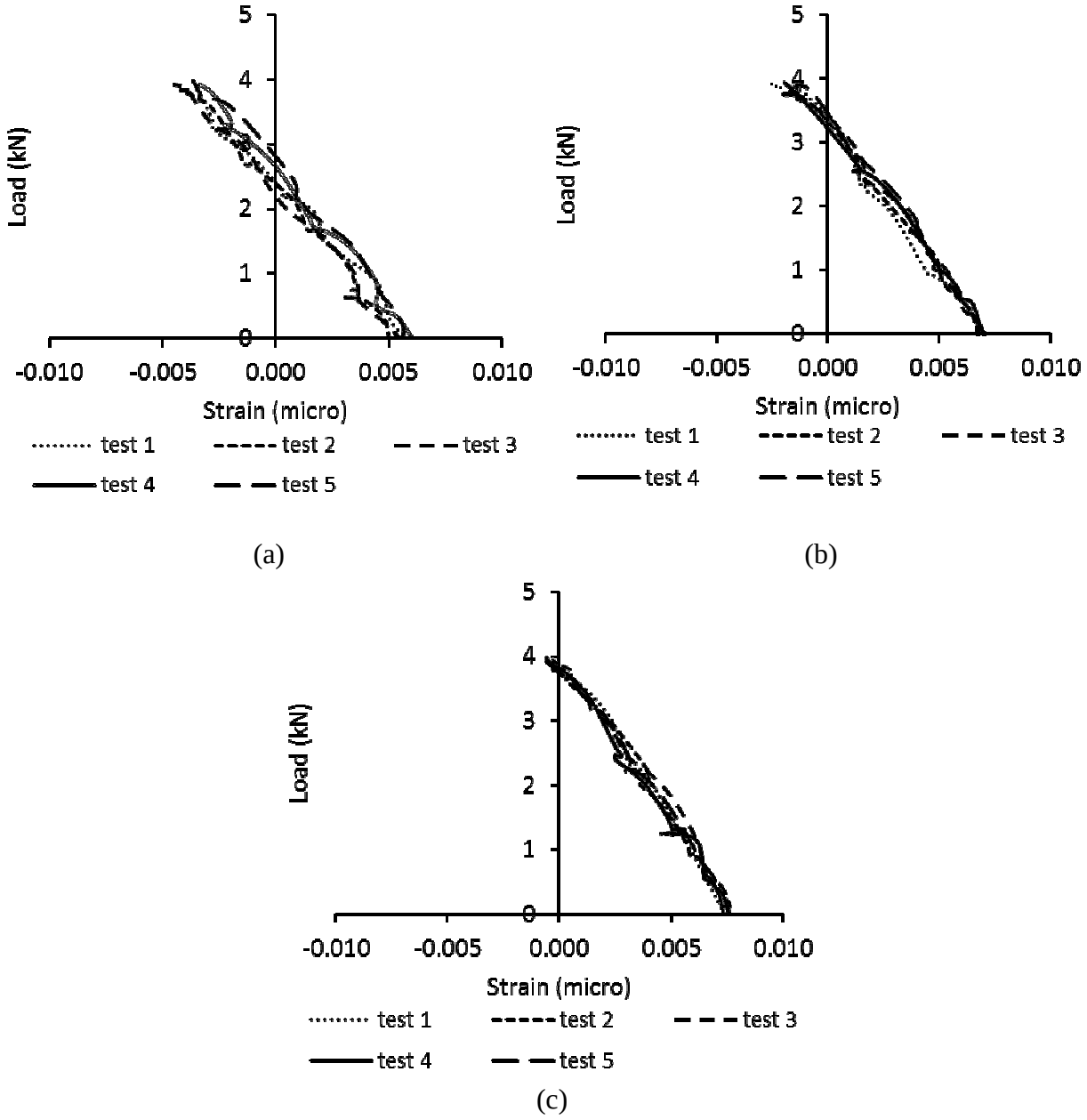

Fig. 4.9 Experimental strain results of 5 subsequent post-tensioned load tests for Specimen 2 (damage scenario 1_2): (a) 2 kN post-tensioning; (b) 4 kN post-tensioning; (c) 6 kN post-tensioning

tensioning levels of 2 kN, 4 kN and 6 kN. Figure 4.8(b) compares the experimental strain results of member C3 to the damaged and control results. Here it is found that the stiffness of the member when damaged is slightly decreased when compared to the control bridge indicating that

additional load is being transferred to it in the presence of local damage. By comparing the results for the post-tensioned bridge to the damaged condition reveals that comparable member stiffness are experienced. However, since the amount of strain experienced by the member is controlled by the level of applied post-tension member strains can be adjusted by designing the required level of post-tension. By applying a higher post-tension load the member strain is decreased. Comparing the results of Figure 4.8(b) to Figure 4.8(c), which presents the numerical models results, similar trends are observed for member strain. When comparing the strain results of the damage to control scenarios using the numerical model, only a small change in strain occurs and when post-tensioning is introduced the amount of compressive strain in the member is proportionally reduced for a linearly increasing level of post-tensioned load. In comparison to the numerical models results the experimental results show the change in strain with post-tension load clusters a bit more than what is theoretically expected. The results from Fig. 4.9 depict the strain response of 5 separate load tests for each of the specified post-tension levels. These results indicate that each of the 5 load tests for each post-tension level achieved very similar strain results indicating that load redistribution occurred consistently throughout the truss system with the application of multiple loads. The results show that the member stiffness is comparable for each scenario between the experimental and numerical results along with the trend of decreasing strain levels which correspond to increasing post-tension loads.

4.7.3 Force Redistribution

The redistribution of member forces in a truss system is a strong indicator of changes to the strength of the structural system. In full scale applications, changes to force distribution can be monitored with simple instruments such as strain gages which provide readings that are easily converted to member force. With the aid of computer simulations a numerical model can be used

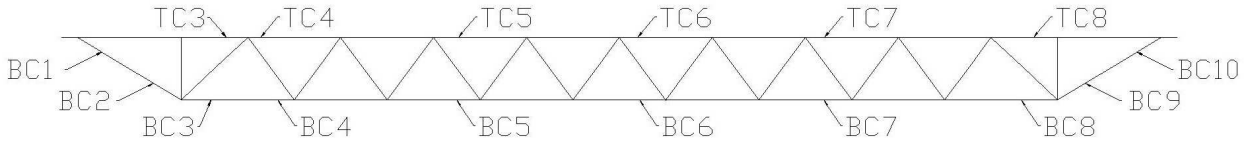

(a)

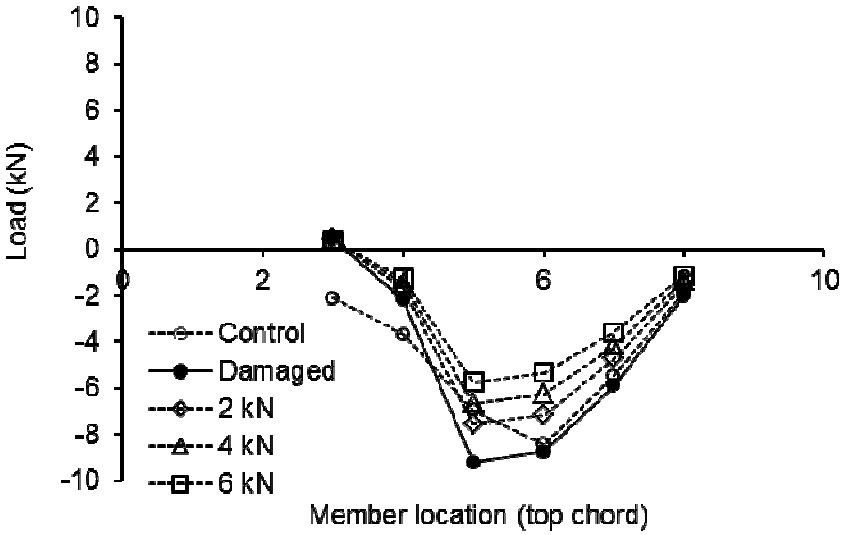

(b)

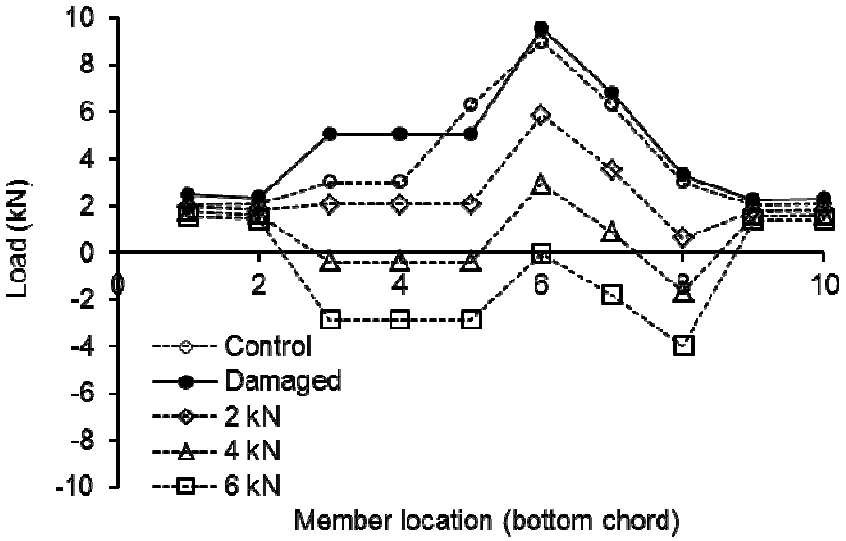

(c)

Fig. 4.10 Variation of top and bottom chord forces for truss 1 of damaged scenario 1_1: (a) member locations; (b) top chord forces; (c) bottom chord forces

to predict the redistribution of member forces for any possible damage scenario. This can be a useful tool to understand the impact that local member degradation has on other truss members.

In this work a numerical model was used to analyze the changes to force distribution when specific members are removed from the system. Fig. 4.10(a) identifies the location of strain measurements on the top and bottom chord of the truss. Fig. 4.10(b) and 4.10(c) summarize the change in strain at these locations when comparing control, damaged, and the three levels of post-tensioning for damage scenario 1_1. Here it is observed that the presence of local damage to web elements results in increased force distribution to the top and bottom chord members except

Table 4.4 Strain distribution, top chord, damage scenario 1_1

Top chord	Control	Damaged		2 kN		4 kN		6 kN	
Member location	F (kN)	F (kN)	Δ^*	F (kN)	Δ^*	F (kN)	Δ^*	F (kN)	Δ^*
TC 3	2.11	-0.45	122%	-0.43	121%	-0.41	119%	-0.37	118%
TC 4	3.69	2.20	40%	1.70	54%	1.49	60%	1.27	66%
TC 5	6.96	9.23	-33%	7.54	-8%	6.65	4%	5.74	17%
TC 6	8.43	8.76	-4%	7.15	15%	6.26	26%	5.33	37%
TC 7	5.47	5.89	-8%	4.74	13%	4.17	24%	3.59	34%
TC 8	1.86	2.02	-9%	1.57	16%	1.37	26%	1.16	37%

*Difference between the control and damaged/strengthened scenario for the numerical model.

Table 4.5 Strain distribution, bottom chord, damage scenario 1_1

Bottom chord	Control	Damaged		2 kN		4 kN		6 kN	
Member location	F (kN)	F (kN)	Δ^*	F (kN)	Δ^*	F (kN)	Δ^*	F (kN)	Δ^*
BC 1	-2.02	-2.47	-22%	-1.97	3%	-1.75	14%	-1.52	25%
BC 2	-2.08	-2.33	-12%	-1.84	12%	-1.63	22%	-1.41	32%
BC 3	-2.99	-5.05	-69%	-2.08	31%	0.39	113%	2.87	196%
BC 4	-2.99	-5.05	-69%	-2.08	31%	0.39	113%	2.87	196%
BC 5	-6.29	-5.05	20%	-2.08	67%	0.39	106%	2.87	146%
BC 6	-9.00	-9.55	-6%	-5.87	35%	-2.93	67%	0.04	100%
BC 7	-6.29	-6.83	-9%	-3.52	44%	-0.87	86%	1.80	129%
BC 8	-2.99	-3.30	-11%	-0.62	79%	1.68	156%	3.99	233%
BC 9	-2.03	-2.24	-11%	-1.77	13%	-1.58	22%	-1.38	32%
BC 10	-2.08	-2.30	-10%	-1.81	13%	-1.60	23%	-1.39	34%

*Difference between the control and damaged/strengthened scenario for the numerical model.

in the section of bottom chord immediately adjacent to the location of the damage on the side of the damage location that is closer to midspan of the truss, member location BC5 Fig. 4.10(c). Whereas member force is found to decrease in the section of the top chord between the existing

undamaged web members in Fig. 4.10(b) location TC4. When the externally draped post-tensioning system is applied the forces in both the top and bottom chords are significantly reduced at all locations and especially at location BC8 farthest away from the damage location. For damage scenario 1_1 the magnitude of change in force compared to the control scenario for location BC8 at 2 kN of post-tensioning is 79%, for 4 kN of post-tensioning it is 156% and for 6 kN of post-tensioning it is 233%. This location experiences the greatest change in member force compared to the control scenario. Additional changes to member force in the top and bottom chords are shown in Tables 4.4 and 4.5. Figure 11(a) identifies the location of force measurements for the tension and compression web members. Fig. 4.11(b) and 4.11(c) summarize the changes in force to these locations between control, damaged, and three levels of post-tensioning in the presence of damage scenario 1_1. For the compression webs a zone of influence is found to be greatest in the web members immediately adjacent to the location of damage. Figures 4.11(b) and 4.11(c) show how forces redistribute when damage scenario 1_1 occurs. In this case compression members C1 and C7 and tension member T6 are greatly influenced by the removal of adjacent web members. Each of these web members experiences an increase of force of around 100% or more compared to the member forces of the control truss. When the strengthening system is employed the member forces in both compression and tension members are significantly reduced. Tension member T6 which experienced an increase in force of 98% in the presence of damage over the control scenario saw that increase drop to a 67% increase with 2 kN of post-tensioning, a 49% increase with 4 kN of post-tensioning and a 29% increase with 6 kN of post-tensioning. Although the initial force level was not recovered a significant portion of the force increase was recovered even with this extreme damage scenario. Similar results were recorded for other members. See Tables 4.6 and 4.7 for additional

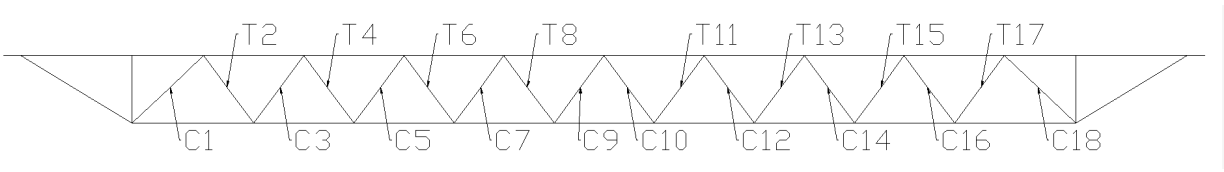

(a)

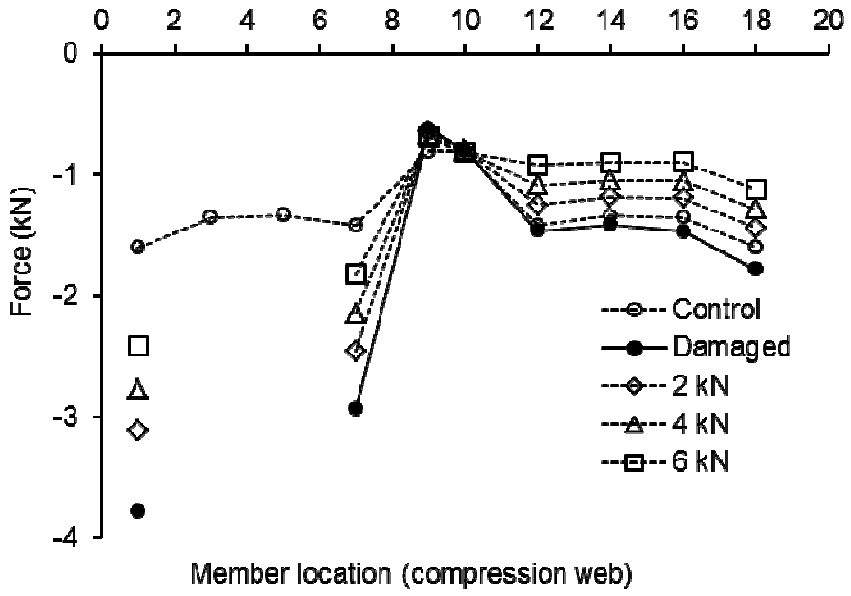

(b)

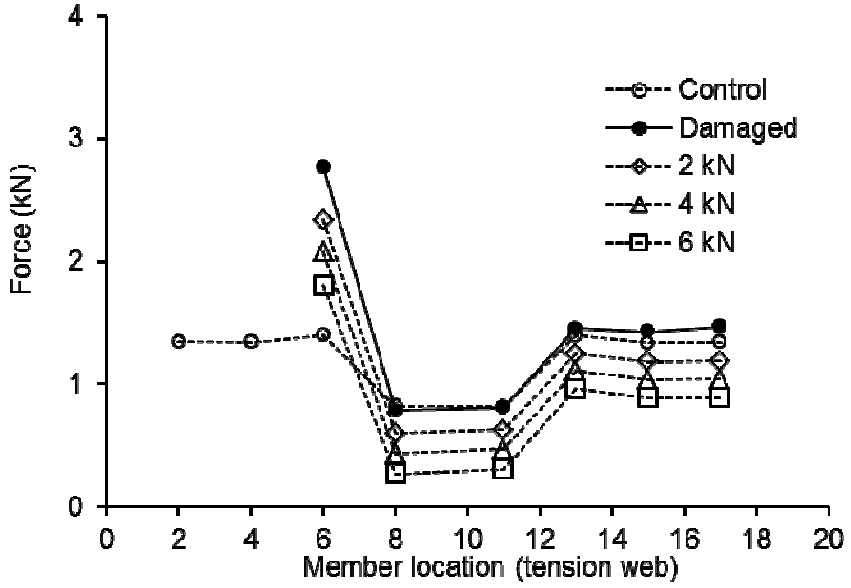

(c)

Fig. 4.11 Variation of forces in compression and tension members for truss 1 of damaged scenario 1_1: (a) member locations; (b) compression members; (c) tension members

Table 4.6 Strain distribution, compression webs, damage scenario 1_1.

Webs-Comp.	Control	Damaged		2 kN		4 kN		6 kN	
Member location	F (kN)	F (kN)	Delta	F (kN)	Δ^*	F (kN)	Δ^*	F (kN)	Δ^*
C 1	1.60	3.78	-136%	3.11	-94%	2.77	-73%	2.41	-51%
C 3	1.35	-	-	-	-	-	-	-	-
C 5	1.33	-	-	-	-	-	-	-	-
C 7	1.42	2.94	-107%	2.46	-73%	2.14	-51%	1.82	-29%
C 9	0.81	0.62	23%	0.64	21%	0.66	18%	0.69	15%
C 10	0.81	0.80	2%	0.80	2%	0.81	1%	0.82	0%
C 12	1.42	1.46	-3%	1.25	12%	1.09	24%	0.92	35%
C 14	1.34	1.41	-6%	1.19	11%	1.05	22%	0.90	32%
C 16	1.36	1.47	-8%	1.20	12%	1.05	23%	0.90	34%
C 18	1.60	1.78	-11%	1.44	10%	1.28	20%	1.12	30%

*Difference between the control and damaged/strengthened scenario for the numerical model.

Table 4.7 Strain distribution, tension webs, damage scenario 1_1.

Web-Tens.	Control	Damaged		2 kN		4 kN		6 kN	
Member location	F (kN)	F (kN)	Δ^*	F (kN)	Δ^*	F (kN)	Δ^*	F (kN)	Δ^*
T 2	-1.35	-	-	-	-	-	-	-	-
T 4	-1.34	-	-	-	-	-	-	-	-
T 6	-1.40	-2.77	-98%	-2.34	-67%	-2.08	-49%	-1.81	-29%
T 8	-0.82	-0.78	4%	-0.60	27%	-0.43	47%	-0.27	67%
T 11	-0.82	-0.81	1%	-0.63	23%	-0.47	42%	-0.31	62%
T 13	-1.40	-1.45	-4%	-1.25	11%	-1.11	21%	-0.96	31%
T 15	-1.34	-1.43	-7%	-1.18	12%	-1.04	22%	-0.89	34%
T 17	-1.34	-1.47	-10%	-1.19	12%	-1.04	23%	-0.89	34%

*Difference between the control and damaged/strengthened scenario for the numerical model.

information on the changes to web member forces for damage scenario 1_1. The distribution of force among truss members is a critical design parameter to consider as it dictates the required size, shape and orientation of the members in the truss system. Therefore when considering a retrofit for the purpose of strengthening a damaged truss system, a careful consideration of the redistribution of member forces should be performed so that existing truss members do not exceed their capacity.

4.7.4 System Redundancy

Truss performance and safety are primary concerns when evaluating the condition of

existing truss bridges. The redundancy of a truss system is an excellent measure to indicate the integrity of the structural system. Frangopol and Curley (1987) identified several definitions of redundancy. The reserve redundant factor, R_2, was defined as;

$$R_2 = \frac{L_{intact}}{L_{design}} = \lambda \tag{4.1}$$

for which L_{intact} is the design failure load of the intact bridge, L_{design} is the design load for the bridge and λ is a multiplier for the load that causes collapse of the intact bridge when compared to the design load. The residual redundant factor, R_3, was defined as

$$R_3 = \frac{L_{damaged}}{L_{intact}} \tag{4.2}$$

for which $L_{damaged}$ is the load capacity of the damaged bridge. The strength redundant factor, R_4, was defined as

$$R_4 = \frac{L_{intact}}{L_{intact} - L_{damaged}} = \frac{\lambda}{(\lambda - \alpha)} \tag{4.3}$$

for which, α, is a multiplier that corresponds to the collapse load for the damaged bridge. In order to apply this method to the numerical modeling procedure used for this work several adaptations were performed. In this work, α, is defined as

$$\alpha = (1 - \beta) \tag{4.4}$$

Also, this work replaced the term R_3 with a term referred to as the damage index, β, which was introduced to quantify the level of damage present for a specific damage scenario and could be experimentally calculated for the scale model bridge. This parameter was intended to determine the degree of strength reduction that occurs when a particular damage scenario is present. This term serves the same purpose as the R_3 term used by Frangopol and Curley (1987).

$$\beta = \frac{k'}{k} = \frac{TL_{damaged}/\delta_{damaged}}{TL_{control}/\delta_{control}} \tag{4.5}$$

The terms, $TL_{damaged}$ and $TL_{control}$ refer to the test load of the control bridge and the test load of the damaged bridge which were each taken to be 4.5 kN for the numerical model. The terms,

$\delta_{damaged}$ and $\delta_{control}$ refer to the deflection of the damaged bridge and the intact bridge where the damaged bridge deflection varied with each damage scenario and the control bridge deflection was numerically predicted to be 3.83 mm. For this work the intact failure load, L_{intact}, was determined to be 18.68 kN and the design load, L_{design}, was chosen to be 11.12 kN. Tables 8, 9 and 10 summarize the redundancy results for post-tension loads of 2 kN, 4 kN and 6 kN. Using this method when the system has no reserve strength, R_4 is equal to 1 and when the system's reserve strength is not influenced by damage, R_4 is infinite. When using this method, a negative

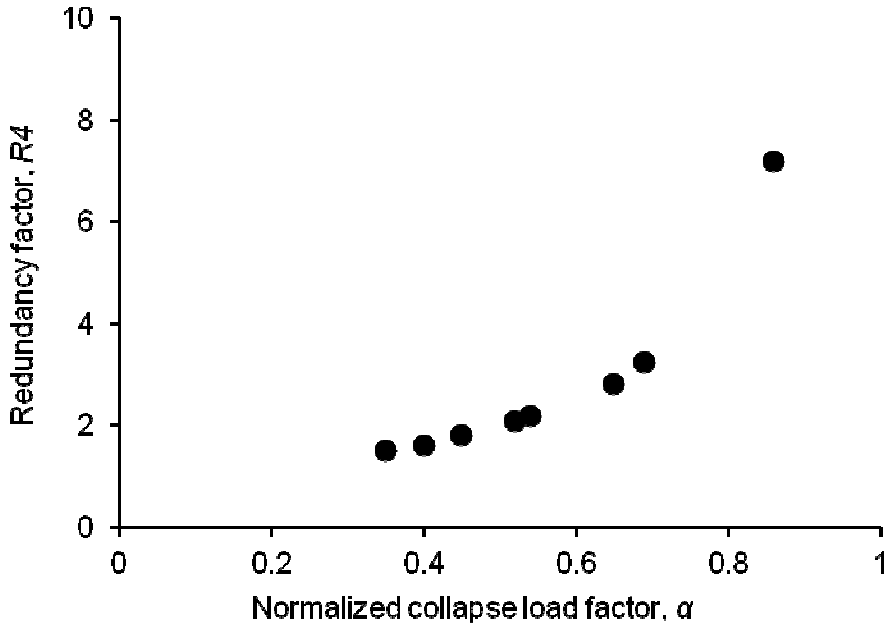

Fig. 4.12 Redundancy factor shown for various collapse load factors shown in Tables 4.11- 4.13

value for the damage index β resulted in the strength redundant factor, R_4 yielding an infinite value and was represented in the tables as a value of 10000. Tables 8, 9 and 10 summarize the redundancy factors. Figure 12 shows a plot of the strength redundant factor with the collapse load factor, α. Here we see that with increasing post tension levels for a given damage scenario, R_4 increases. The increase in the strength redundant factor is dependent upon the degree of damage present. For one of the most severe damage scenarios, for example Specimen ID 4, the

presence of damage in truss 1 is so severe that the change in the strength redundant factor is minimal when post-tensioning is increased from 2 to 6 kN. Whereas for a less severe damage location such as Specimen ID 2, the strength redundancy is recovered to an acceptable level between post-tensioning loads of 4 and 6 kN. These results were typical for other damage scenarios and indicate that for less severe damage scenarios this method of strengthening could prove beneficial.

Table 4.8 Summary of redundancy factor for 2kN of post-tensioning

Specimen ID	Damage Scenario	Truss 1			Truss 2		
Control	None	β	α	$R4^*$	β	α	$R4^*$
1	1_1	0.55	0.45	1.80	-0.10	1.10	10000
2	1_2	0.35	0.65	2.82	0.00	1.00	10000
3	1_3	0.36	0.64	2.81	-0.01	1.01	10000
4	1_1 & 1_3	0.67	0.33	1.50	0.01	0.99	124.55
5	1_1 & 1_4	0.73	0.27	1.37	0.01	0.99	67.03
6	1_1 & 2_1	0.56	0.44	1.78	0.62	0.38	1.60
7	1_1 & 2_2	0.56	0.44	1.80	0.49	0.51	2.05
8	1_1 & 2_3	0.56	0.44	1.80	0.49	0.51	2.06
9	1_1 & 2_4	0.56	0.44	1.79	0.62	0.38	1.60
10	1_2 & 2_2	0.36	0.64	2.80	0.48	0.52	2.07
11	1_2 & 2_3	0.36	0.64	2.81	0.48	0.52	2.07
12	1_1, 2_1 & 2_3	0.56	0.44	1.78	0.72	0.28	1.39
13	1_1, 2_1 & 2_4	0.57	0.43	1.77	0.77	0.23	1.31
14	1_2, 2_1 & 2_3	0.36	0.64	2.74	0.72	0.28	1.39
15	1_2, 2_1 & 2_4	0.37	0.63	2.71	0.76	0.24	1.31
16	1_3, 2_1 & 2_3	0.36	0.64	2.74	0.72	0.28	1.39

4.7.5 Dynamic Behavior

In accordance with Zein and Gassman (2010) using a numerical model to perform a dynamic analysis is a reasonable procedure if the model has been previously validated using a static analysis first. Based on the assumption that the previous, *Static Behavior*, discussion was valid the following presents the results of a dynamic analysis which assumed the same loading conditions. Here the CFRP was included in the physical model in order to account for its

interaction with the existing truss members under dynamic conditions.

Table 4.9 Summary of redundancy factor for 4kN of post-tensioning

Specimen ID	Damage Scenario	Truss 1			Truss 2		
Control	None	β	α	R4*	β	α	R4*
1	1_1	0.46	0.54	2.18	-0.11	1.11	10000
2	1_2	0.14	0.86	7.18	-0.01	1.01	10000
3	1_3	0.14	0.86	7.11	-0.01	1.01	10000
4	1_1 & 1_3	0.60	0.40	1.67	0.00	1.00	426.56
5	1_1 & 1_4	0.68	0.32	1.46	0.01	0.99	117.06
6	1_1 & 2_1	0.47	0.53	2.13	0.62	0.38	1.61
7	1_1 & 2_2	0.46	0.54	2.16	0.48	0.52	2.06
8	1_1 & 2_3	0.46	0.54	2.16	0.48	0.52	2.06
9	1_1 & 2_4	0.47	0.53	2.14	0.622	0.38	1.61
10	1_2 & 2_2	0.14	0.86	6.91	0.482	0.52	2.07
11	1_2 & 2_3	0.14	0.86	7.03	0.482	0.52	2.07
12	1_1, 2_1 & 2_3	0.47	0.53	2.12	0.718	0.28	1.39
13	1_1, 2_1 & 2_4	0.48	0.52	2.10	0.765	0.24	1.31
14	1_2, 2_1 & 2_3	0.16	0.84	6.38	0.717	0.28	1.39
15	1_2, 2_1 & 2_4	0.17	0.83	6.03	0.764	0.24	1.31
16	1_3, 2_1 & 2_3	0.16	0.84	6.32	0.717	0.28	1.39

4.7.5.1 Mode shape

RISA 3-D was used to perform a dynamic analysis of the control, damaged and subsequently strengthened bridge conditions. Mode shapes were generated for the control, the damaged, and the three levels of post-tensioning that were used to strengthen the bridge. Fig. 4.13 compares the first four modes of the control bridge to the equivalent modes of the damaged and strengthened bridge for specimen 1. This figure illustrates that equivalent mode shapes will change mode number when the stiffness of the truss system is altered and the load paths are changed. The mode shape of lower modes such as 1 and 2 were relatively unchanged by the presence of either damage or strengthening, however for higher order modes such as modes 3 and 4 greater differences were observed in the mode shape of equivalent modes. Fig. 4.13 shows that mode 1 represents lateral sway and mode 2 represents a longitudinal shift which is

Table 4.10 Summary of redundancy factor for 6kN of post-tensioning

Specimen ID	Damage Scenario	Truss 1			Truss 2		
Control	None	β	α	R4*	β	α	R4*
1	1_1	0.31	0.69	3.25	-0.11	1.11	10000
2	1_2	-0.31	1.31	10000	-0.01	1.01	10000
3	1_3	-0.31	1.31	10000	-0.01	1.01	10000
4	1_1 & 1_3	0.48	0.52	2.08	0.00	1.00	10000
5	1_1 & 1_4	0.62	0.38	1.62	0.00	1.00	548.14
6	1_1 & 2_1	0.32	0.68	3.10	0.62	0.38	1.61
7	1_1 & 2_2	0.31	0.69	3.18	0.48	0.52	2.07
8	1_1 & 2_3	0.31	0.69	3.19	0.48	0.52	2.07
9	1_1 & 2_4	0.32	0.68	3.11	0.620	0.38	1.61
10	1_2 & 2_2	-0.30	1.30	10000	0.481	0.52	2.08
11	1_2 & 2_3	-0.31	1.31	10000	0.481	0.52	2.08
12	1_1, 2_1 & 2_3	0.33	0.67	3.05	0.717	0.28	1.39
13	1_1, 2_1 & 2_4	0.34	0.66	2.98	0.764	0.24	1.31
14	1_2, 2_1 & 2_3	-0.27	1.27	10000	0.716	0.28	1.40
15	1_2, 2_1 & 2_4	-0.25	1.25	10000	0.763	0.24	1.31
16	1_3, 2_1 & 2_3	-0.27	1.27	10000	0.717	0.28	1.40

*Note: A redundancy factor R4=1/β of 10000 signifies that the damage deflection was less than the control bridge.

independent of the bridge condition. At modes 3 and 4 of the control truss, which correspond to twist about the center of the bridge and camber of the truss, changes were observed to the mode number for the equivalent mode shape. These changes at higher order modes are a result of the changed stiffness of the system and the force distribution amongst truss elements when the post-tensioning system is applied. The sensitivity of the bridge to changes is confirmed by the frequency changes as discussed in the next section.

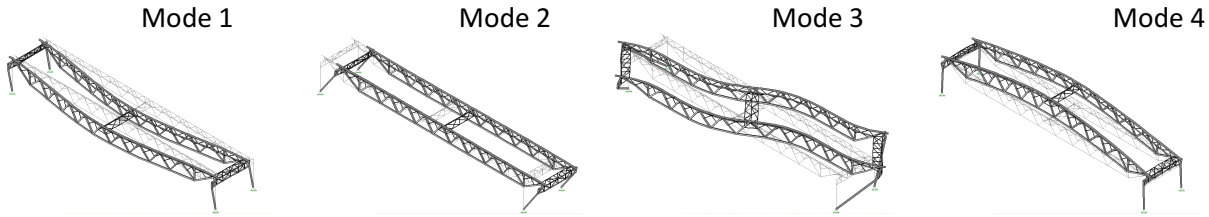

(a)

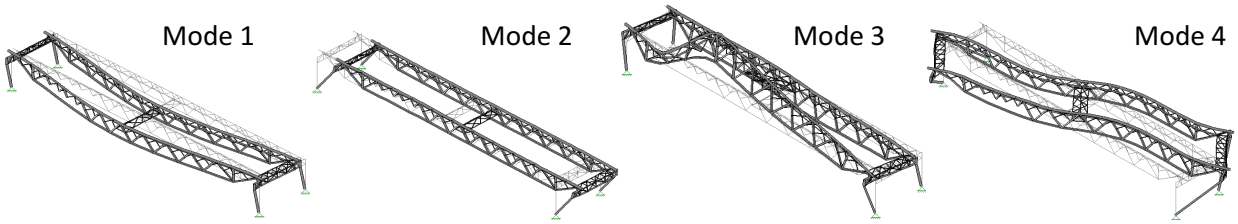
Mode 1
Mode 2
Mode 3
Mode 4

(b)

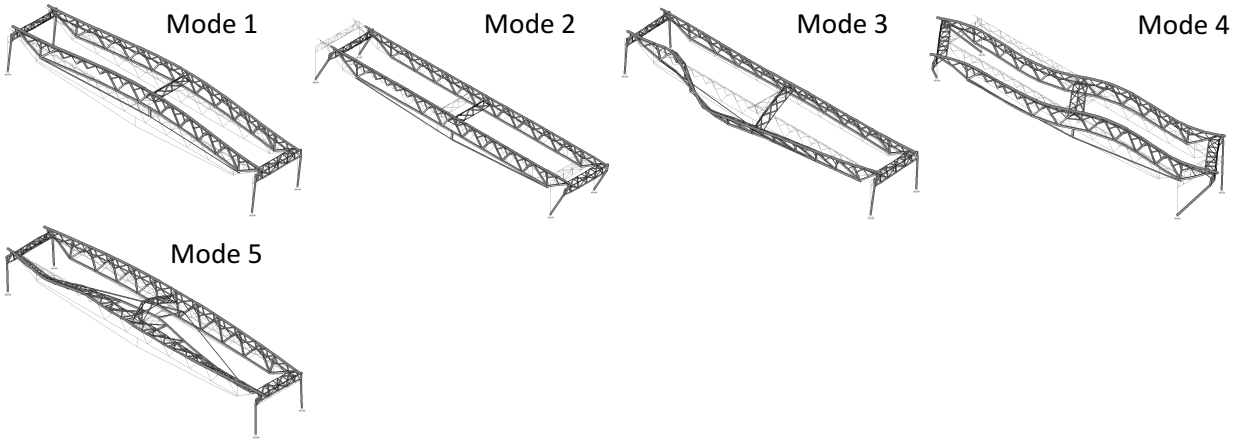
Mode 1
Mode 2
Mode 3
Mode 4
Mode 5

(c)

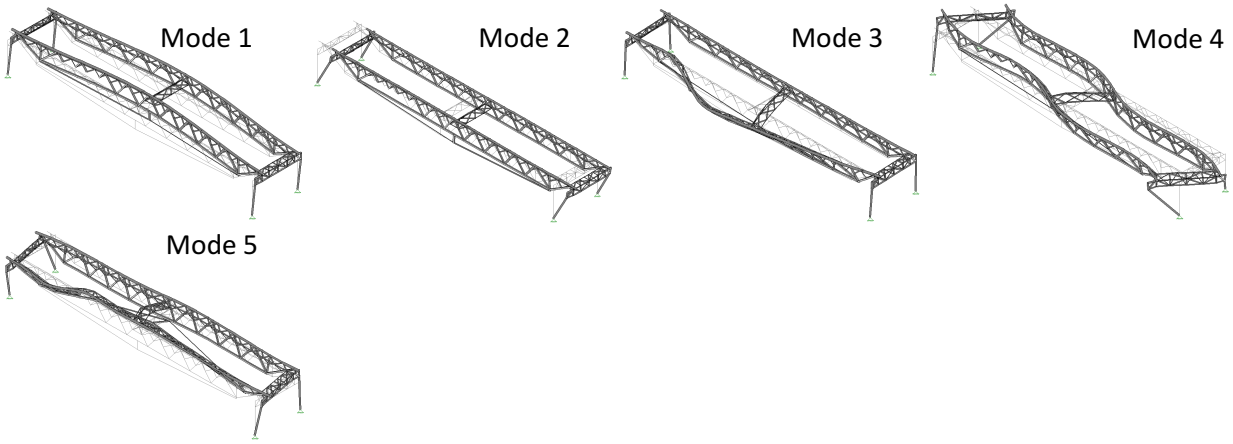
Mode 1
Mode 2
Mode 3
Mode 4
Mode 5

(d)

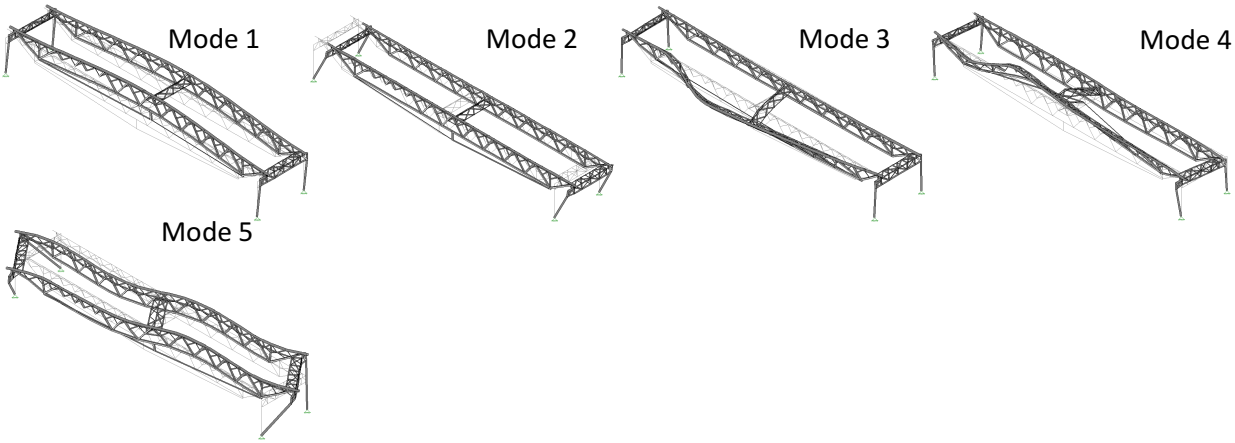
Mode 1
Mode 2
Mode 3
Mode 4
Mode 5

(e)

Fig. 4.13 Comparison of mode shapes: (a) control; (b) damaged (Specimen 1); (c) 2 kN strengthened (Specimen 1); (d) 4 kN strengthened (Specimen 1); (e) 6 kN strengthened (Specimen 1)

4.7.5.2 Frequency

The detection of damage by changes to the bridge frequency has potential to be a useful tool as frequency can be measured quickly and it can provide reliable results. The use of frequency as a method for damage detection is a reasonable method because of the principles that govern the frequency of a structure. The structural frequency (f) relates directly to the stiffness of the system (k_e) and inversely to the mass of the system (m):

$$f = 2\pi\sqrt{\frac{k_e}{m}} \tag{4.6}$$

Table 4.11 Frequency of Trusses - 2kN

Specimen ID		Mode and frequency							
		1		2		3		4	
		Hz	Δ^a	Hz	Δ^a	Hz	Δ^a	Hz	Δ^a
Control		0.94	-	1.41	-	5.28	-	8.17	-
Strengthened: (2 kN)	1	0.95	-1.2%	1.47	-4.5%	5.3	-0.3%	5.78	29.2%
	2	0.95	-1.2%	1.47	-4.5%	5.57	-5.6%	5.9	27.8%
	3	0.95	-1.2%	1.47	-4.5%	5.27	0.2%	5.78	29.3%
	4	0.95	-0.9%	1.47	-4.5%	4.6	13.0%	5.6	31.4%
	5	0.95	-0.9%	1.47	-4.5%	4.3	18.6%	5.77	29.3%
	6	0.92	1.7%	1.44	-1.8%	5.15	2.5%	5.3	35.1%
	7	0.92	1.7%	1.44	-1.8%	5.17	2.2%	5.49	32.8%
	8	0.92	1.7%	1.44	-1.8%	5.2	1.6%	5.45	33.2%
	9	0.92	1.7%	1.44	-1.8%	5.16	2.3%	5.29	35.2%
	10	0.92	1.7%	1.44	-1.8%	5.23	1.0%	5.67	30.6%
	11	0.92	1.7%	1.44	-1.8%	5.27	0.1%	5.6	31.5%
	12	0.92	2.0%	1.43	-1.7%	4.53	14.2%	5.22	36.1%
	13	0.92	1.9%	1.43	-1.7%	4.24	19.7%	5.22	36.1%
	14	0.92	2.0%	1.43	-1.7%	4.53	14.3%	5.27	35.5%
	15	0.92	2.0%	1.43	-1.7%	4.24	19.7%	5.45	33.3%
	16	0.92	2.0%	1.43	-1.7%	4.53	14.3%	5.28	35.4%

Table 4.12 Frequency of Trusses - 4kN

Specimen ID		Mode and frequency							
		1		2		3		4	
		Hz	Δ^a	Hz	Δ^a	Hz	Δ^a	Hz	Δ^a
Control		0.94	-	1.41	-	5.28	-	8.17	-
Strengthened: (4 kN)	1	0.93	1.4%	1.44	-1.9%	4.83	8.5%	5.67	30.7%
	2	0.93	1.5%	1.44	-1.9%	4.75	10.0%	5.58	31.7%
	3	0.93	1.4%	1.44	-1.9%	4.79	9.4%	5.66	30.7%
	4	0.92	1.7%	1.44	-1.8%	4.2	20.5%	5.14	37.1%
	5	0.92	1.7%	1.44	-1.8%	4.01	24.1%	5.66	30.7%
	6	0.88	6.3%	1.37	3.0%	4.55	13.8%	5.05	38.2%
	7	0.88	6.3%	1.37	3.0%	4.49	14.9%	5.01	38.6%
	8	0.88	6.3%	1.37	3.0%	4.53	14.2%	4.98	39.1%
	9	0.88	6.3%	1.37	3.0%	4.56	13.7%	5.04	38.4%
	10	0.88	6.4%	1.37	3.0%	4.52	14.5%	4.82	41.0%
	11	0.88	6.3%	1.37	3.0%	4.61	12.8%	4.66	43.0%
	12	0.88	6.5%	1.37	3.0%	4.1	22.4%	4.79	41.4%
	13	0.88	6.5%	1.37	3.0%	3.91	25.9%	4.81	41.1%
	14	0.88	6.6%	1.37	3.0%	4.09	22.5%	4.59	43.8%
	15	0.88	6.5%	1.37	3.0%	3.9	26.2%	4.85	40.6%
	16	0.88	6.6%	1.37	3.0%	4.08	22.8%	4.8	41.2%

*Note: The table depicts frequencies of damage and strengthened scenarios which correlate with the control bridge's first four modes.

The results of this work indicate that the stiffness of a strengthened truss bridge is unaffected by the application of the proposed strengthening scheme. This results in relatively unchanged frequencies for the strengthened scenarios when compared to the damaged scenarios. The results, shown in Tables 4.11-4.13, identify that the frequency of a strengthened truss decreases indicating that the stiffness of the truss is reduced with increasing levels of post-tension. These results are graphically depicted with Fig. 4.13. Based on the static results, cumulative deflection increases at higher post-tension levels. This is evident by the difference between camber and deflection under applied load. This increased cumulative deflection indicates a decrease in truss stiffness. These results indicate that measuring frequency to detect the recovery of system

Table 4.13 Frequency of Trusses - 6kN

Specimen ID		Mode and frequency							
		1		2		3		4	
		Hz	Δ^a	Hz	Δ^a	Hz	Δ^a	Hz	Δ^a
Control		0.94	-	1.41	-	5.28	-	8.17	-
Strengthened: (6 kN)	1	0.9	3.9%	1.4	0.6%	4.35	17.6%	5.4	34.0%
	2	0.9	3.9%	1.4	0.6%	4.07	23.0%	5.46	33.2%
	3	0.9	3.9%	1.4	0.6%	4.3	18.5%	5.41	33.8%
	4	0.9	4.3%	1.4	0.7%	3.78	28.4%	4.65	43.1%
	5	0.9	4.1%	1.4	0.7%	3.74	29.1%	5.06	38.1%
	6	0.84	10.4%	1.31	7.2%	4.11	22.1%	4.52	44.7%
	7	0.84	10.4%	1.31	7.2%	3.93	25.6%	4.34	46.9%
	8	0.84	10.4%	1.31	7.2%	3.96	25.1%	4.33	47.0%
	9	0.84	10.4%	1.31	7.2%	4.11	22.1%	4.52	44.7%
	10	0.84	10.5%	1.31	7.2%	3.97	24.8%	3.99	51.2%
	11	0.84	10.5%	1.31	7.2%	3.88	26.5%	4.08	50.1%
	12	0.84	10.6%	1.31	7.2%	3.71	29.7%	4.19	48.8%
	13	0.84	10.5%	1.31	7.2%	3.63	31.3%	4.5	44.9%
	14	0.84	10.6%	1.31	7.2%	3.72	29.6%	3.87	52.6%
	15	0.84	10.6%	1.31	7.2%	3.59	32.0%	4.14	49.3%
	16	0.84	10.6%	1.31	7.2%	3.69	30.2%	3.98	51.3%

*Note: The table depicts frequencies of damage and strengthened scenarios which correlate with the control bridge's first four modes.

reliability may not be an effective method for this proposed strengthening method. However, since the purpose of the strengthening technique is to increase the load capacity and provide alternative load paths this proposed strengthening method is still valid.

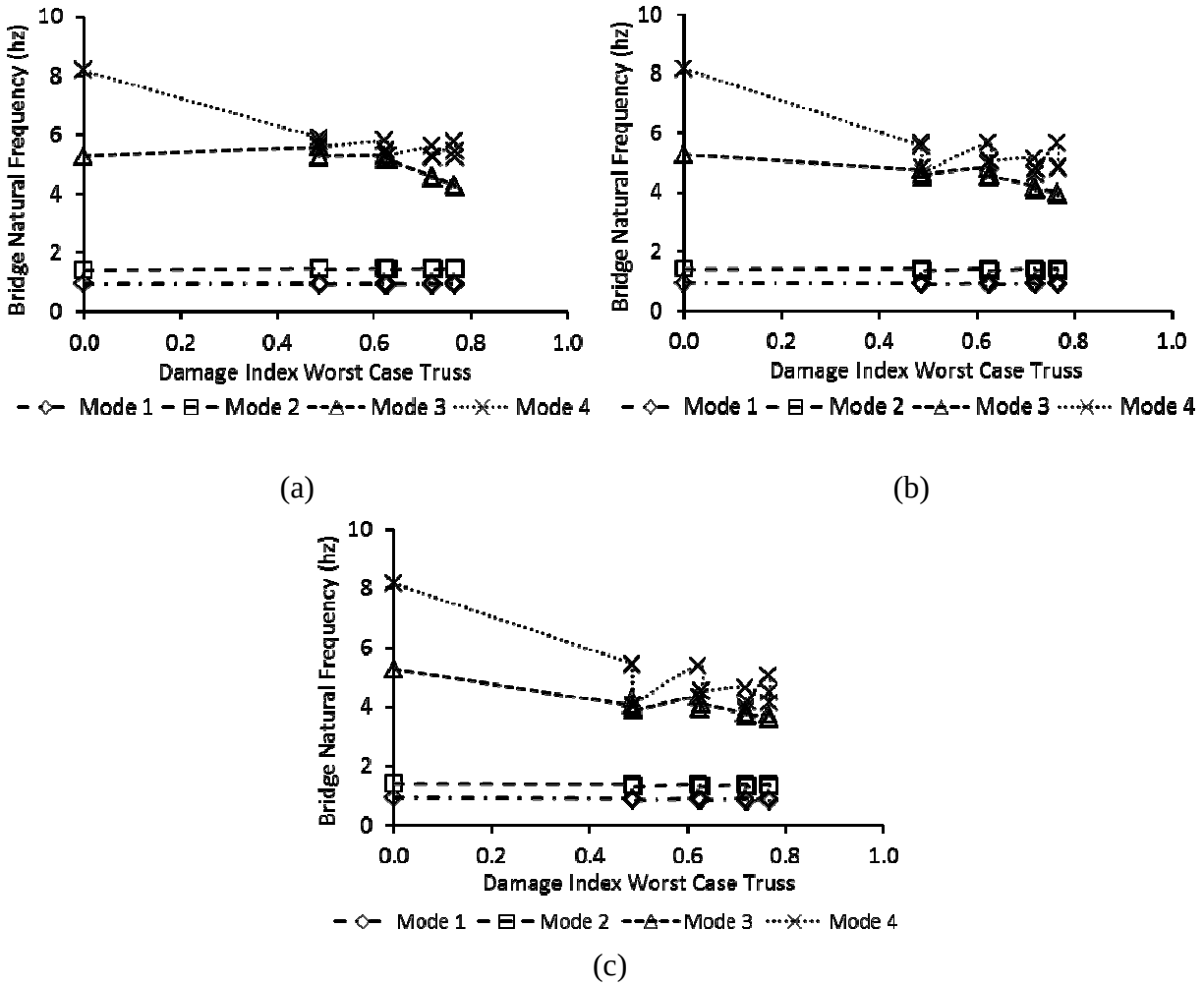

Fig. 4.14 Natural frequency response with the worst case damage index: (a) 2kN (b) 4kN (c) 6kN

4.8 SUMMARY AND CONCLUSIONS

An examination was performed to determine the effect that a novel approach to strengthening a damaged steel truss bridge has on the overall performance of the structure. To perform the examination a scale model bridge was experimentally tested and a numerical model was used to validate the results. Once the static response parameters of the experimental tests were validated with the numerical model, the numerical model was extended to further examine the relationship between the strengthening technique and the susceptibility of the bridge to failure. In total, 16 damage scenarios were tested and then each scenario was strengthened using

three levels of post-tensioning, 2 kN, 4 kN and 6 kN. The static analysis was used to evaluate; 1) a damage index which quantified the level of damage that was present, 2) the transfer of load between members when post-tensioning was applied and 3) the reliability of the bridge during various conditions. In addition to the static analysis, a dynamic analysis was conducted using the numerical model to determine the effects of strengthening on the mode shapes and mode frequencies. The following was concluded:

- The damage index revealed that the proposed strengthening method was successful in reducing overall truss deflection for any degree of localized damage.
- The ability to control member forces in the presence of damage was most significantly illustrated by members adjacent to the location of damage. These members experienced the greatest degree of force redistribution; however it is not always an increase in member force that occurs when a member is damaged.
- The reliability of a truss subject to the proposed strengthening scheme is influenced by both the level of damage present and the level of post-tensioning applied. With an appropriately selected level of post-tensioning the reliability of a damaged truss bridge can be increased. Less severe levels of damage, as indicated by the damage index, respond more favorably to the proposed strengthening method.
- Extreme damage conditions where multiple web members were severely damaged pose the greatest risk for system reliability. Damage locations 1 and 4 were of primary concern. Damage to interior truss web members had less influence on the overall performance of the system.
- Higher order modes are more susceptible to changes in frequency when damage is present and when this strengthening system was applied. The externally post-tensioned

CFRP did not influence the frequency variation because the contribution of the CFRP to the global stiffness of the system was not significant.

CHAPTER 5. SUMMARY AND CONCLUSIONS

5.1 INTRODUCTION

An experimental investigation was performed to confirm the results of a numerical model. The investigation considered the effects of localized damage and a subsequent strengthening technique on the performance of the structural system. A static analysis was performed on the experimental steel truss bridge which evaluated the truss deflection at midspan and member strain for the various truss conditions. In total 16 damage conditions were evaluated and 3 levels of post-tensioning were considered for their effect on recovering the performance of the bridge when damage was present. The following summarizes the results:

5.2 SUMMARY

- Localized truss damage greatly effects the serviceability of the bridge as truss deflection was found to increase exponentially for damage indices greater than 0.5. With the application of an externally draped post-tensioned strengthening system it is possible to control the service deflection and recover the degree of damage, as represented by the damage index. The level of applied post-tension was found to correlate directly with the amount of deflection that was recovered.
- Current methods of load rating bridges as outlined by AASHTO approximated the results form numerical modeling with reasonable accuracy. An inventory rating greater than 1.5 was recommended to provide safe operation of truss bridges.
- Member force was redistributed to members adjacent to the location of damage as represented by the member safety index. Similarly, the element strain energy was determined to increase in members adjacent to the location of damage. The proposed strengthening system was found to reduce overall member forces and thereby effectively

reduce member strain energy. This result is useful for both damaged and undamaged truss systems.

- A dynamic analysis was determined to provide an indication of change to the stiffness of the structural system which could be useful for detecting the presence of damage. Higher order modes showed a greater sensitivity to stiffness changes which was evident by the change in frequency and mode shape. The numerical model predicted changes to natural frequency which correlated well with the damage index for damaged conditions. The results of a dynamic analysis for the strengthened truss revealed that the strengthening system does not provide additional stiffness to the system as the system frequency was found to decrease with increasing post-tension loads. This result was consistent with the static analysis which revealed that the truss stiffness was slightly reduced with increasing levels of post-tension.

5.3 CONCLUSIONS

Steel truss bridges have inherent deficiencies when it comes to retaining load carrying capacity when local web members are damaged. Generally speaking, most truss designs lack the redundancy within their structural system to sustain a working load if any of the component elements sustains a fatal degree of deterioration. However, heavy class trusses which can support moment transfer across member connections do have an inherent greater degree of system redundancy when compared to light class trusses which completely lack redundancy. The level of system redundancy can be effectively increased by applying the proposed strengthening system and adjusting the level of applied post-tensioning force. With this process member forces can be adjusted as the load distribution can be altered. The proposed strengthening system has several advantages for repairing damaged and deficient steel truss bridges, however there is still

future work that needs to be completed for this strengthening technique to be applied in full scale applications.

5.4 RECOMMENDATIONS FOR FUTURE WORK

This work has proposed several methods for analyzing the issues associated with damaged steel truss bridges. It also examined a proposed strengthening technique using a state of the art construction material. The scope of the findings was however superficial in determining detailed facts about the issues that are associated with the problems which aging steel truss bridges face. In light of the previous fact much work is still required to determine the efficacy of the proposed strengthening method as a probable means of strengthening existing steel truss bridges. Some of the proposed future work should include the following:

- A more detailed investigation as to the effects that load transfer between trusses has on performance of an undamaged truss when the adjacent truss incurs damage. This effect was not effectively considered with the modeling technique used for this work. A more thorough modeling process to account for load transfer and truss interaction would no doubt improve the accuracy of the model.
- Refinement of a technique which is suitable for comparing data that is quantifiable with field measuring processes to the output capabilities of the numerical modeling procedure. In addition to a more refined process, a unified technique that would be applicable for both un-strengthened and strengthened truss scenarios would be ideal.
- Further investigation as to the effect that strengthening has on the natural frequency of the bridge. This work indicated that with increased post-tension levels the natural frequency decreased which indicates a reduction in system stiffness. Further testing to confirm these effects would be required.

- Additional experimental testing of the proposed strengthening technique on damage scenarios where all truss elements are in place and the individual local member capacities are slightly reduced by a decreased member cross section would better approximate field conditions which are much more likely to occur.
- Finally, design guidelines and codes must be formulated to govern the criteria required for analysis and design of the proposed externally draped post-tensioning technique using carbon fiber reinforced polymer tendons.

REFERENCES

AASHTO. 1989. Guide specifications for strength evaluation of existing steel and concrete bridges, American Association of State Highway and Transportation Officials, Washington, D.C.

AASHTO. 2003. Manual for condition evaluation of bridges (2003 interim revisions), American Association of State Highway and Transportation Officials, Washington, D.C.

Alampalli, S. and Kunin, J. 2003. Load testing of an FRP bridge deck on a truss bridge, Applied Composite Materials, 10, 85-102.

Albrect, P and Lenwan, A. 2008. Design of prestressing tendons for strengthening steel truss bridges, Journal of Bridge Engineering, 13(5), 449-454

ASCE. 2010. Report card for America's infrastructure, American Society of Civil Engineers, Reston, VA.

Ayyub, B.M., Ibrahim, A. Schelling, D. 1990. Post-tensioned trusses: analysis and design, Journal of Structural Engineering, 116(6), 1491-1506

Ayyub, B.M. and Ibrahim, A. 1990. Post-tensioned trusses: reliability and redundancy, Journal of Structural Engineering, 116(6), 1507-1521

Azizinamini, A. 2002. Full scale testing of old steel truss bridge, Journal of Constructional Steel Research, 58, 843-858.

Bakis, C.E., Bank, L. C., Brown, V. L. Consenza, E., Davalos, J. F., Lesko, J. J., Machida, A., Rizkalla, S. H., Triantafillou, T. C. 2002. Fiber-Reinforced polymer composites for construction - state-of-the-art review, Journal of Composites for Construction, 6(2), 73-87.

Csagoly, P.F. and Jaeger, L.G. 1979. Multi-load-path structures for highway bridges, Transportation Research Board 711, National Academy of Sciences, Washington D.C.

Frangopol, D. M. and Curley, J.P. 1987. Effects of damage and redundancy on structural reliability, Journal of Structural Engineering, 113(7), 1533-1539.

Ghosn, M. and Moses, F. 1998. Redundancy in highway bridge superstructures (NCHRP 406), Transportation Research Board, Washington, D.C.

Han, B. K. and Park S. K. 2005. Parametric study of truss bridges by the post-tensioning method, Canadian Journal of Civil Engineering, 32, 420-429

Hao, S. 2010. I-35W bridge collapse, Journal of Bridge Engineering, 15(5), 608-614.

Hickey, L., Roberts-Wollmann, C., Cousons, T., Sotelino, E., and Easterling, W.S. 2009. Live load test and failure analysis for the steel deck truss bridge over the New River in Virginia, Final Contract Report FHWA/VTRC 09-CR8, Virginia Transportation Research Council, Charlottesville, VA.

Hollaway, L.C. and Cadei, J. 2002. Progress in the technique of upgrading metallic structures with advanced polymer composites. Progress in Structural Engineering and Materials, 4, 131-148

Kim, Y.J., Green M.F., and Fallis G.J. 2008. Repair of Bridge Girder Damaged by Impact Loads with Prestressed CFRP Sheets. Journal of Bridge Engineering. 13(1). 15-23.

Kim, Y.J., Green, M.F. and Wight, G.R. 2008. Live load distributions on an impact-damaged prestressed concrete girder bridge repaired using prestressed CFRP sheets, Journal of Bridge Engineering, 13(2), 202-210.

Kim, Y.J. and Harries, Kent, A. 2012. Predictive response of notched steel beams repaired with CFRP strips including bond-slip behavior, International Journal of Structural Stability and Dynamics.

Kim, Y.J. and Harries, K.A. 2010. Modeling of timber beams strengthened with various CFRP composites, Engineering Structures, 32, 3225-3234.

Kim, Y. J. and Yoon, D. K. 2010. Identifying critical sources of bridge deterioration in cold regions through the constructed bridges in North Dakota, Journal of Bridge Engineering, 15(5), 542-552.

Lenett, M., Hunt, V., Helmicki, A., and Turer, A. 2001. Field testing and evaluation of the Ironton-Russsell truss bridge, Proceedings of Structures Congress, ASCE, Washington, D.C.

MacDougall, C., Green, M. and Amato, L. 2010. CFRP tendons for the repair of post-tensioned unbounded concrete buildings, Journal of Performance of Constructed Facilities.

Nagavi, R. S. and Aktan, A. E. 2003. Nonlinear behavior of heavy class steel truss bridges, Journal of Structural Engineering, 129(8), 1113-1121.

Nowak, A.S. 1993. Calibration of LRFD bridge design code, NCHRP Report 12-33, Transportation Research Board, Washington, D.C.

Nowak, A.S. 1995. Calibration of LRFD bridge code, Journal of Structural Engineering, 121(8), 1245-1251.

Pandey, P.C. and Barai, S.V. 1997. Structural sensitivity as a measure of redundancy, Journal of Structural Engineering, 360-364.

Salawu, O.S. 1997. Detection of structural damage through changes in frequency: a review, Engineering Structures, 19(9), 718-723

Teng, J.G., Chen, J.F., Smith, S.T., and Lam, L. 2003. Behaviour and strength of FRP-strengthened RC structures: a state-of-the-art review, Structures and Buildings, 156(1), 51-62.

Zein, A. S. and Gassman, S.L. 2010. Frequency spectrum analysis of impact-echo waveforms for T-beams, Journal of Bridge Engineering, 15(6), 705-714.

Zhao, X.L., and Zhang, L. 2006. State-of-the-art review on FRP strengthened steel structures, Engineering Structures, 29, 1808-1823.

APPENDIX A. BRIDGE MODE SHAPES

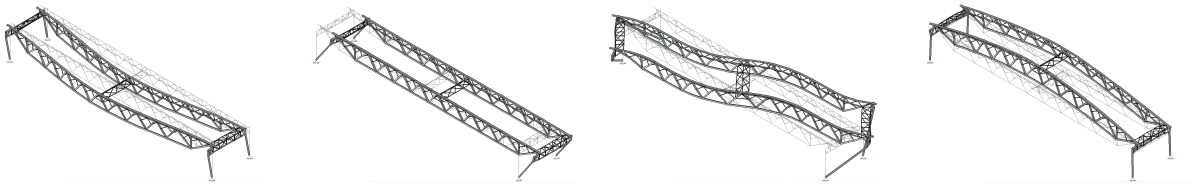

(a) (b) (c) (d)

Fig. A.1 Mode shape of control truss during service load level of 4.45 kN: (a) mode 1; (b) mode 2; (c) mode 3; (d) mode 4

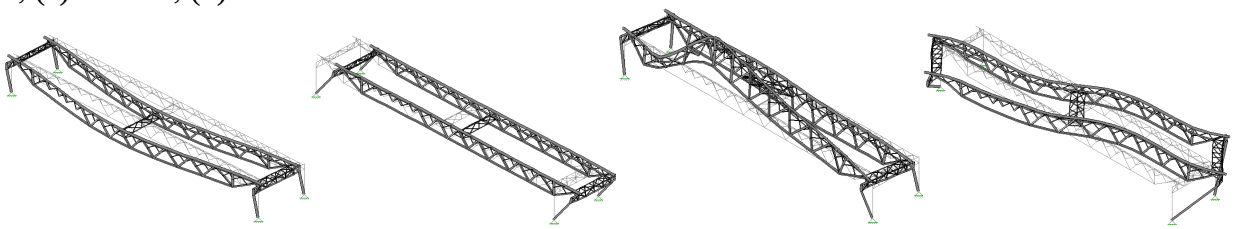

(a) (b) (c) (d)

Fig. A.2 Mode shapes of damaged truss during service load level of 4.45 kN (Specimen 1): (a) mode 1; (b) mode 2; (c) mode 3; (d) mode 4

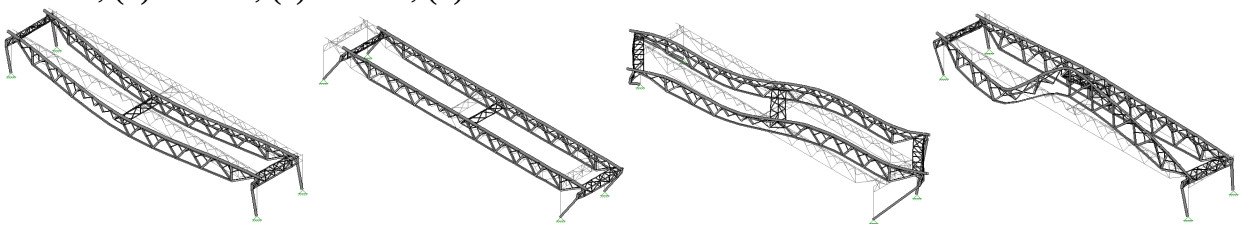

(a) (b) (c) (d)

Fig. A.3 Mode shapes of damaged truss during service load level of 4.45 kN (Specimen 2): (a) mode 1; (b) mode 2; (c) mode 3; (d) mode 4

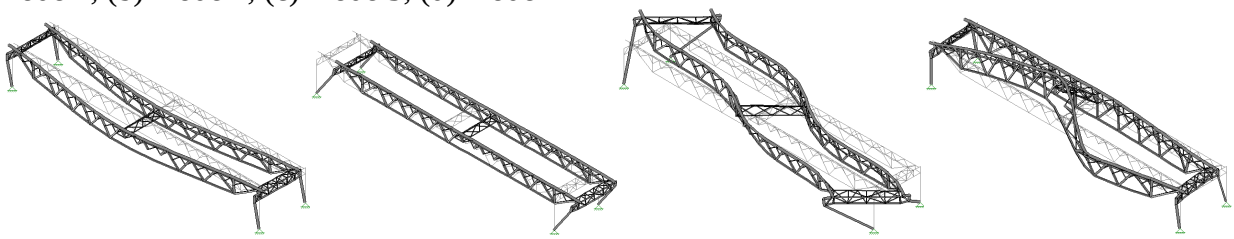

(a) (b) (c) (d)

Fig. A.4 Mode shapes of damaged truss during service load level of 4.45 kN (Specimen 3): (a) mode 1; (b) mode 2; (c) mode 3; (d) mode 4

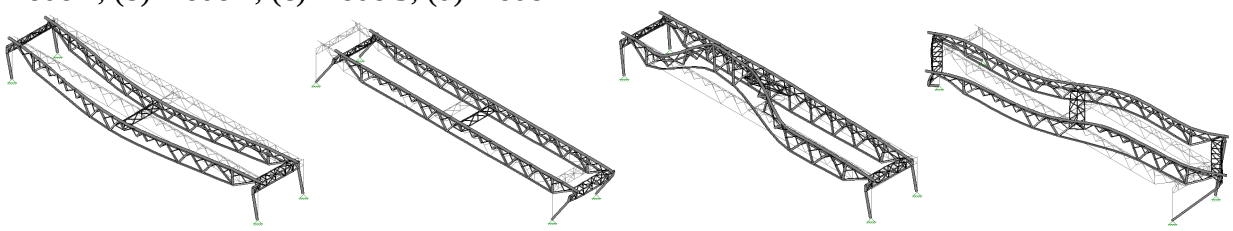

(a) (b) (c) (d)

Fig. A.5 Mode shapes of damaged truss during service load level of 4.45 kN (Specimen 4): (a) mode 1; (b) mode 2; (c) mode 3; (d) mode 4

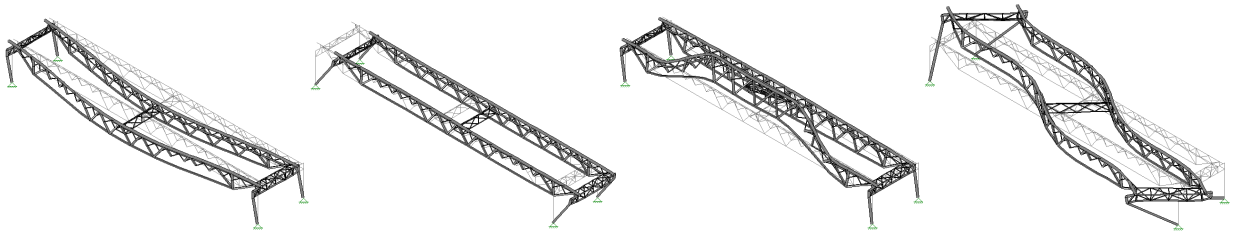

(a) (b) (c) (d)

Fig. A.6 Mode shapes of damaged truss during service load level of 4.45 kN (Specimen 5): (a) mode 1; (b) mode 2; (c) mode 3; (d) mode 4

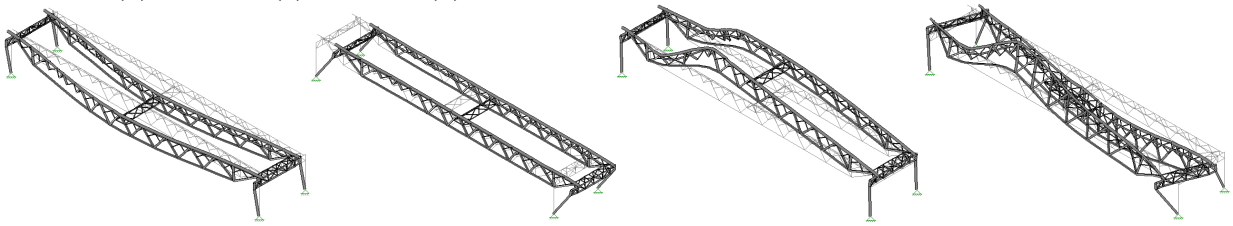

(a) (b) (c) (d)

Fig. A.7 Mode shapes of damaged truss during service load level of 4.45 kN (Specimen 6): (a) mode 1; (b) mode 2; (c) mode 3; (d) mode 4

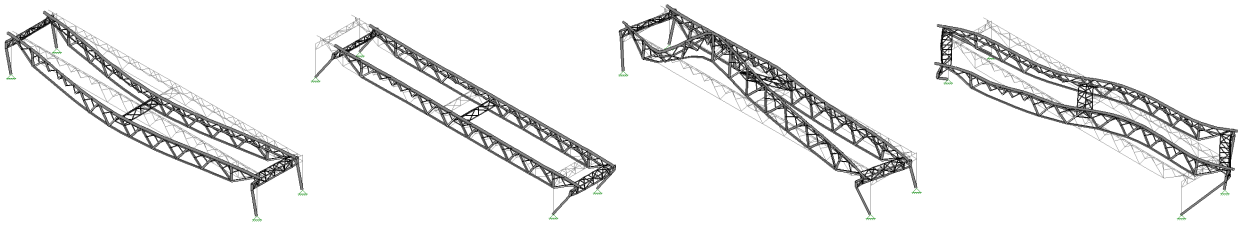

(a) (b) (c) (d)

Fig. A.8 Mode shapes of damaged truss during service load level of 4.45 kN (Specimen 7): (a) mode 1; (b) mode 2; (c) mode 3; (d) mode 4

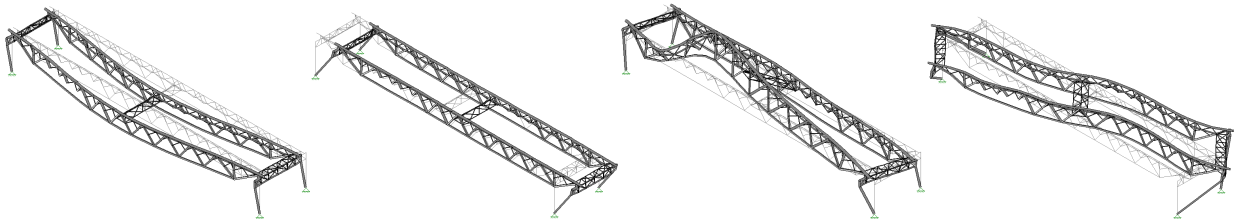

(a) (b) (c) (d)

Fig. A.9 Mode shapes of damaged truss during service load level of 4.45 kN (Specimen 8): (a) mode 1; (b) mode 2; (c) mode 3; (d) mode 4

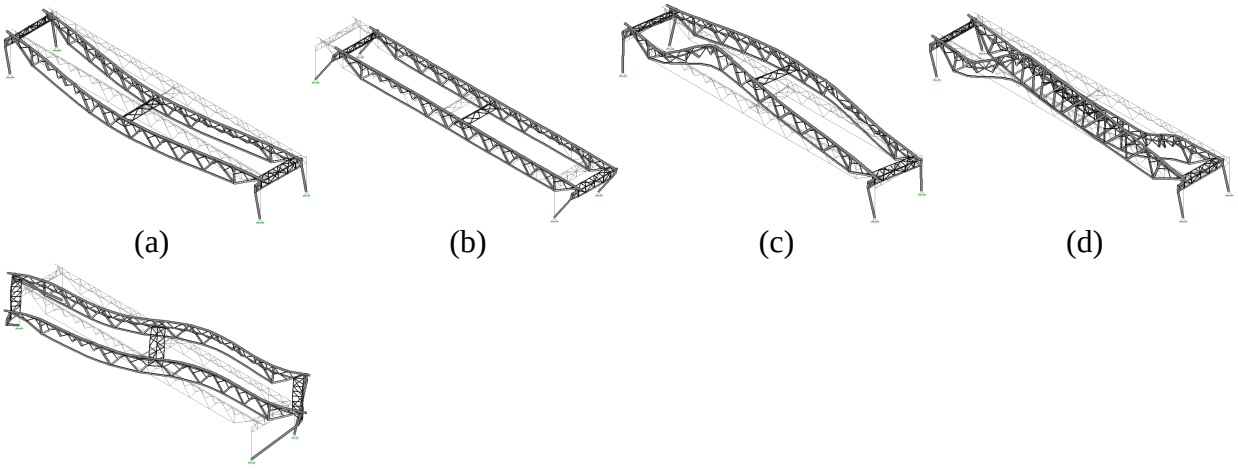

(a) (b) (c) (d)

(e)

Fig. A.10 Mode shapes of damaged truss during service load level of 4.45 kN (Specimen 9): (a) mode 1; (b) mode 2; (c) mode 3; (d) mode 4; (e) mode 5

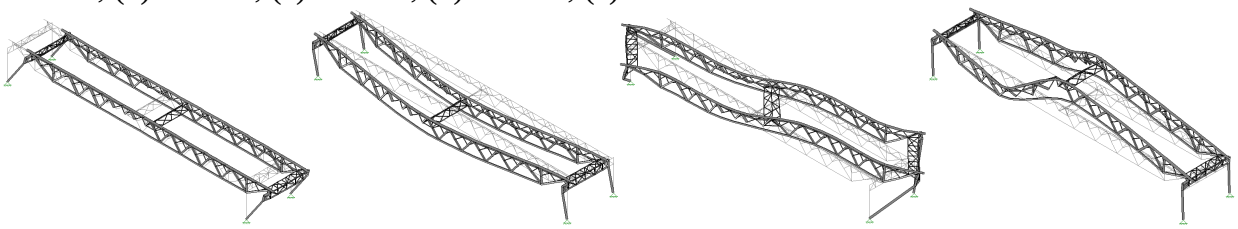

(a) (b) (c) (d)

Fig. A.11 Mode shapes of damaged truss during service load level of 4.45 kN (Specimen 10): (a) mode 1; (b) mode 2; (c) mode 3; (d) mode 4

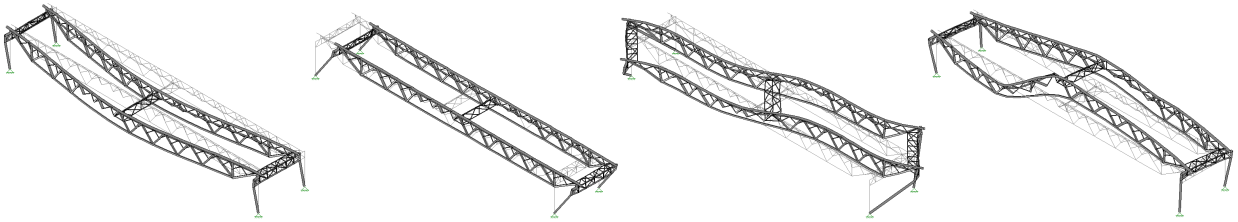

(a) (b) (c) (d)

Fig. A.12 Mode shapes of damaged truss during service load level of 4.45 kN (Specimen 11): (a) mode 1; (b) mode 2; (c) mode 3; (d) mode 4

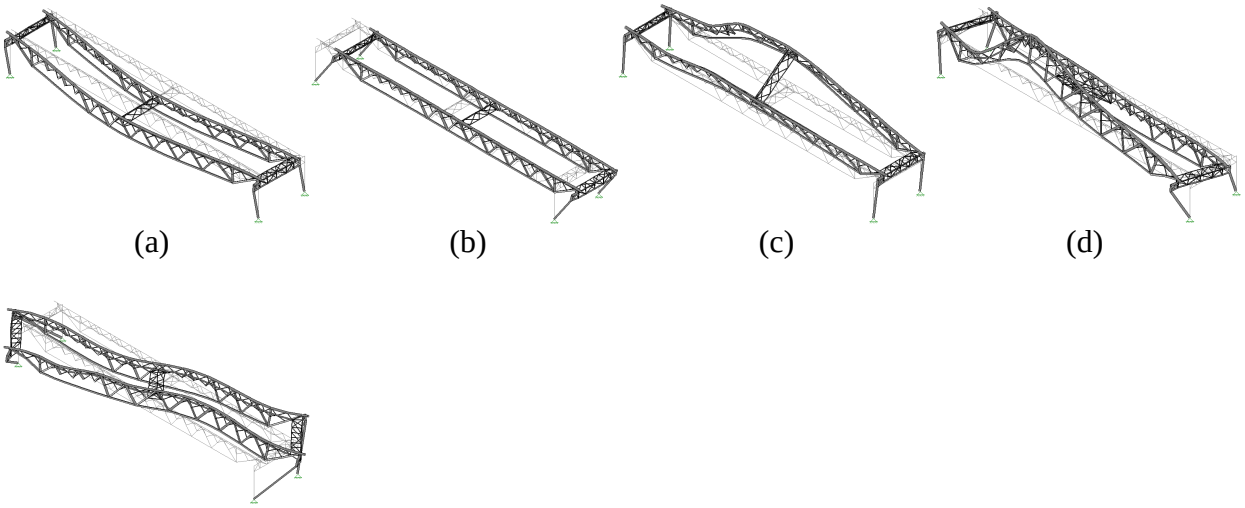

(a) (b) (c) (d)

(e)

Fig. A.13 Mode shapes of damaged truss during service load level of 4.45 kN (Specimen 12): (a) mode 1; (b) mode 2; (c) mode 3; (d) mode 4; (e) mode 5

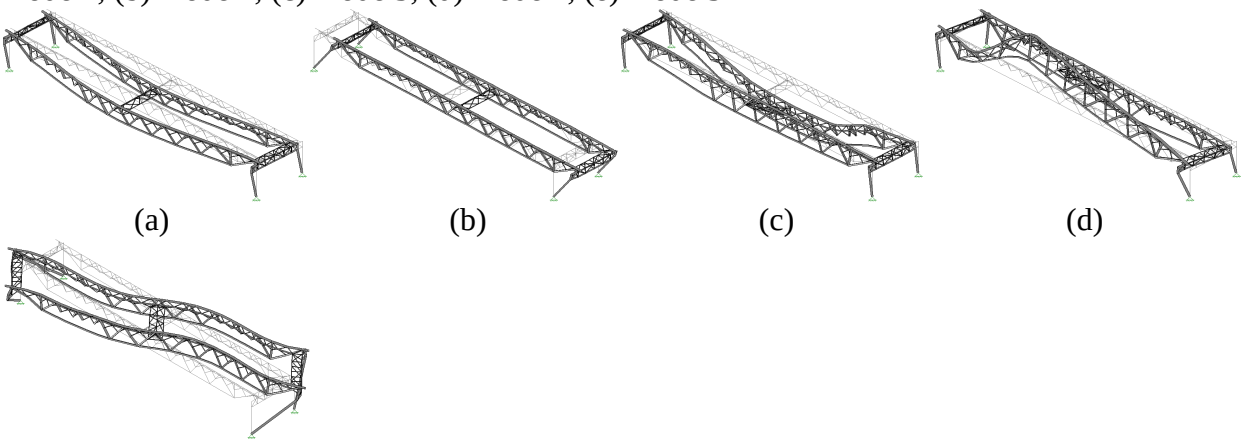

(a) (b) (c) (d)

(e)

Fig. A.14 Mode shapes of damaged truss during service load level of 4.45 kN (Specimen 13): (a) mode1; (b) mode 2; (c) mode 3; (d) mode 4; (e) mode 5

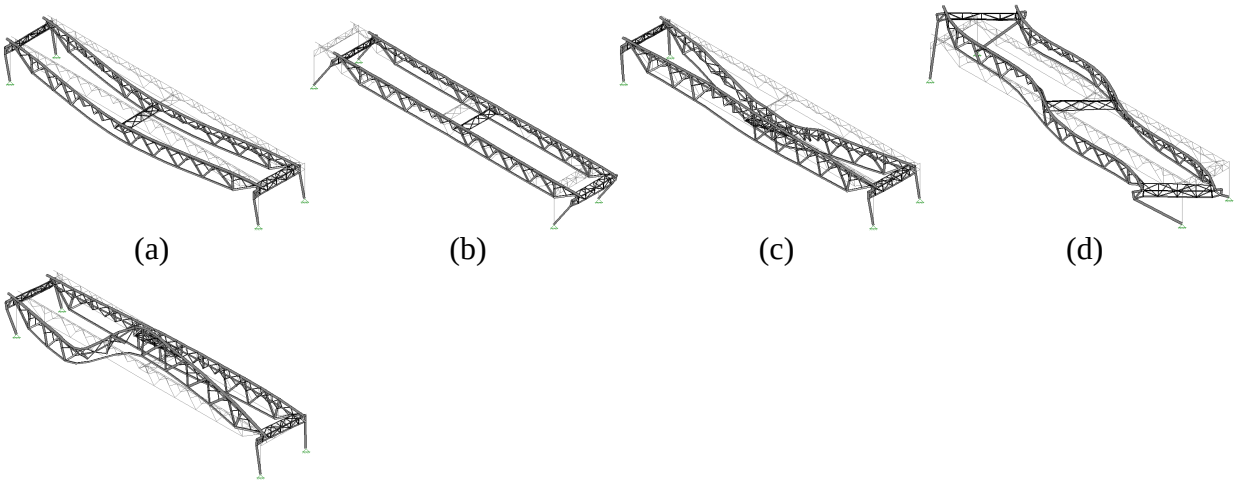

(a) (b) (c) (d)

(e)

Fig. A.15 Mode shapes of damaged truss during service load level of 4.45 kN (Specimen 14): (a) mode1; (b) mode 2; (c) mode 3; (d) mode 4; (e) mode 5

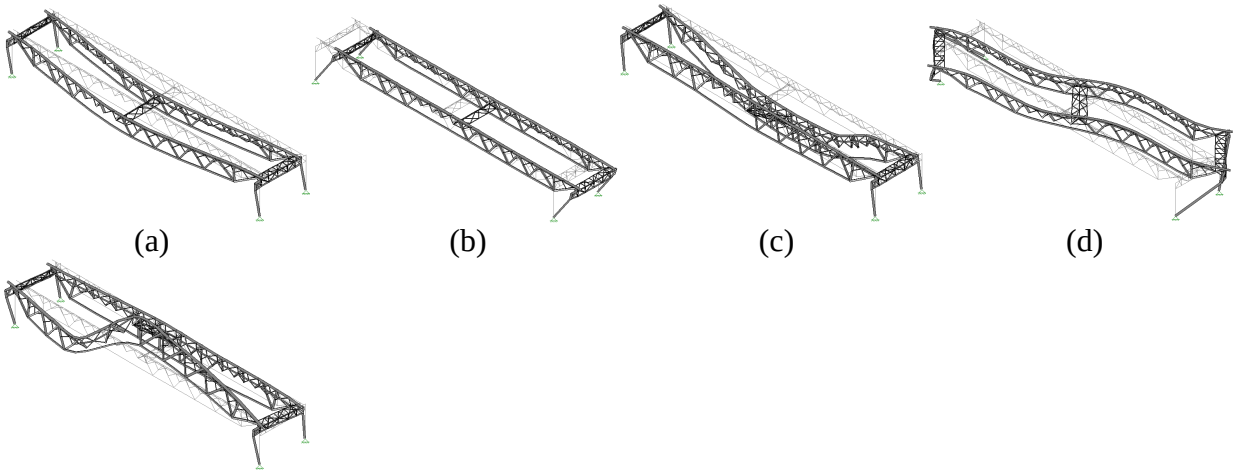

(a) (b) (c) (d)

(e)

Fig. A.16 Mode shapes of damaged truss during service load level of 4.45 kN (Specimen 15): (a) mode1; (b) mode 2; (c) mode 3; (d) mode 4; (e) mode 5

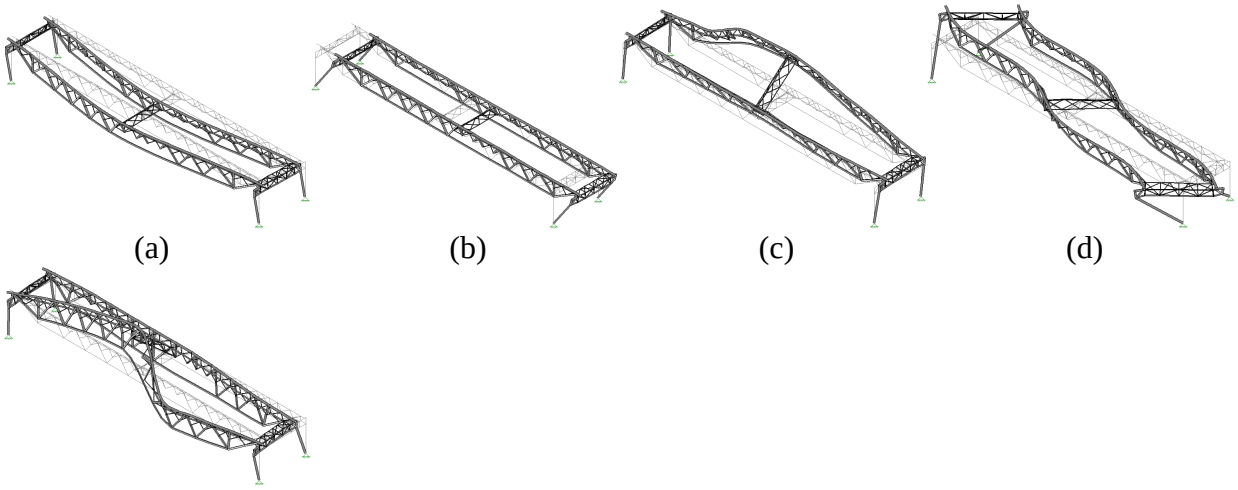

(a) (b) (c) (d)

(e)

Fig. A.17 Mode shapes of damaged truss during service load level of 4.45 kN (Specimen 16): (a) mode1; (b) mode 2; (c) mode 3; (d) mode 4; (e) mode 5

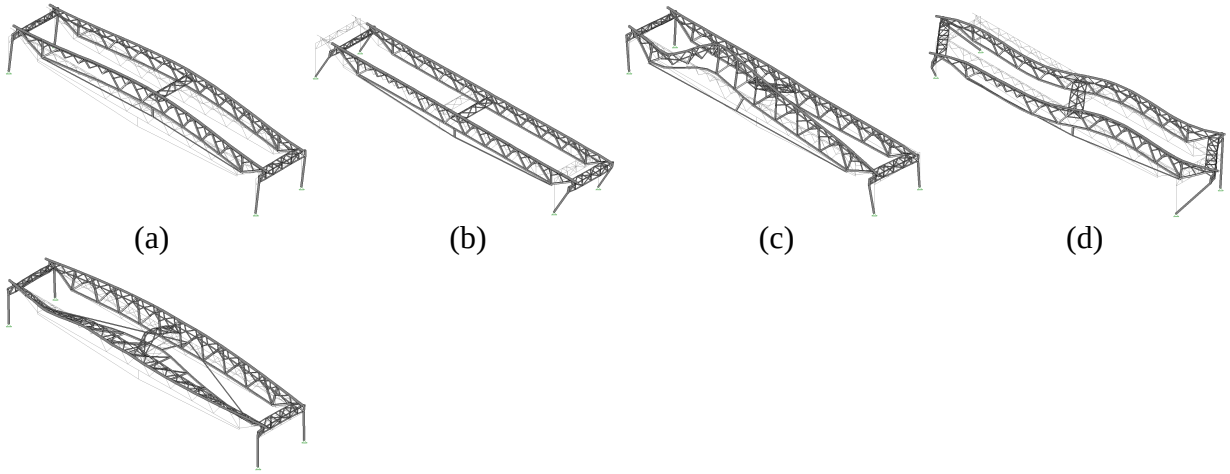

(a) (b) (c) (d)

(e)

Fig. A.18 Mode shapes of the strengthened truss during a service load level of 4.45 kN; 2 kN of post-tensioning load (Specimen 1): (a) mode1; (b) mode 2; (c) mode 3; (d) mode 4; (e) mode 5

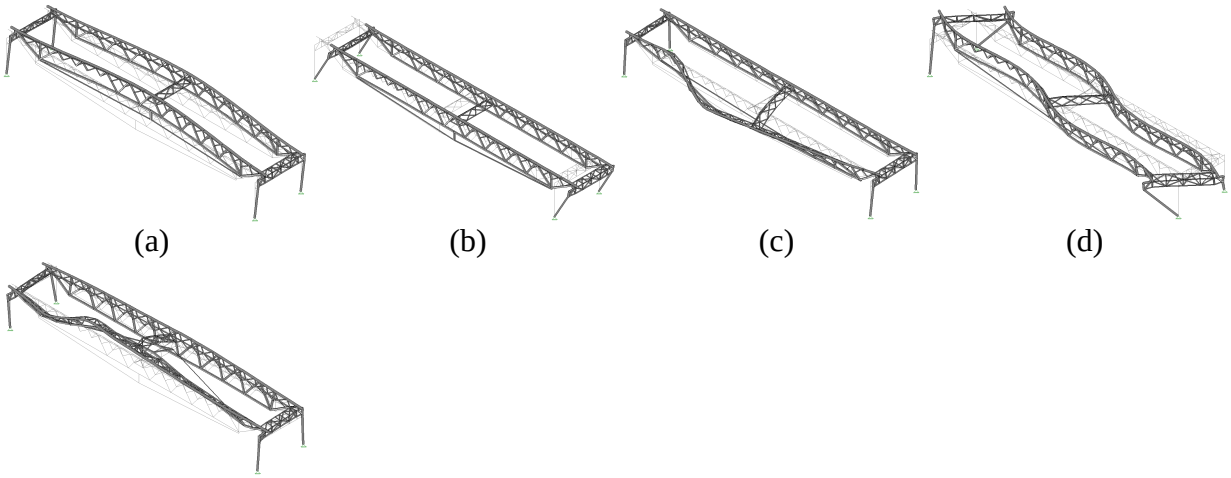

(a) (b) (c) (d)

(e)

Fig. A.19 Mode shapes of the strengthened truss during a service load level of 4.45 kN; 4 kN of post-tensioning load (Specimen 1): (a) mode1; (b) mode 2; (c) mode 3; (d) mode 4; (e) mode 5

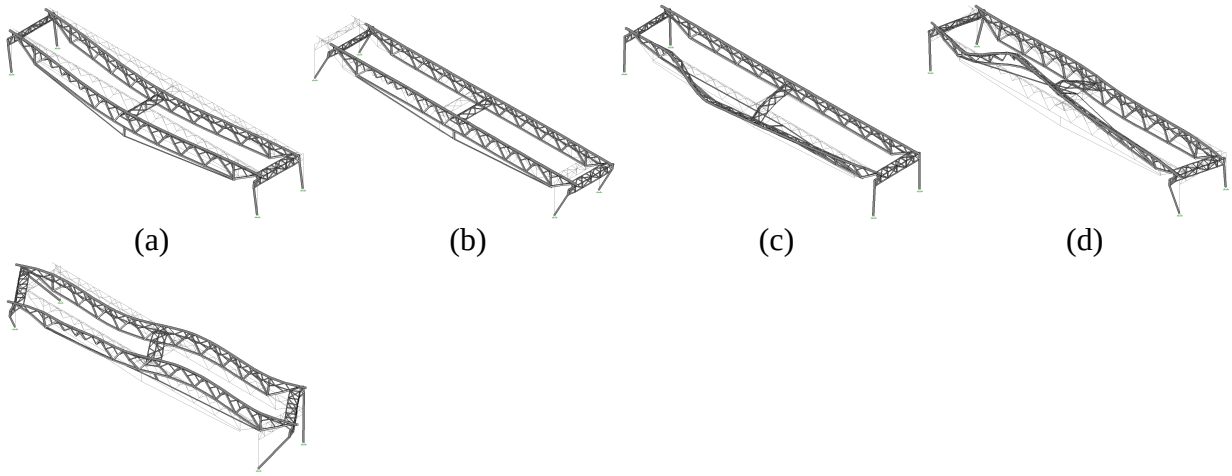

(a) (b) (c) (d)

(e)

Fig. A.20 Mode shapes of the strengthened truss during a service load level of 4.45 kN; 6 kN of post-tensioning load (Specimen 1): (a) mode1; (b) mode 2; (c) mode 3; (d) mode 4; (e) mode 5

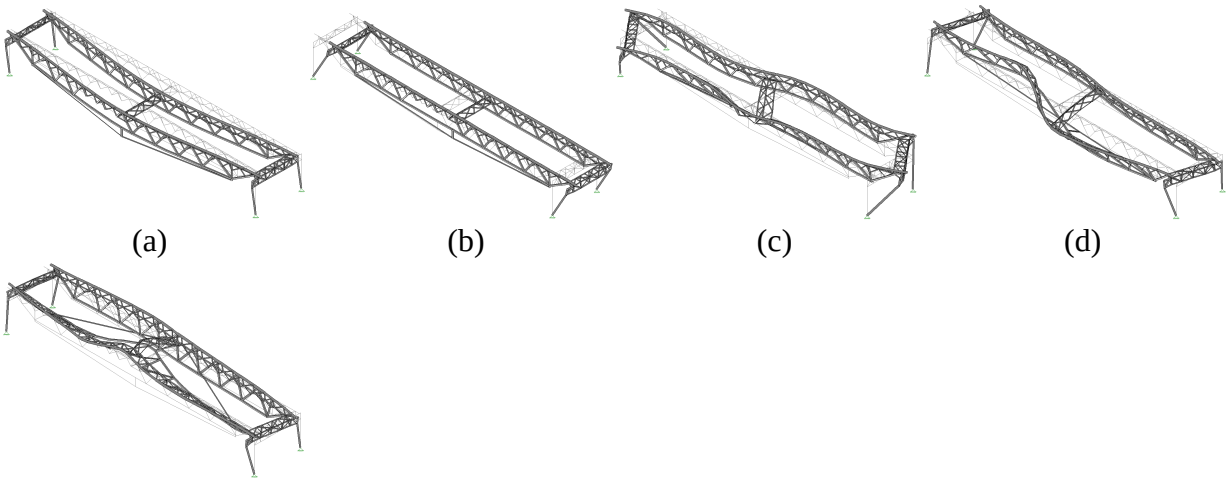

(a) (b) (c) (d)

(e)

Fig. A.21 Mode shapes of the strengthened truss during a service load level of 4.45 kN; 2 kN of post-tensioning load (Specimen 2): (a) mode1; (b) mode 2; (c) mode 3; (d) mode 4; (e) mode 5

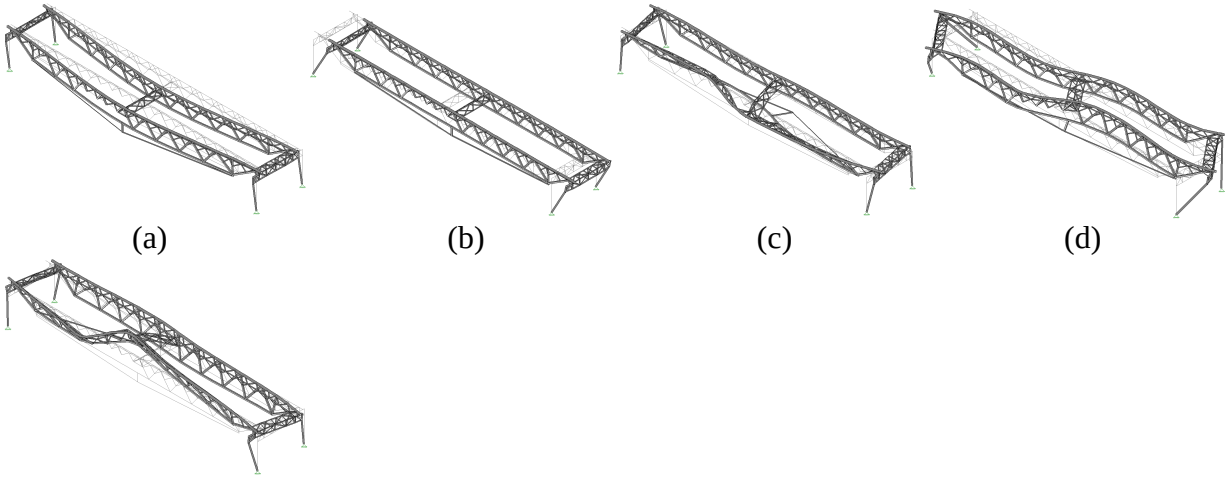

(a) (b) (c) (d)

(e)

Fig. A.22 Mode shapes of the strengthened truss during a service load level of 4.45 kN; 4 kN of post-tensioning load (Specimen 2): (a) mode1; (b) mode 2; (c) mode 3; (d) mode 4; (e) mode 5

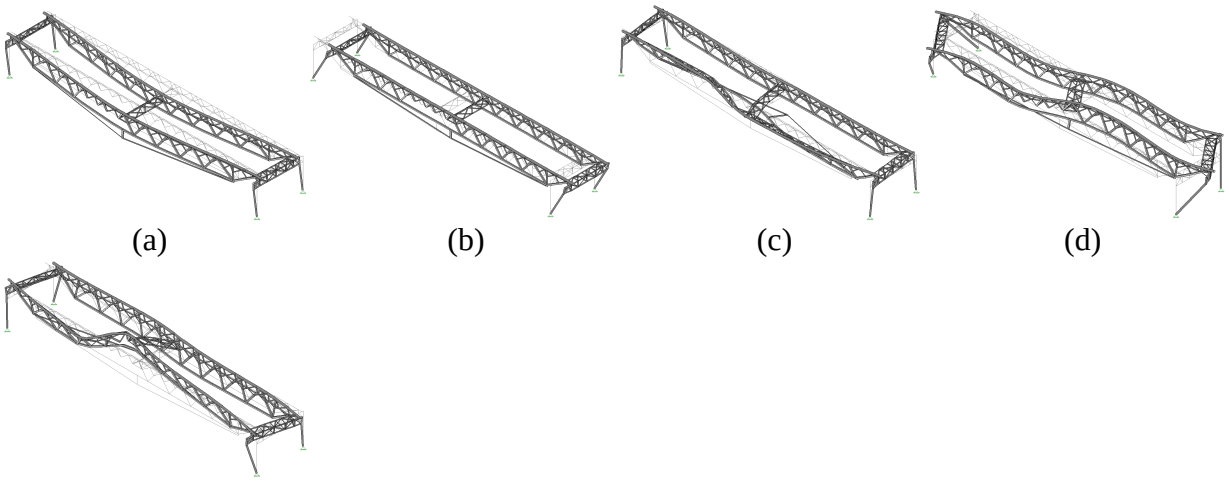

(a) (b) (c) (d)

(e)

Fig. A.23 Mode shapes of the strengthened truss during a service load level of 4.45 kN; 6 kN of post-tensioning load (Specimen 2): (a) mode1; (b) mode 2; (c) mode 3; (d) mode 4; (e) mode 5

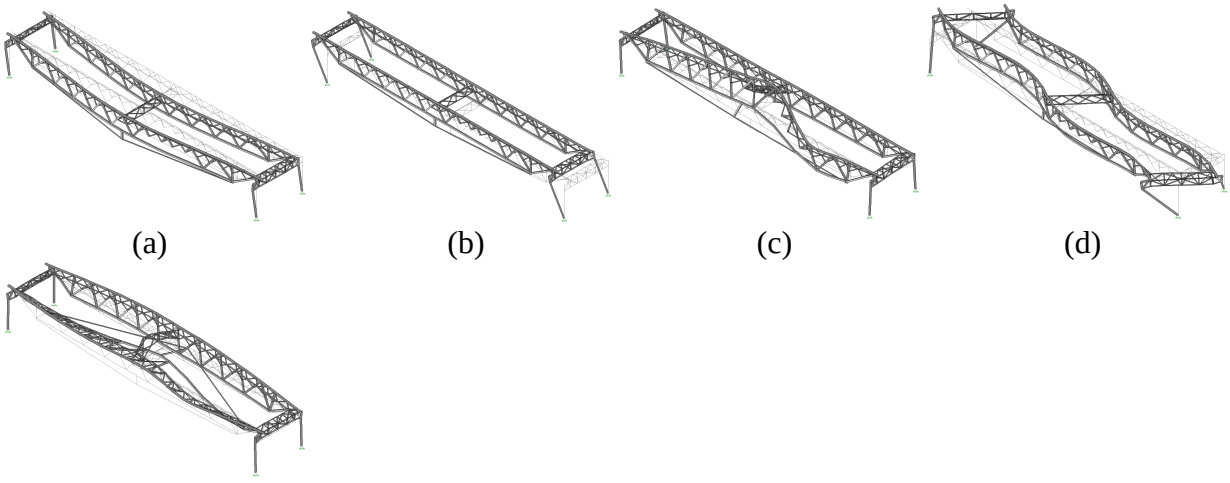

(a) (b) (c) (d)

(e)

Fig. A.24 Mode shapes of the strengthened truss during a service load level of 4.45 kN; 2 kN of post-tensioning load (Specimen 3): (a) mode1; (b) mode 2; (c) mode 3; (d) mode 4; (e) mode 5

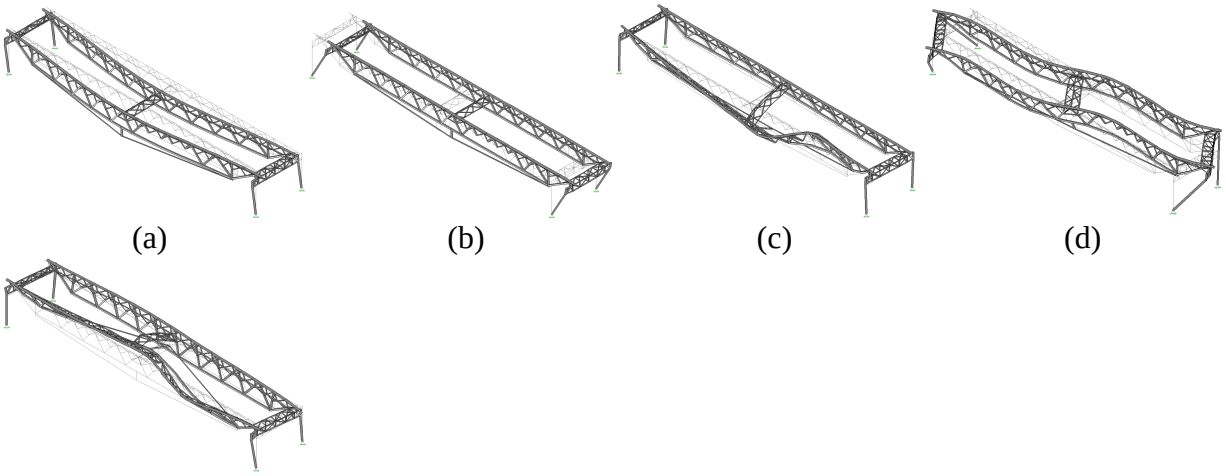

(a) (b) (c) (d)

(e)

Fig. A.25 Mode shapes of the strengthened truss during a service load level of 4.45 kN; 4 kN of post-tensioning load (Specimen 3): (a) mode1; (b) mode 2; (c) mode 3; (d) mode 4; (e) mode 5

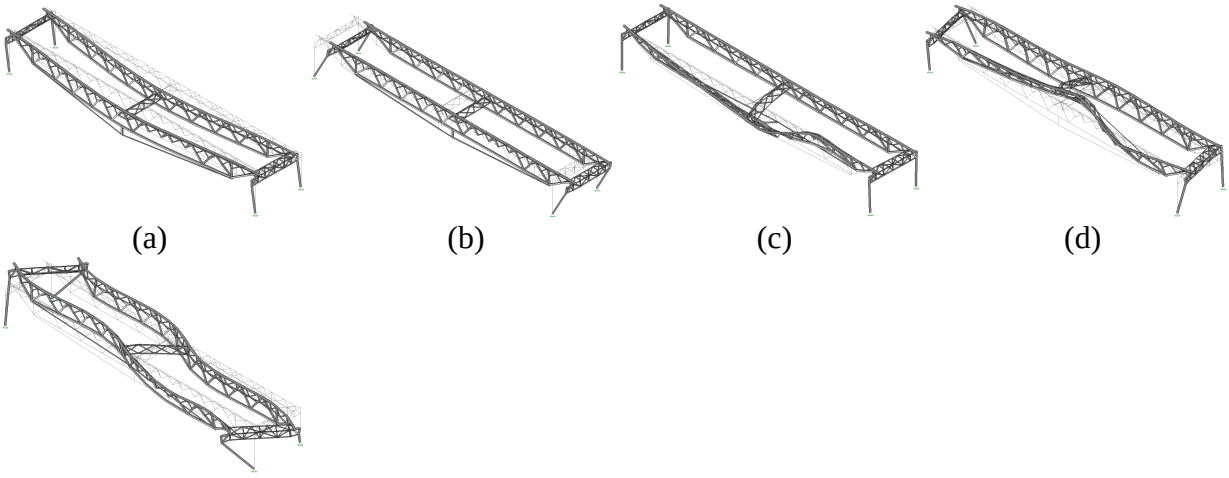

(a) (b) (c) (d)

(e)

Fig. A.26 Mode shapes of the strengthened truss during a service load level of 4.45 kN; 6 kN of post-tensioning load (Specimen 3): (a) mode1; (b) mode 2; (c) mode 3; (d) mode 4; (e) mode 5

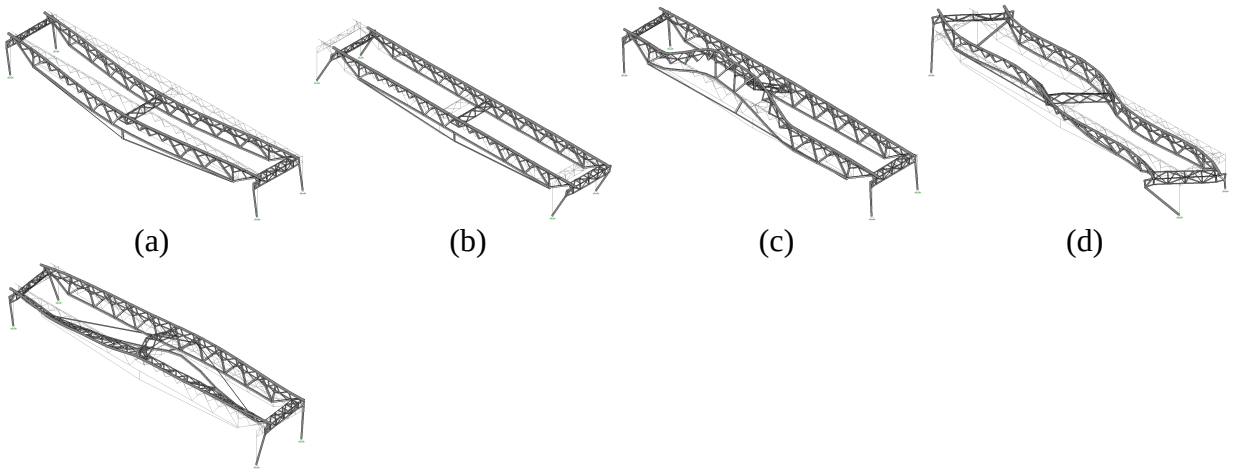

(a) (b) (c) (d)

(e)

Fig. A.27 Mode shapes of the strengthened truss during a service load level of 4.45 kN; 2 kN of post-tensioning load (Specimen 4): (a) mode1; (b) mode 2; (c) mode 3; (d) mode 4; (e) mode 5

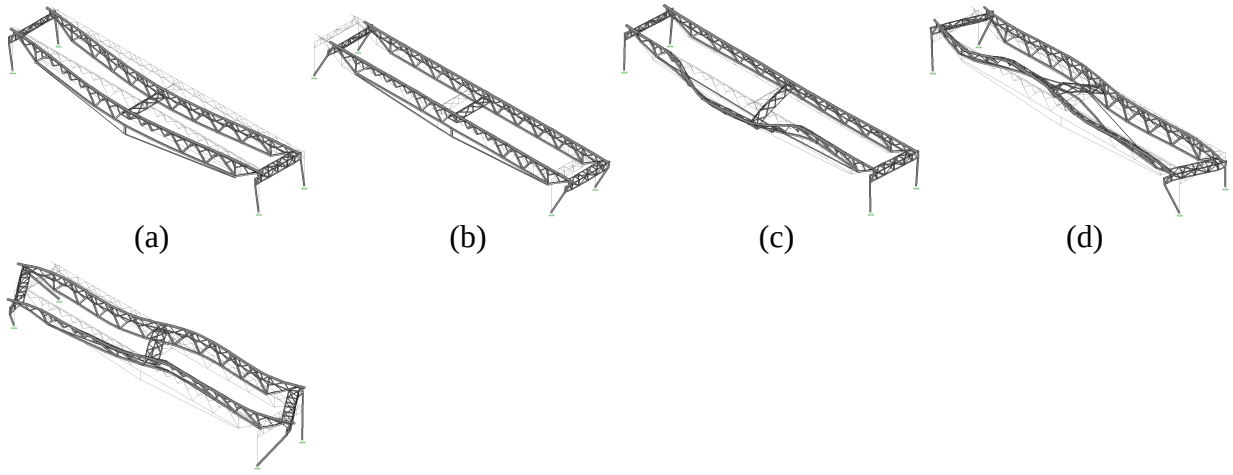

(a) (b) (c) (d)

(e)

Fig. A.28 Mode shapes of the strengthened truss during a service load level of 4.45 kN; 4 kN of post-tensioning load (Specimen 4): (a) mode1; (b) mode 2; (c) mode 3; (d) mode 4; (e) mode 5

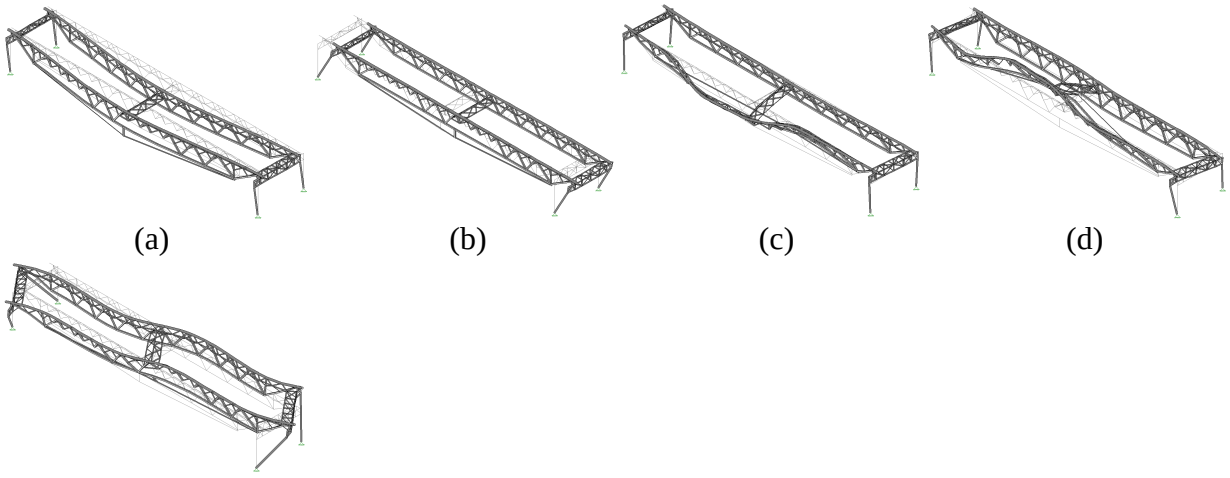

(a) (b) (c) (d)

(e)

Fig. A.29 Mode shapes of the strengthened truss during a service load level of 4.45 kN; 6 kN of post-tensioning load (Specimen 4): (a) mode1; (b) mode 2; (c) mode 3; (d) mode 4; (e) mode 5

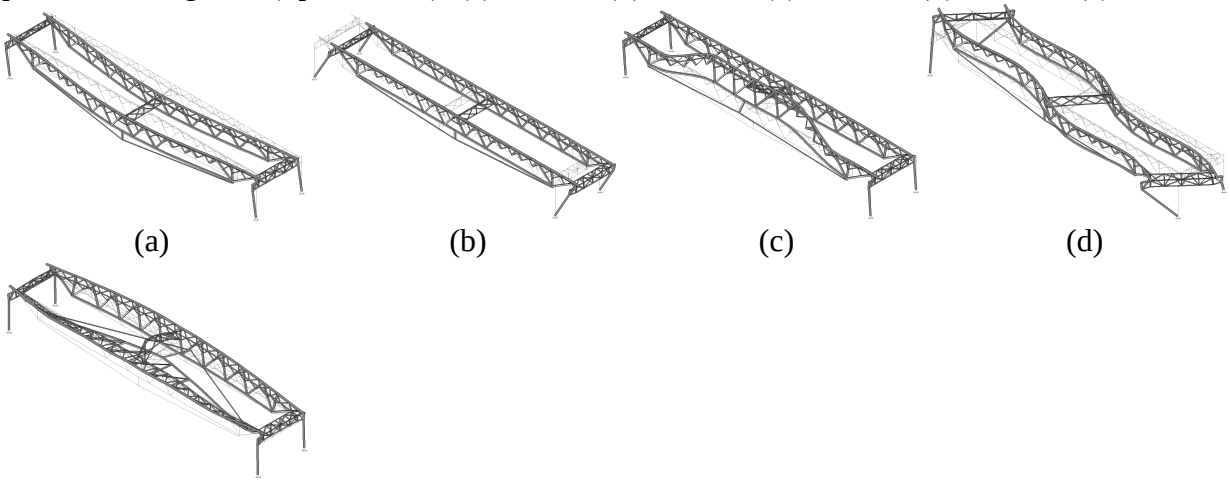

(a) (b) (c) (d)

(e)

Fig. A.30 Mode shapes of the strengthened truss during a service load level of 4.45 kN; 2 kN of post-tensioning load (Specimen 5): (a) mode1; (b) mode 2; (c) mode 3; (d) mode 4; (e) mode 5

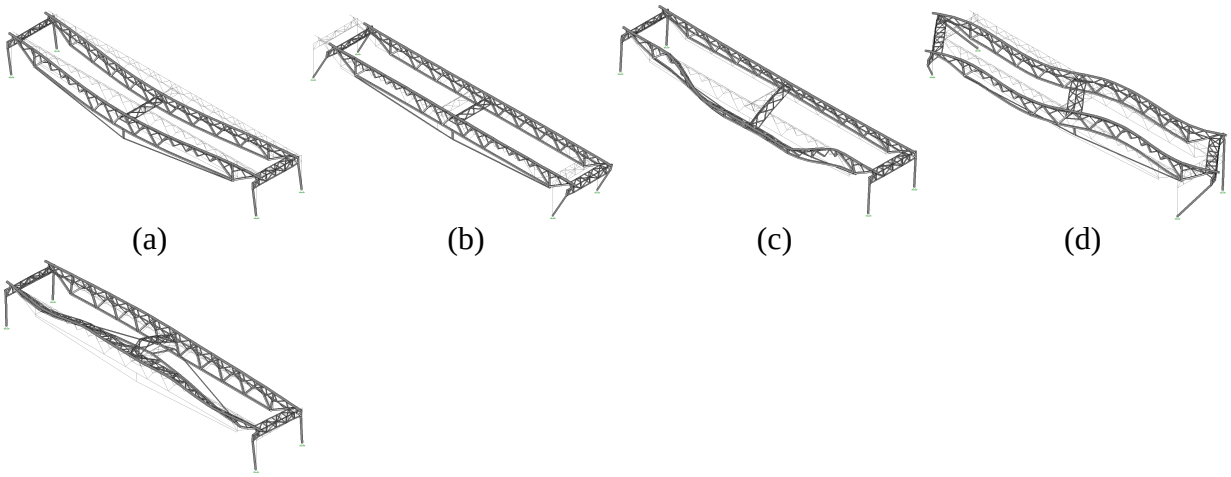

(a) (b) (c) (d)

(e)

Fig. A.31 Mode shapes of the strengthened truss during a service load level of 4.45 kN; 4 kN of post-tensioning load (Specimen 5): (a) mode1; (b) mode 2; (c) mode 3; (d) mode 4; (e) mode 5

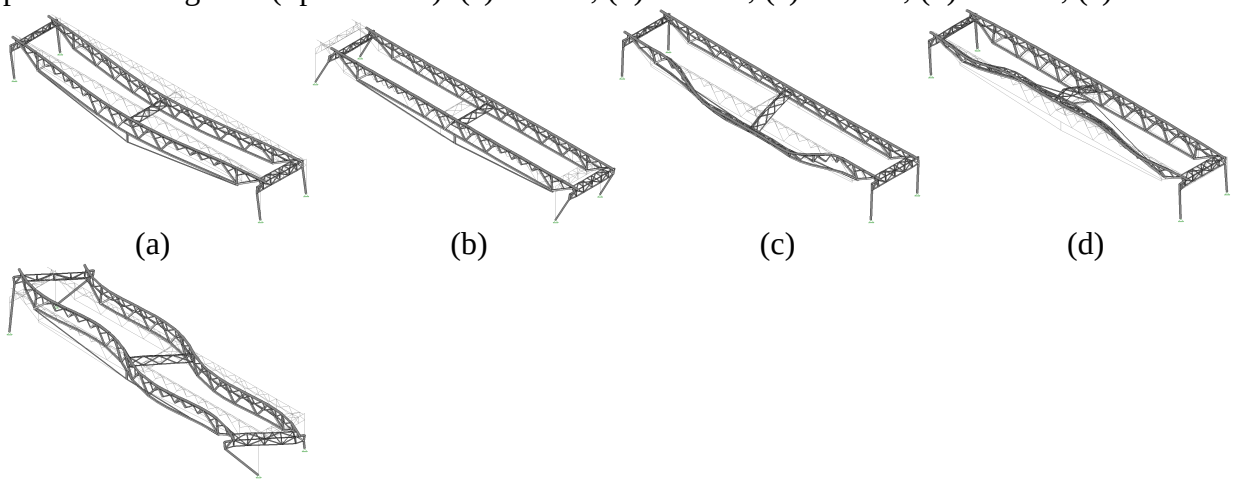

(a) (b) (c) (d)

(e)

Fig. A.32 Mode shapes of the strengthened truss during a service load level of 4.45 kN; 6 kN of post-tensioning load (Specimen 5): (a) mode1; (b) mode 2; (c) mode 3; (d) mode 4; (e) mode 5

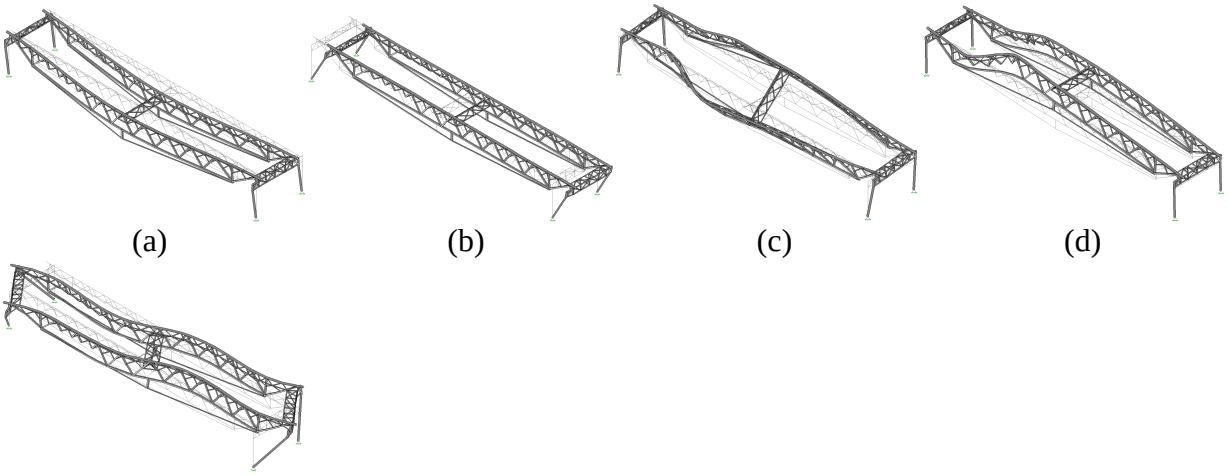

(a) (b) (c) (d)

(e)

Fig. A.33 Mode shapes of the strengthened truss during a service load level of 4.45 kN; 2 kN of post-tensioning load (Specimen 6): (a) mode1; (b) mode 2; (c) mode 3; (d) mode 4; (e) mode 5

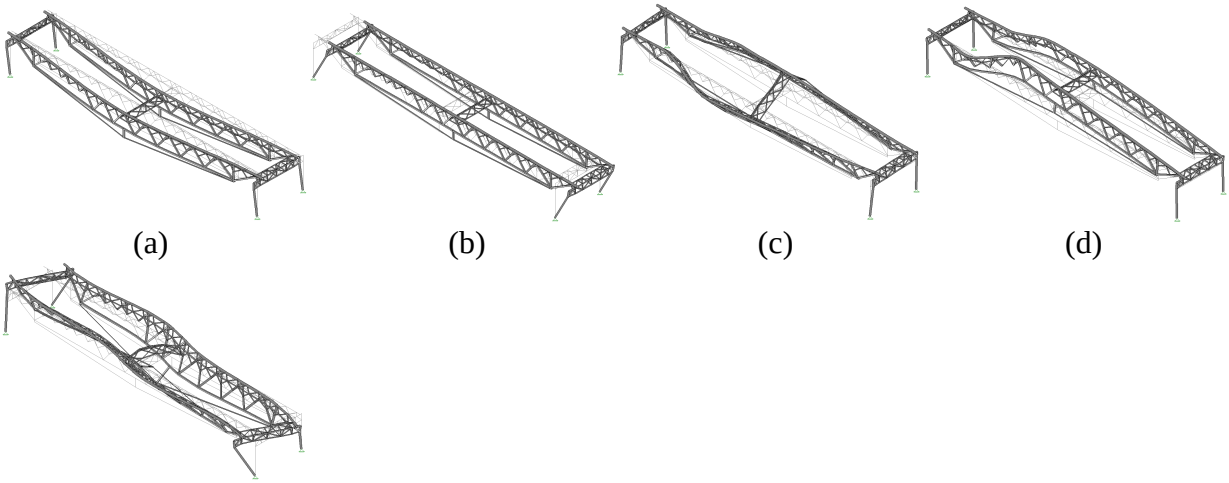

(a) (b) (c) (d)

(e)

Fig. A.34 Mode shapes of the strengthened truss during a service load level of 4.45 kN; 4 kN of post-tensioning load (Specimen 6): (a) mode1; (b) mode 2; (c) mode 3; (d) mode 4; (e) mode 5

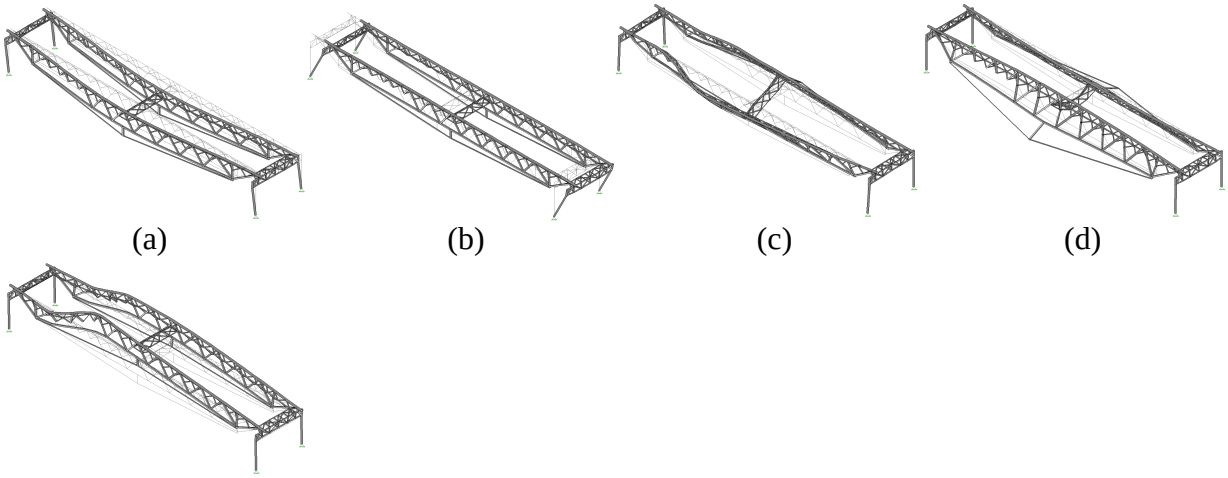

(a) (b) (c) (d)

(e)

Fig. A.35 Mode shapes of the strengthened truss during a service load level of 4.45 kN; 6 kN of post-tensioning load (Specimen 6): (a) mode1; (b) mode 2; (c) mode 3; (d) mode 4; (e) mode 5

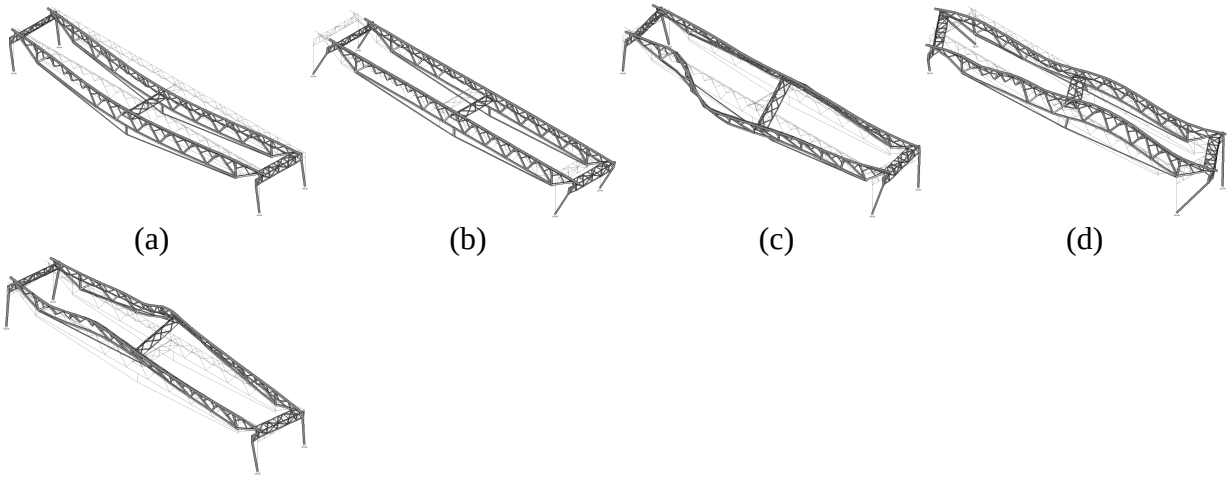

(a) (b) (c) (d)

(e)

Fig. A.36 Mode shapes of the strengthened truss during a service load level of 4.45 kN; 2 kN of post-tensioning load (Specimen 7): (a) mode1; (b) mode 2; (c) mode 3; (d) mode 4; (e) mode 5

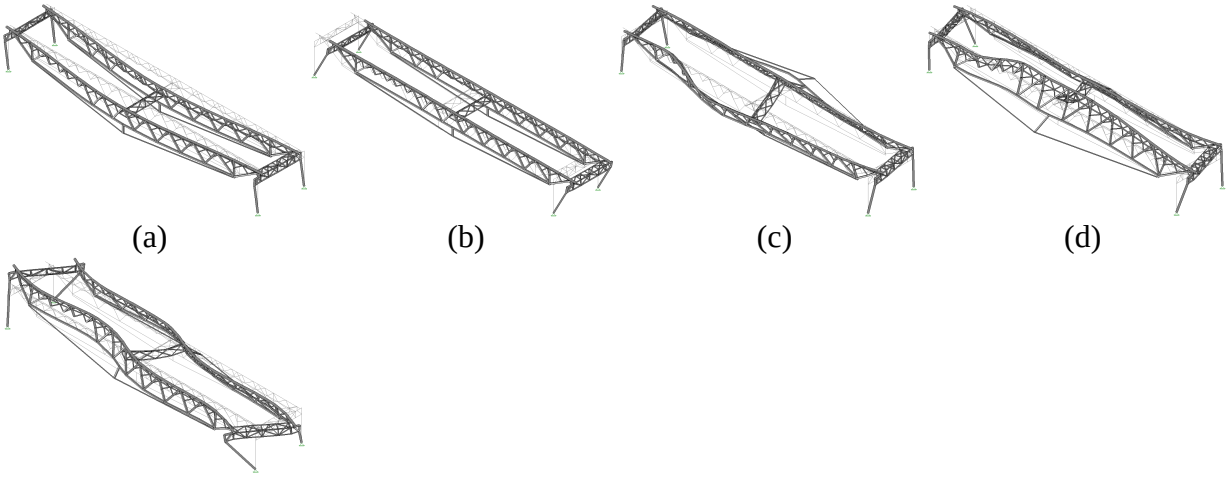

(a) (b) (c) (d)

(e)

Fig. A.37 Mode shapes of the strengthened truss during a service load level of 4.45 kN; 4 kN of post-tensioning load (Specimen 7): (a) mode1; (b) mode 2; (c) mode 3; (d) mode 4; (e) mode 5

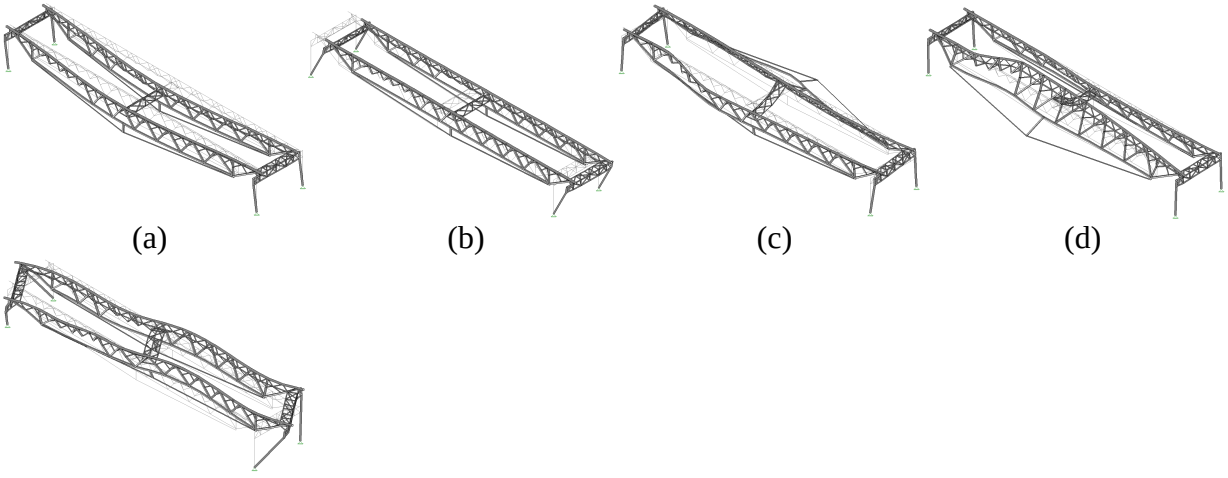

(a) (b) (c) (d)

(e)

Fig. A.38 Mode shapes of the strengthened truss during a service load level of 4.45 kN; 6 kN of post-tensioning load (Specimen 7): (a) mode1; (b) mode 2; (c) mode 3; (d) mode 4; (e) mode 5

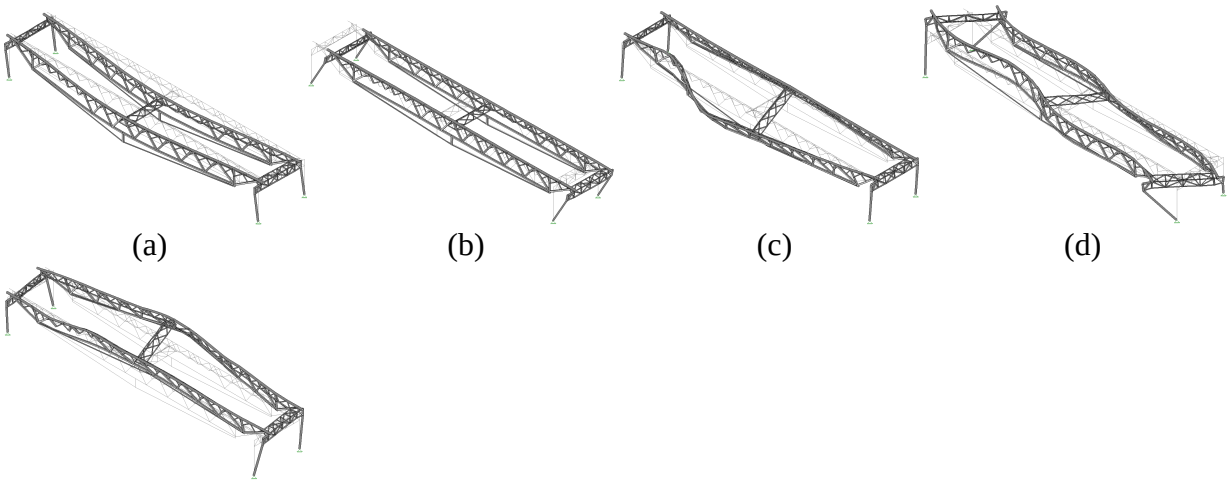

(a) (b) (c) (d)

(e)

Fig. A.39 Mode shapes of the strengthened truss during a service load level of 4.45 kN; 2 kN of post-tensioning load (Specimen 8): (a) mode1; (b) mode 2; (c) mode 3; (d) mode 4; (e) mode 5

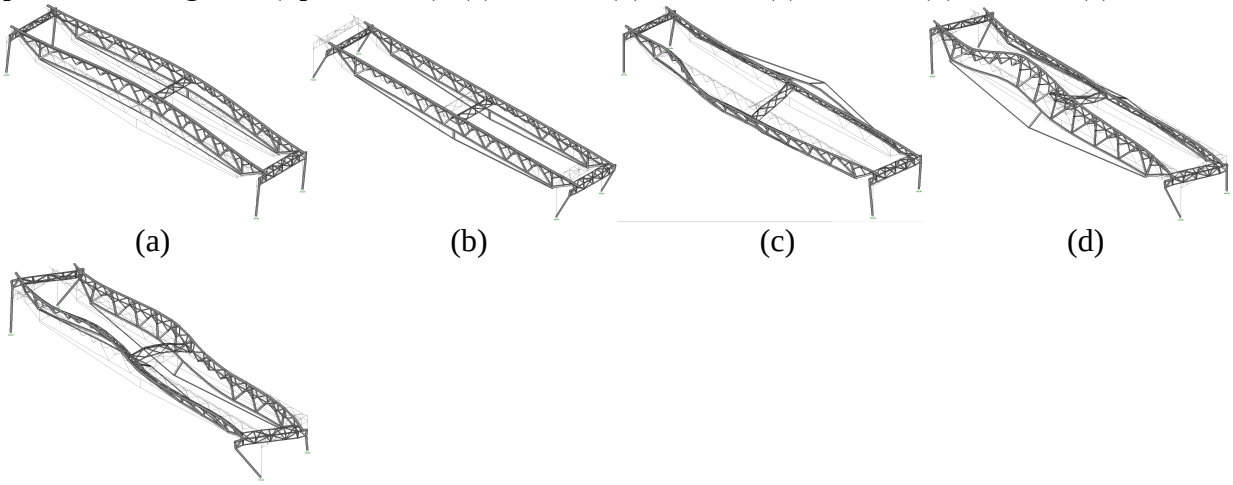

(a) (b) (c) (d)

(e)

Fig. A.40 Mode shapes of the strengthened truss during a service load level of 4.45 kN; 4 kN of post-tensioning load (Specimen 8): (a) mode1; (b) mode 2; (c) mode 3; (d) mode 4; (e) mode 5

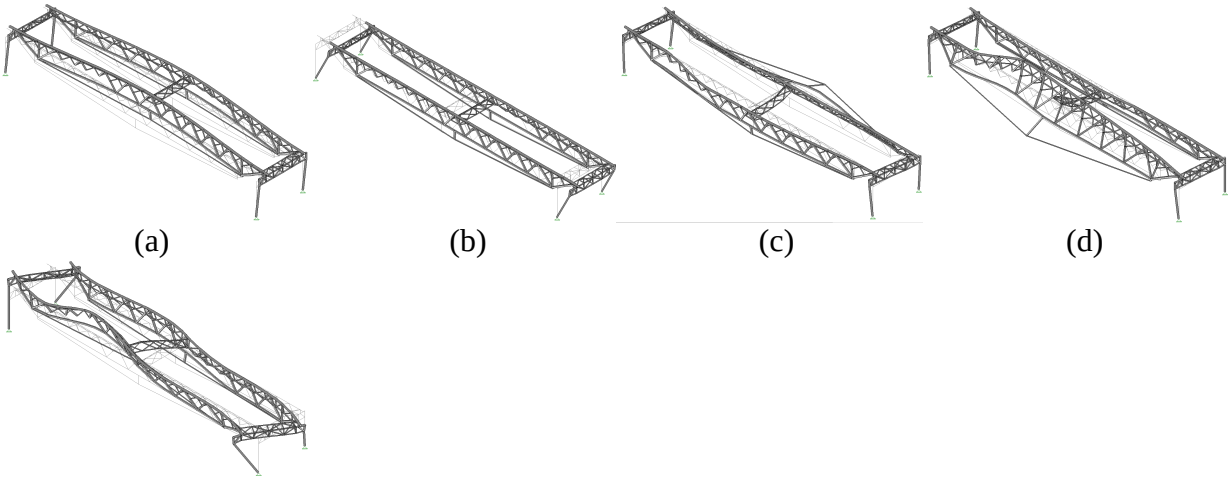

(a) (b) (c) (d)

(e)

Fig. A.41 Mode shapes of the strengthened truss during a service load level of 4.45 kN; 6 kN of post-tensioning load (Specimen 8): (a) mode1; (b) mode 2; (c) mode 3; (d) mode 4; (e) mode 5

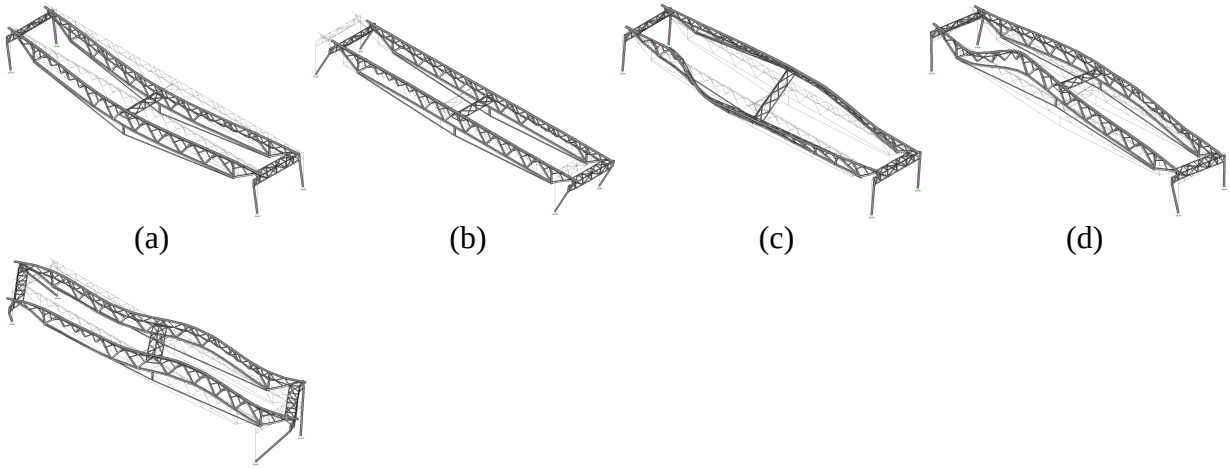

(a) (b) (c) (d)

(e)

Fig. A.42 Mode shapes of the strengthened truss during a service load level of 4.45 kN; 2 kN of post-tensioning load (Specimen 9): (a) mode1; (b) mode 2; (c) mode 3; (d) mode 4; (e) mode 5

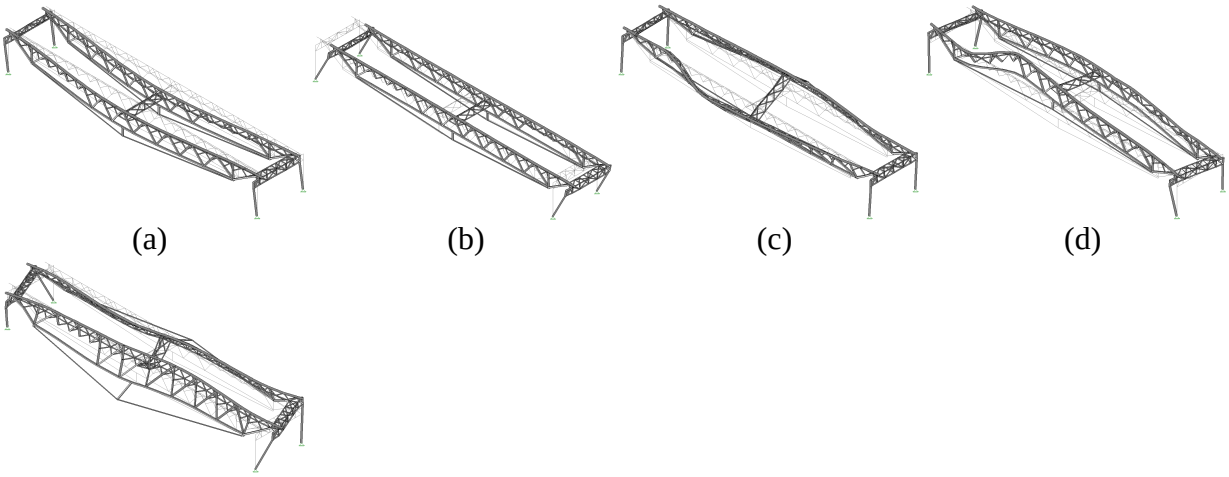

(a) (b) (c) (d)

(e)

Fig. A.43 Mode shapes of the strengthened truss during a service load level of 4.45 kN; 4 kN of post-tensioning load (Specimen 9): (a) mode1; (b) mode 2; (c) mode 3; (d) mode 4; (e) mode 5

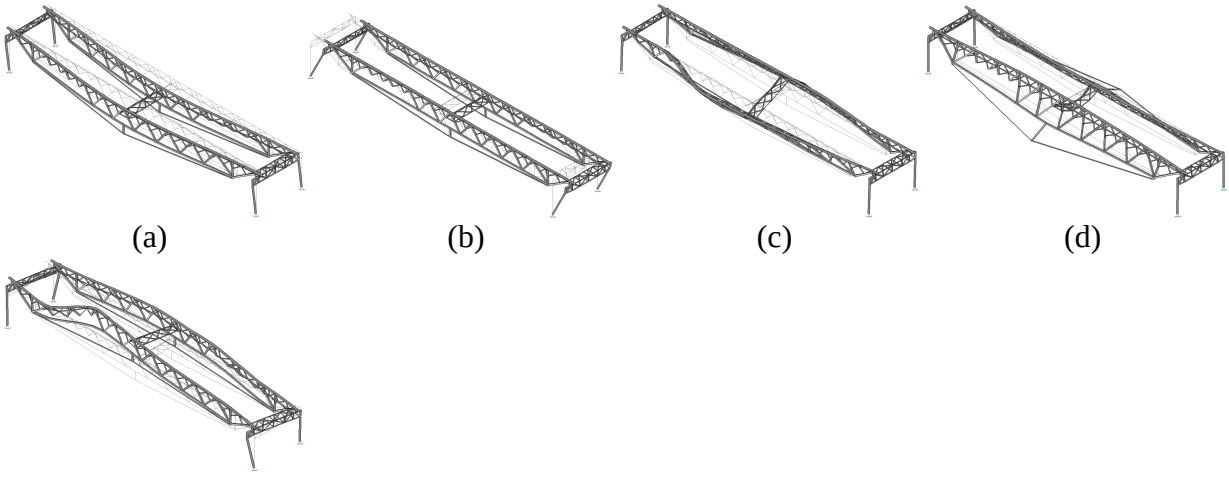

(a) (b) (c) (d)

(e)

Fig. A.44 Mode shapes of the strengthened truss during a service load level of 4.45 kN; 6 kN of post-tensioning load (Specimen 9): (a) mode1; (b) mode 2; (c) mode 3; (d) mode 4; (e) mode 5

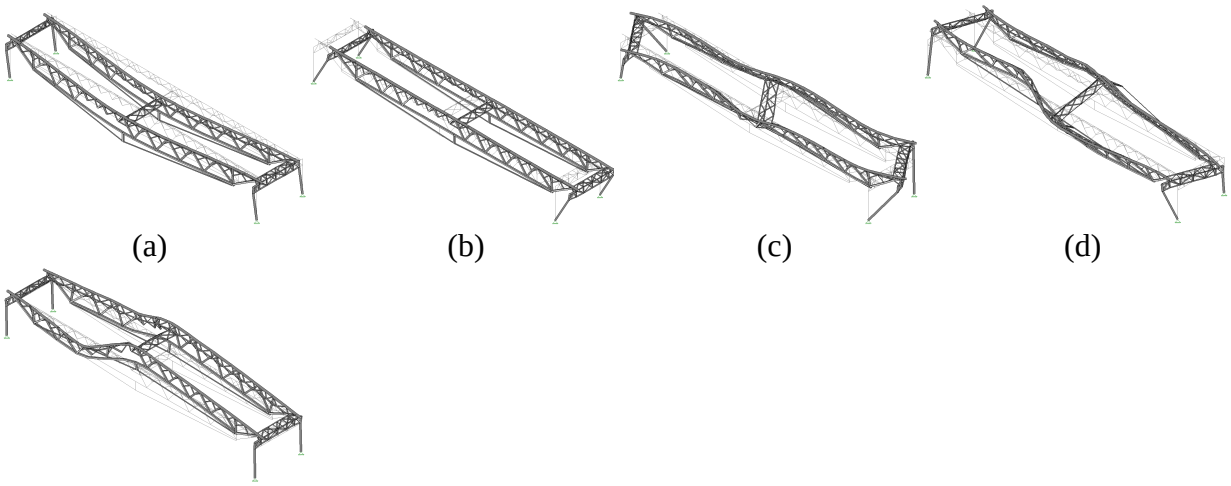

(a) (b) (c) (d)

(e)

Fig. A.45 Mode shapes of the strengthened truss during a service load level of 4.45 kN; 2 kN of post-tensioning load (Specimen 10): (a) mode1; (b) mode 2; (c) mode 3; (d) mode 4; (e) mode 5

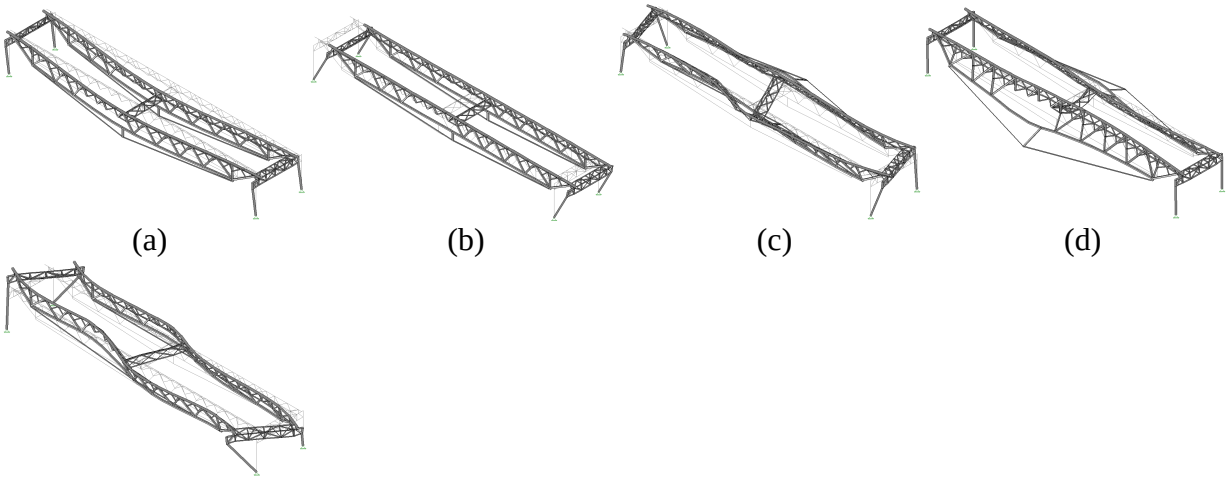

(a) (b) (c) (d)

(e)

Fig. A.46 Mode shapes of the strengthened truss during a service load level of 4.45 kN; 4 kN of post-tensioning load (Specimen 10): (a) mode1; (b) mode 2; (c) mode 3; (d) mode 4; (e) mode 5

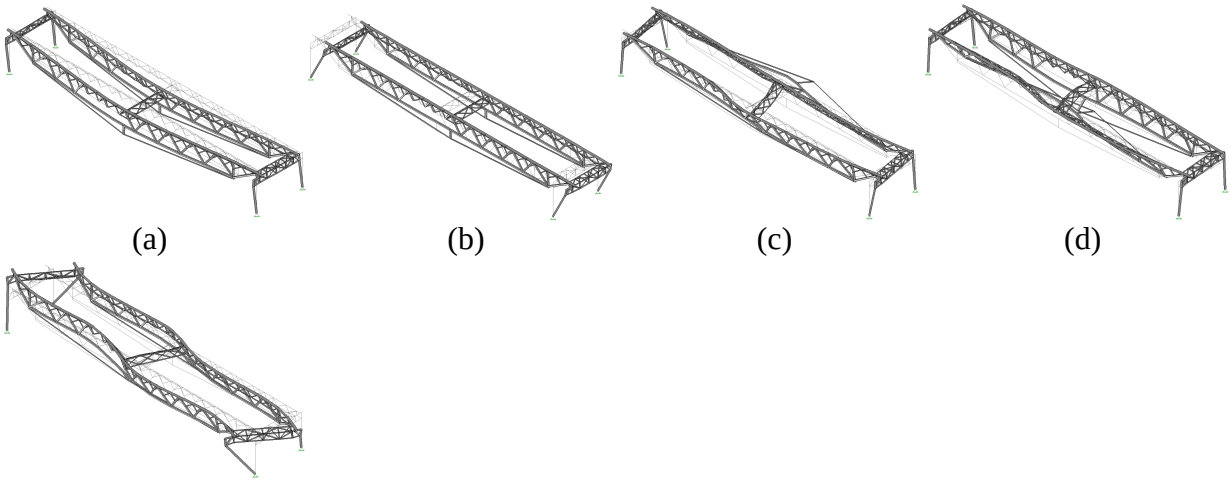

(a) (b) (c) (d)

(e)

Fig. A.47 Mode shapes of the strengthened truss during a service load level of 4.45 kN; 6 kN of post-tensioning load (Specimen 10): (a) mode1; (b) mode 2; (c) mode 3; (d) mode 4; (e) mode 5

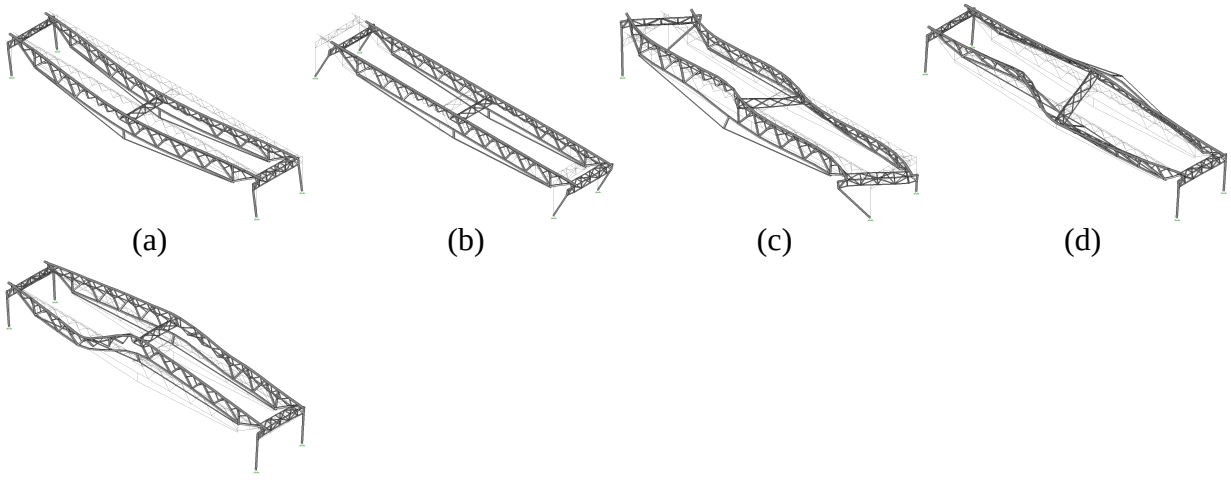

(a) (b) (c) (d)

(e)

Fig. A.48 Mode shapes of the strengthened truss during a service load level of 4.45 kN; 2 kN of post-tensioning load (Specimen 11): (a) mode1; (b) mode 2; (c) mode 3; (d) mode 4; (e) mode 5

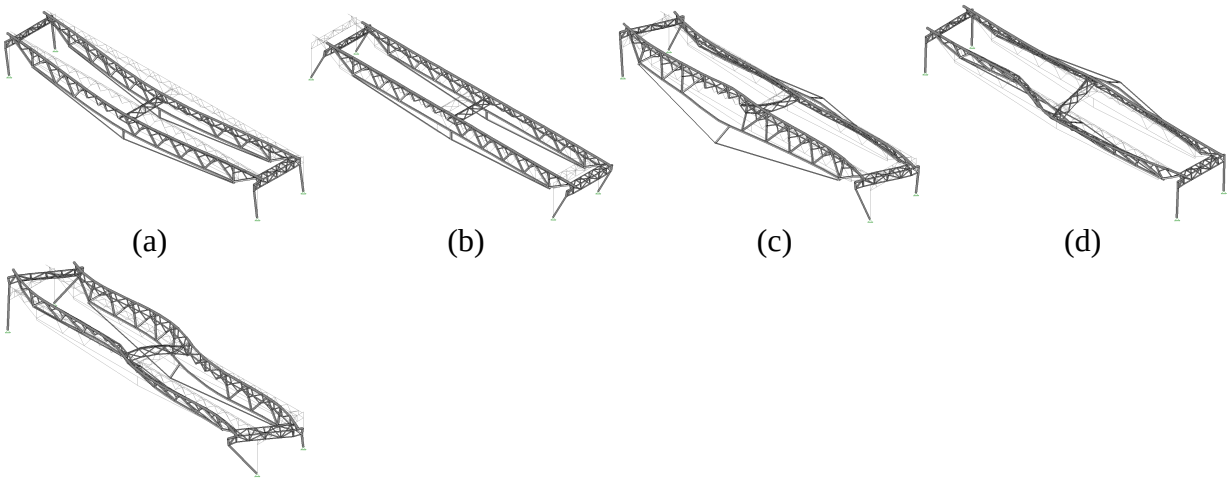

(a) (b) (c) (d)

(e)

Fig. A.49 Mode shapes of the strengthened truss during a service load level of 4.45 kN; 4 kN of post-tensioning load (Specimen 11): (a) mode1; (b) mode 2; (c) mode 3; (d) mode 4; (e) mode 5

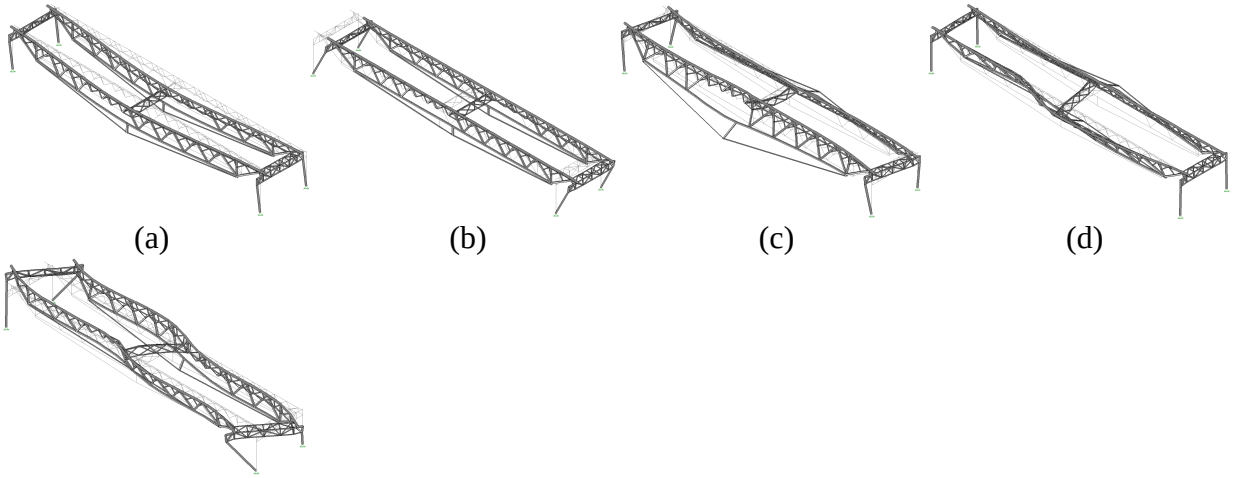

(a) (b) (c) (d)

(e)

Fig. A.50 Mode shapes of the strengthened truss during a service load level of 4.45 kN; 6 kN of post-tensioning load (Specimen 11): (a) mode1; (b) mode 2; (c) mode 3; (d) mode 4; (e) mode 5

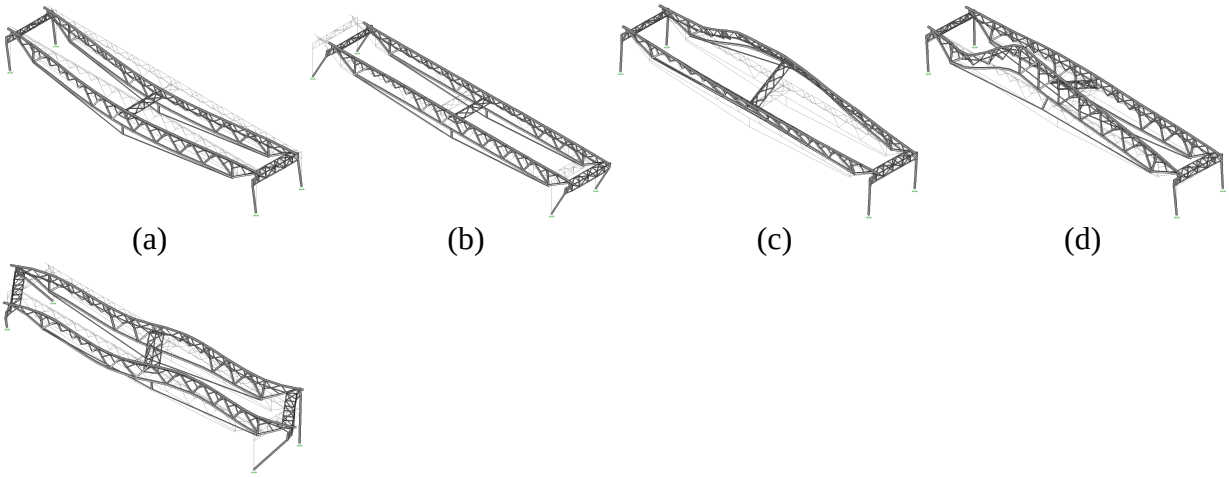

(a) (b) (c) (d)

(e)

Fig. A.51 Mode shapes of the strengthened truss during a service load level of 4.45 kN; 2 kN of post-tensioning load (Specimen 12): (a) mode1; (b) mode 2; (c) mode 3; (d) mode 4; (e) mode 5

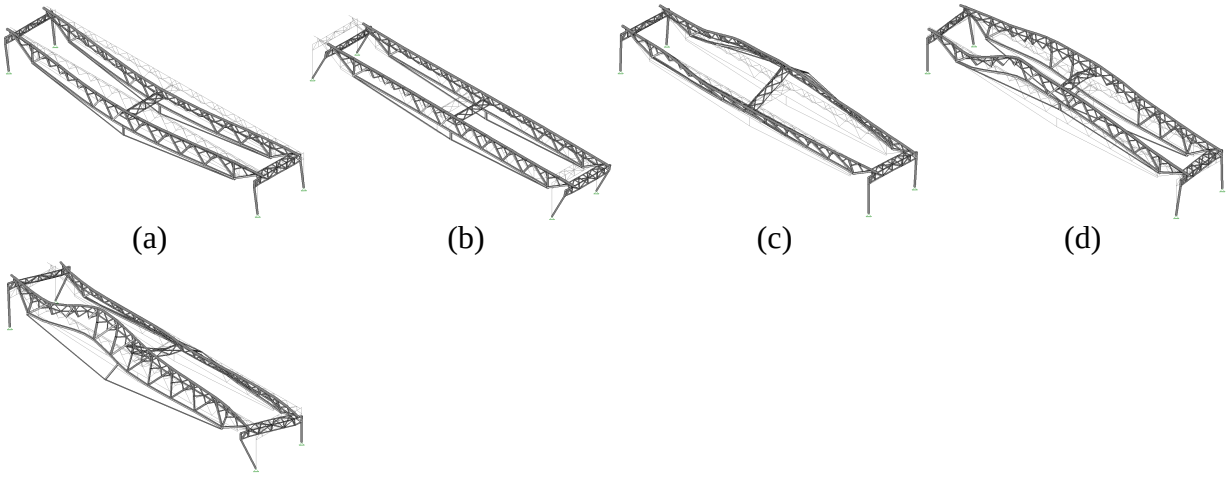

(a) (b) (c) (d)

(e)

Fig. A.52 Mode shapes of the strengthened truss during a service load level of 4.45 kN; 4 kN of post-tensioning load (Specimen 12): (a) mode1; (b) mode 2; (c) mode 3; (d) mode 4; (e) mode 5

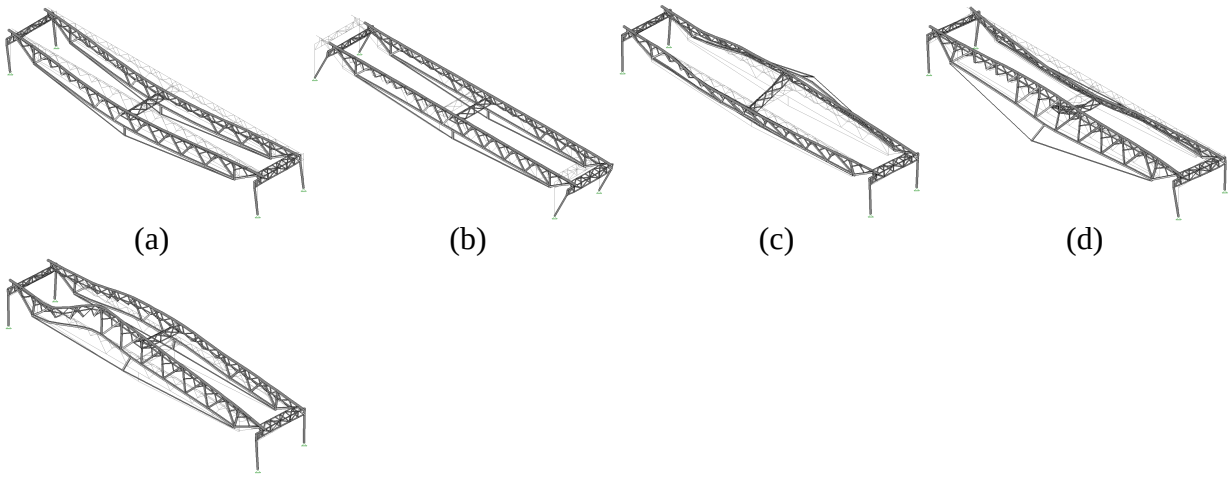

(a) (b) (c) (d)

(e)

Fig. A.53 Mode shapes of the strengthened truss during a service load level of 4.45 kN; 6 kN of post-tensioning load (Specimen 12): (a) mode1; (b) mode 2; (c) mode 3; (d) mode 4; (e) mode 5

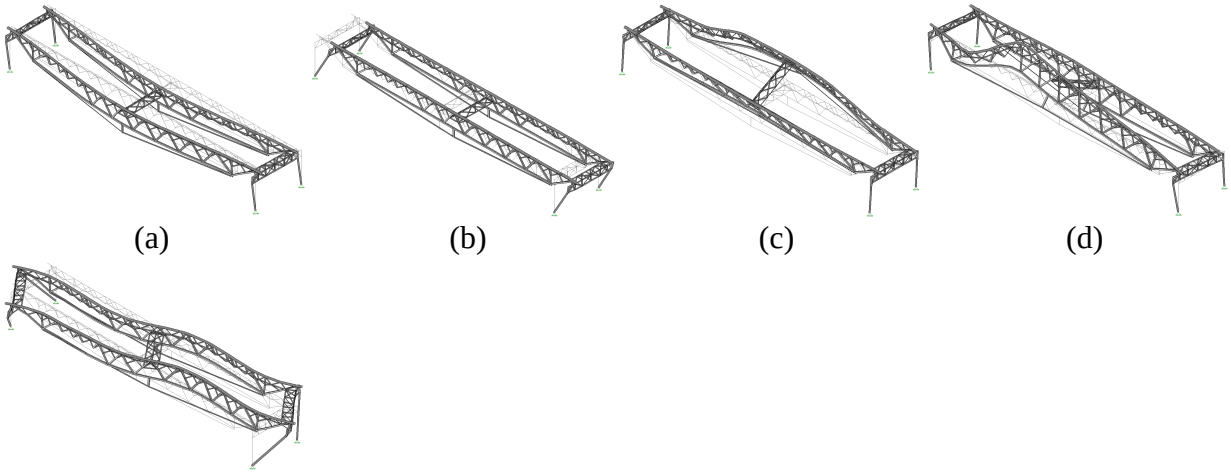

(a) (b) (c) (d)

(e)

Fig. A.54 Mode shapes of the strengthened truss during a service load level of 4.45 kN; 2 kN of post-tensioning load (Specimen 13): (a) mode1; (b) mode 2; (c) mode 3; (d) mode 4; (e) mode 5

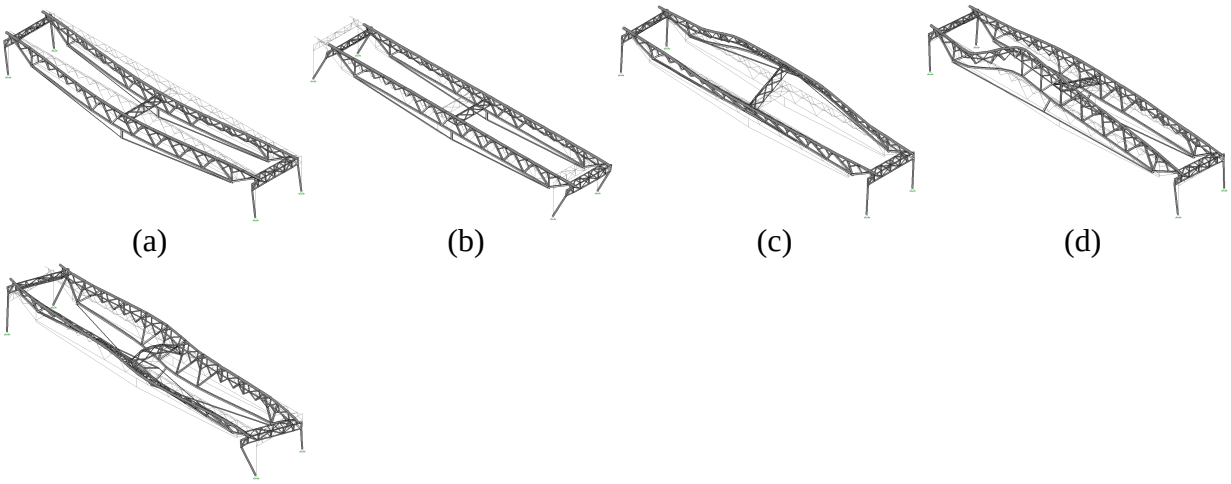

(a) (b) (c) (d)

(e)

Fig. A.55 Mode shapes of the strengthened truss during a service load level of 4.45 kN; 4 kN of post-tensioning load (Specimen 13): (a) mode1; (b) mode 2; (c) mode 3; (d) mode 4; (e) mode 5

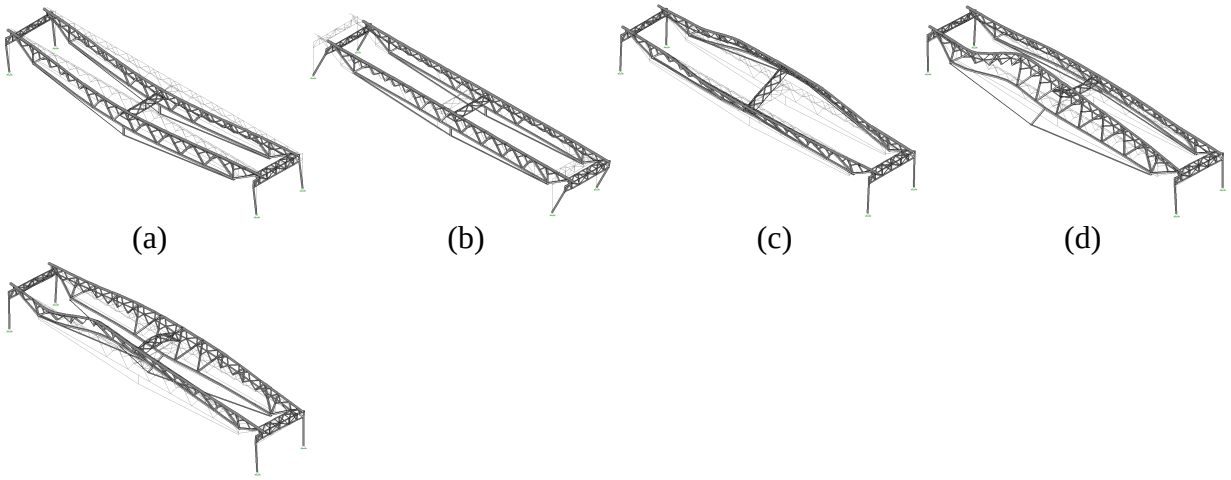

(a) (b) (c) (d)

(e)

Fig. A.56 Mode shapes of the strengthened truss during a service load level of 4.45 kN; 6 kN of post-tensioning load (Specimen 13): (a) mode1; (b) mode 2; (c) mode 3; (d) mode 4; (e) mode 5

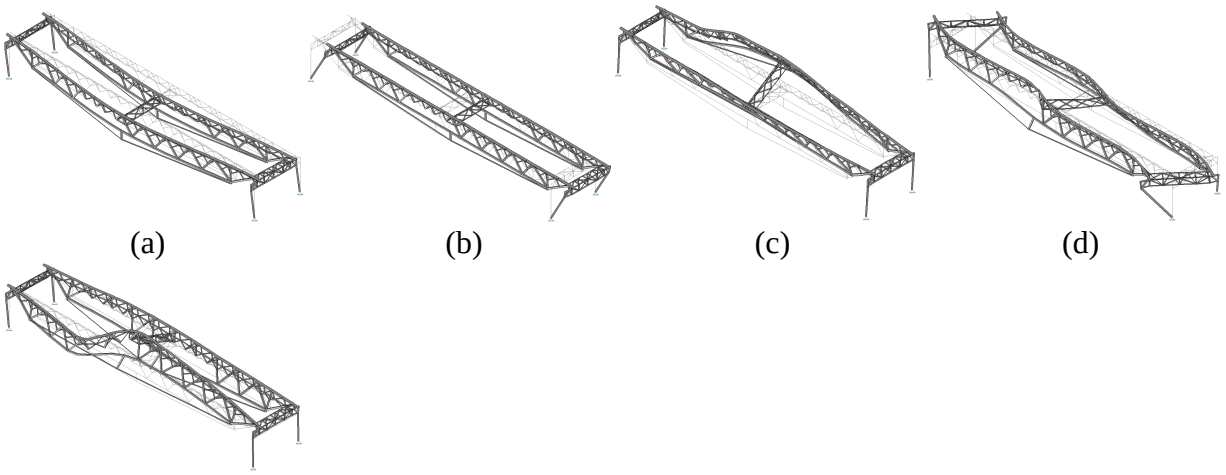

(a) (b) (c) (d)

(e)

Fig. A.57 Mode shapes of the strengthened truss during a service load level of 4.45 kN; 2 kN of post-tensioning load (Specimen 14): (a) mode1; (b) mode 2; (c) mode 3; (d) mode 4; (e) mode 5

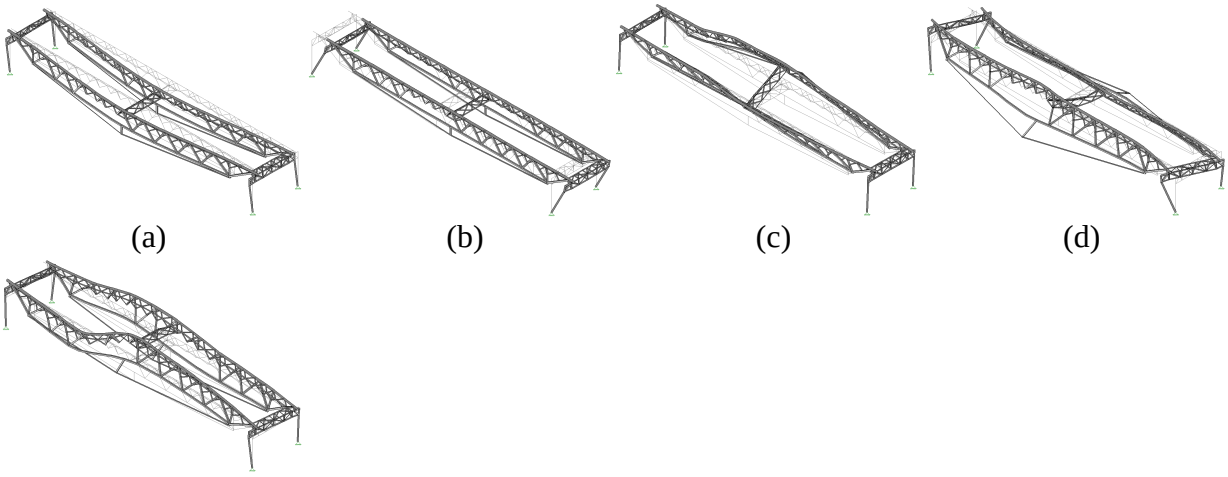

(a) (b) (c) (d)

(e)

Fig. A.58 Mode shapes of the strengthened truss during a service load level of 4.45 kN; 4 kN of post-tensioning load (Specimen 14): (a) mode1; (b) mode 2; (c) mode 3; (d) mode 4; (e) mode 5

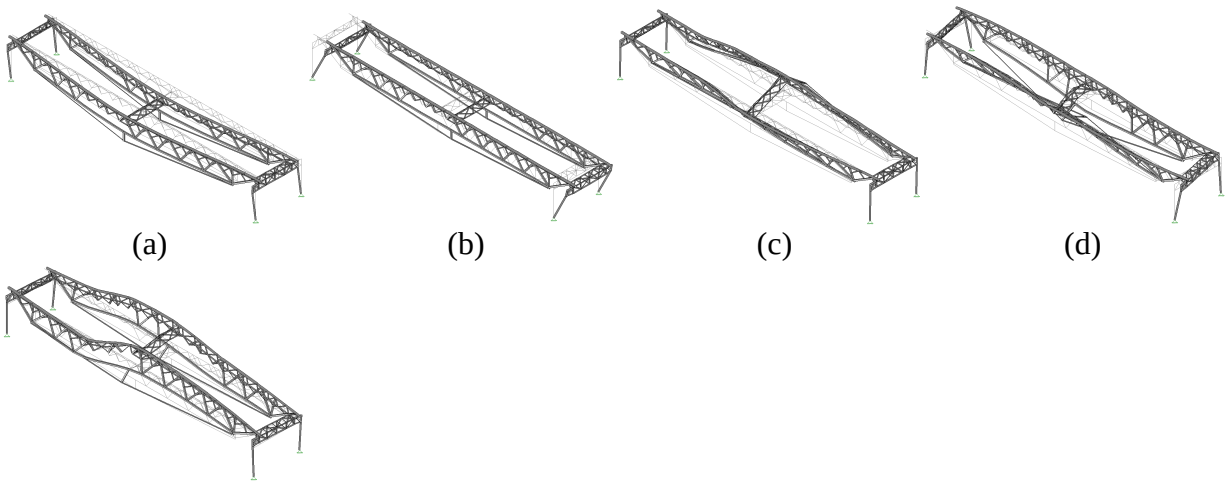

(a) (b) (c) (d)

(e)

Fig. A.59 Mode shapes of the strengthened truss during a service load level of 4.45 kN; 6 kN of post-tensioning load (Specimen 14): (a) mode1; (b) mode 2; (c) mode 3; (d) mode 4; (e) mode 5

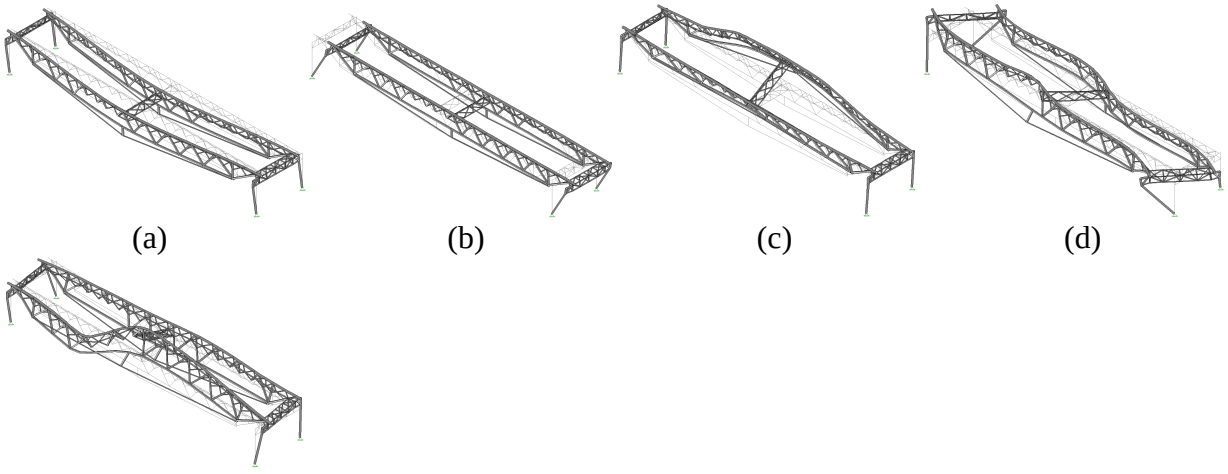

(a) (b) (c) (d)

(e)

Fig. A.60 Mode shapes of the strengthened truss during a service load level of 4.45 kN; 2 kN of post-tensioning load (Specimen 15): (a) mode1; (b) mode 2; (c) mode 3; (d) mode 4; (e) mode 5

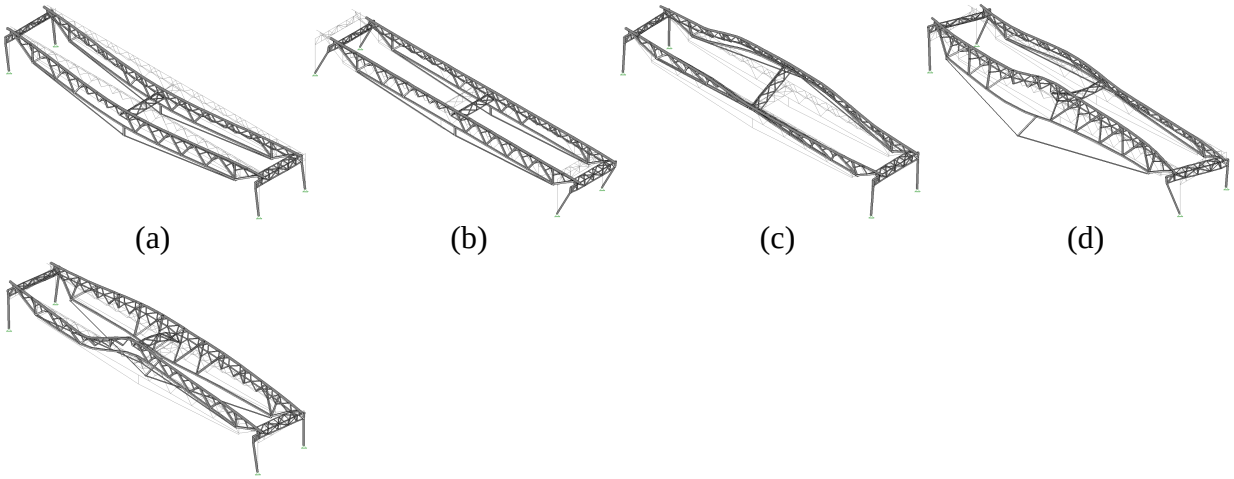

(a) (b) (c) (d)

(e)

Fig. A.61 Mode shapes of the strengthened truss during a service load level of 4.45 kN; 4 kN of post-tensioning load (Specimen 15): (a) mode1; (b) mode 2; (c) mode 3; (d) mode 4; (e) mode 5

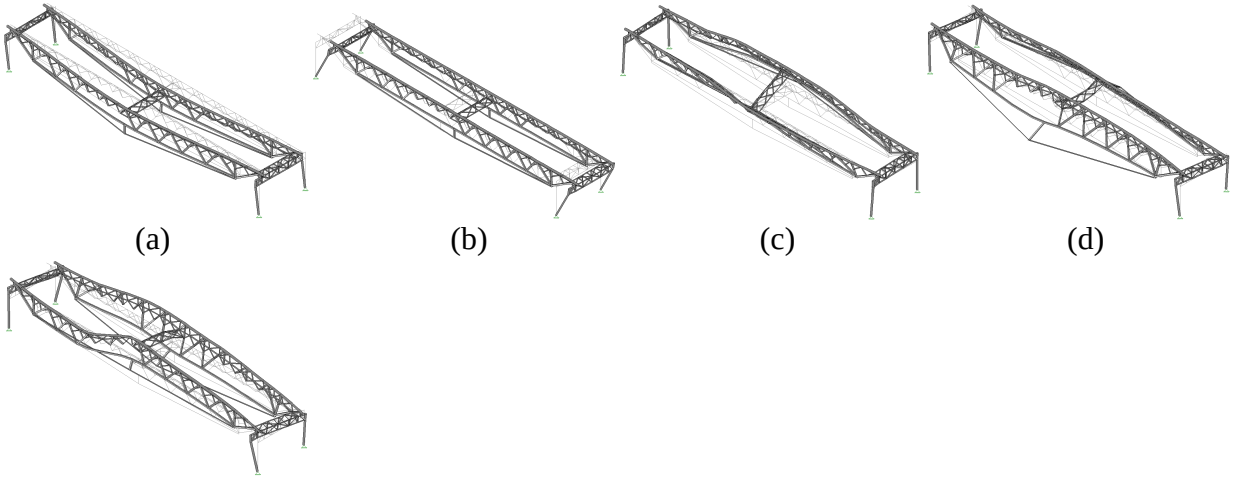

(a) (b) (c) (d)

(e)

Fig. A.62 Mode shapes of the strengthened truss during a service load level of 4.45 kN; 6 kN of post-tensioning load (Specimen 15): (a) mode1; (b) mode 2; (c) mode 3; (d) mode 4; (e) mode 5

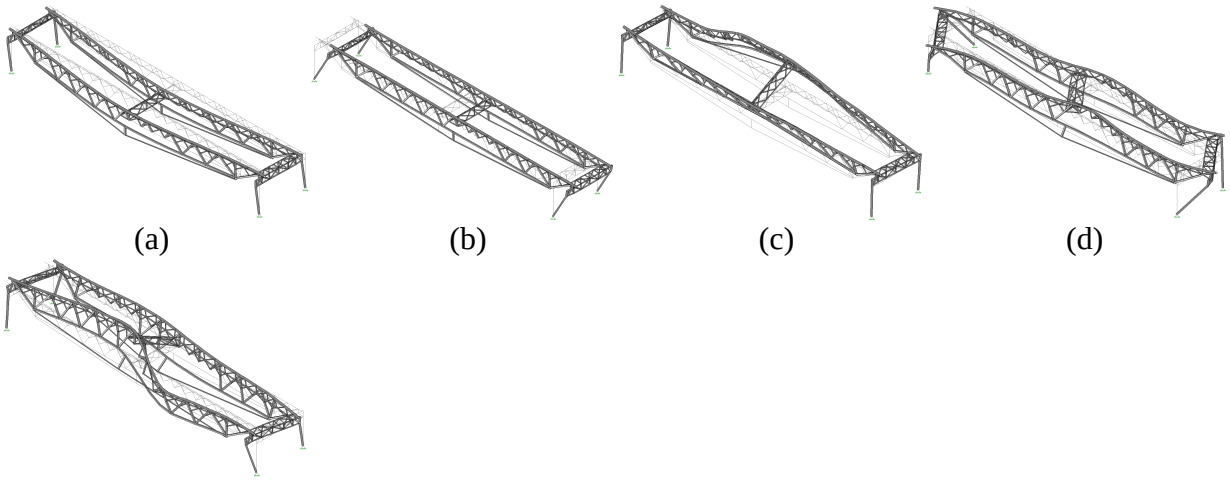

(a) (b) (c) (d)

(e)

Fig. A.63 Mode shapes of the strengthened truss during a service load level of 4.45 kN; 2 kN of post-tensioning load (Specimen 16): (a) mode1; (b) mode 2; (c) mode 3; (d) mode 4; (e) mode 5

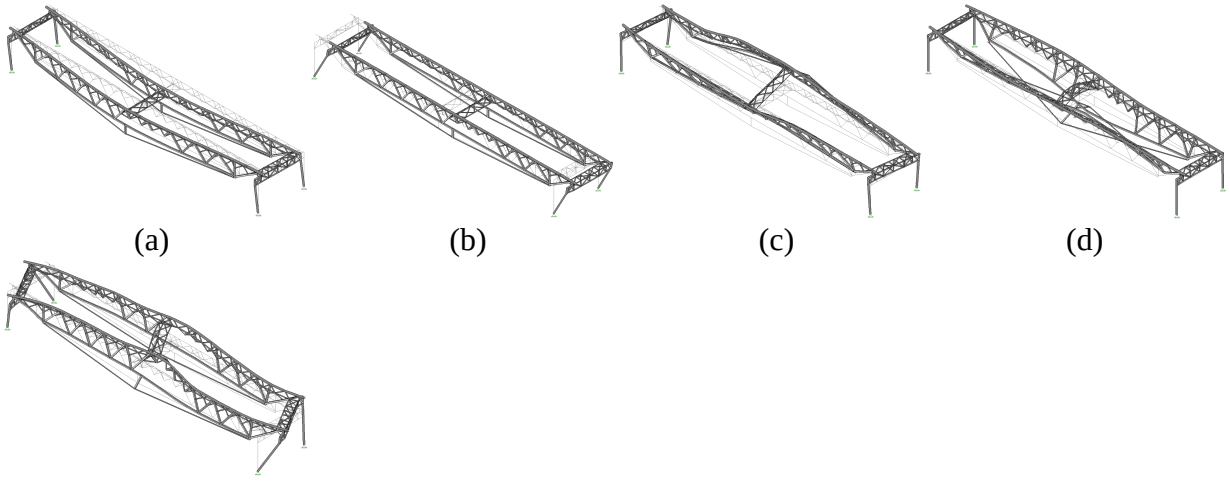

(a) (b) (c) (d)

(e)

Fig. A.64 Mode shapes of the strengthened truss during a service load level of 4.45 kN; 4 kN of post-tensioning load (Specimen 16): (a) mode1; (b) mode 2; (c) mode 3; (d) mode 4; (e) mode 5

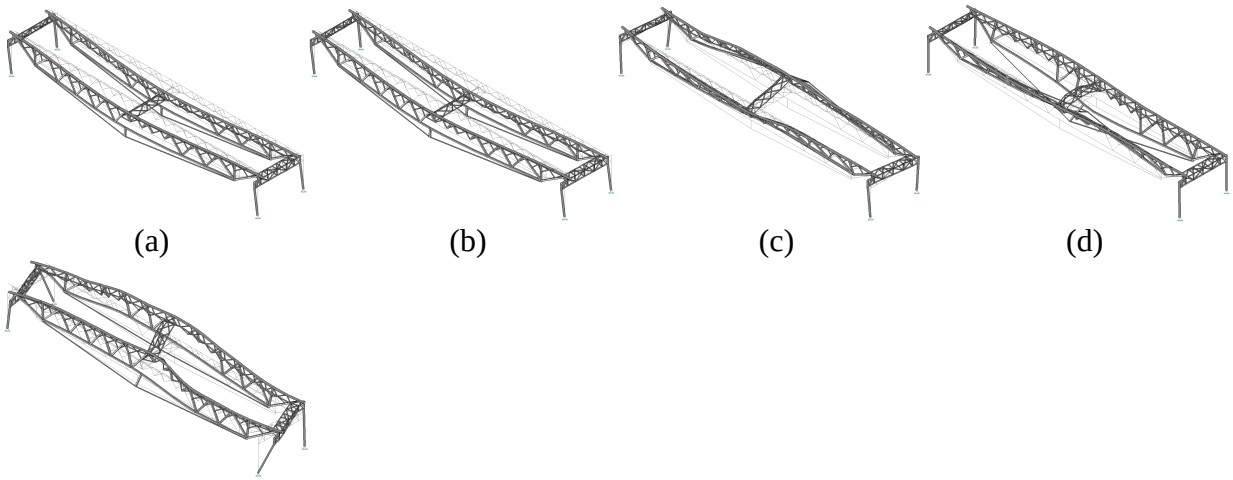

(a) (b) (c) (d)

(e)

Fig. A.65 Mode shapes of the strengthened truss during a service load level of 4.45 kN; 6 kN of post-tensioning load (Specimen 16): (a) mode1; (b) mode 2; (c) mode 3; (d) mode 4; (e) mode 5

APPENDIX B. MEMBER STRAIN

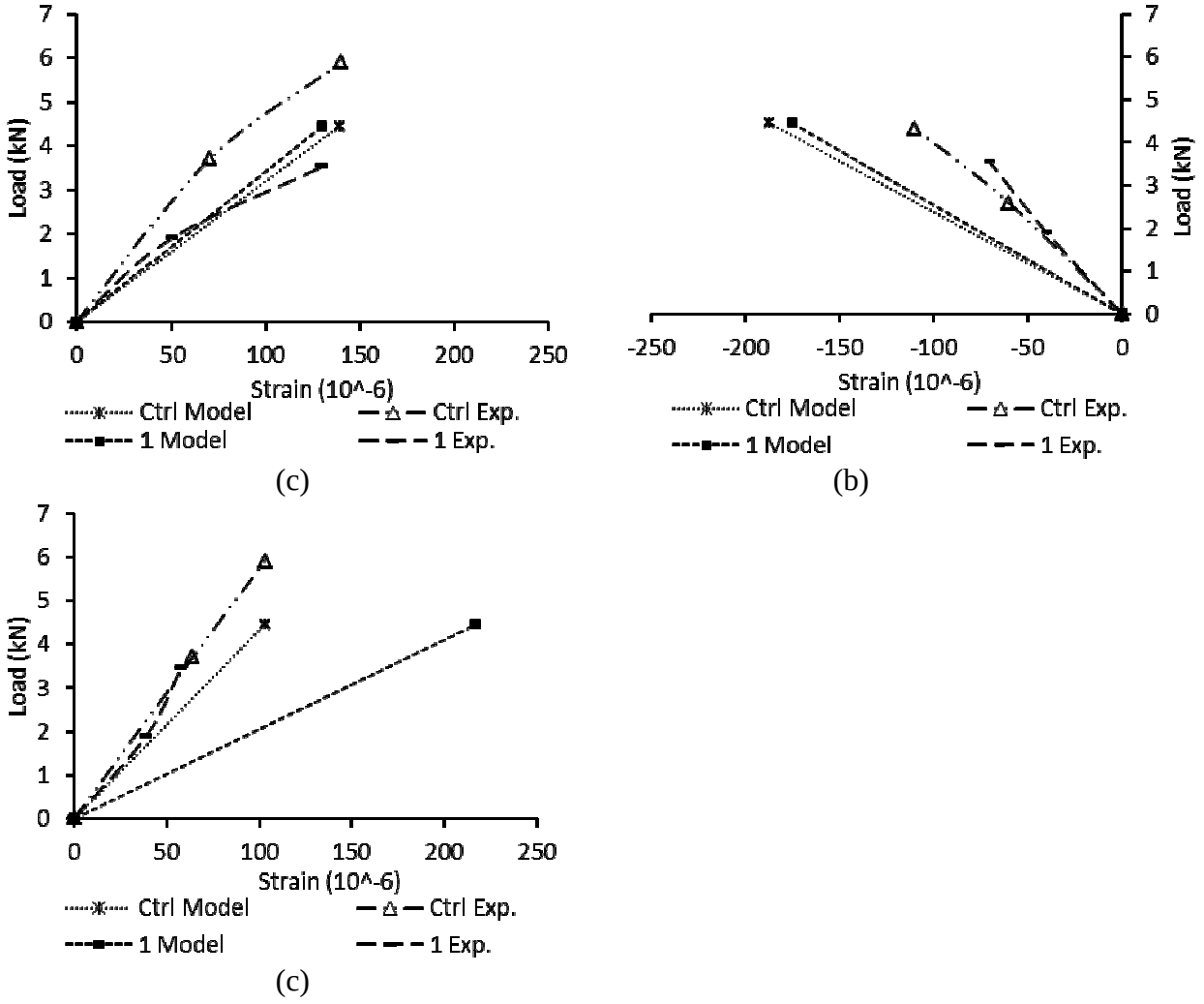

Fig. B.1 Strain response Specimen 1, Truss 1: (a) Top chord; (b) Bottom chord; (c) Web 1

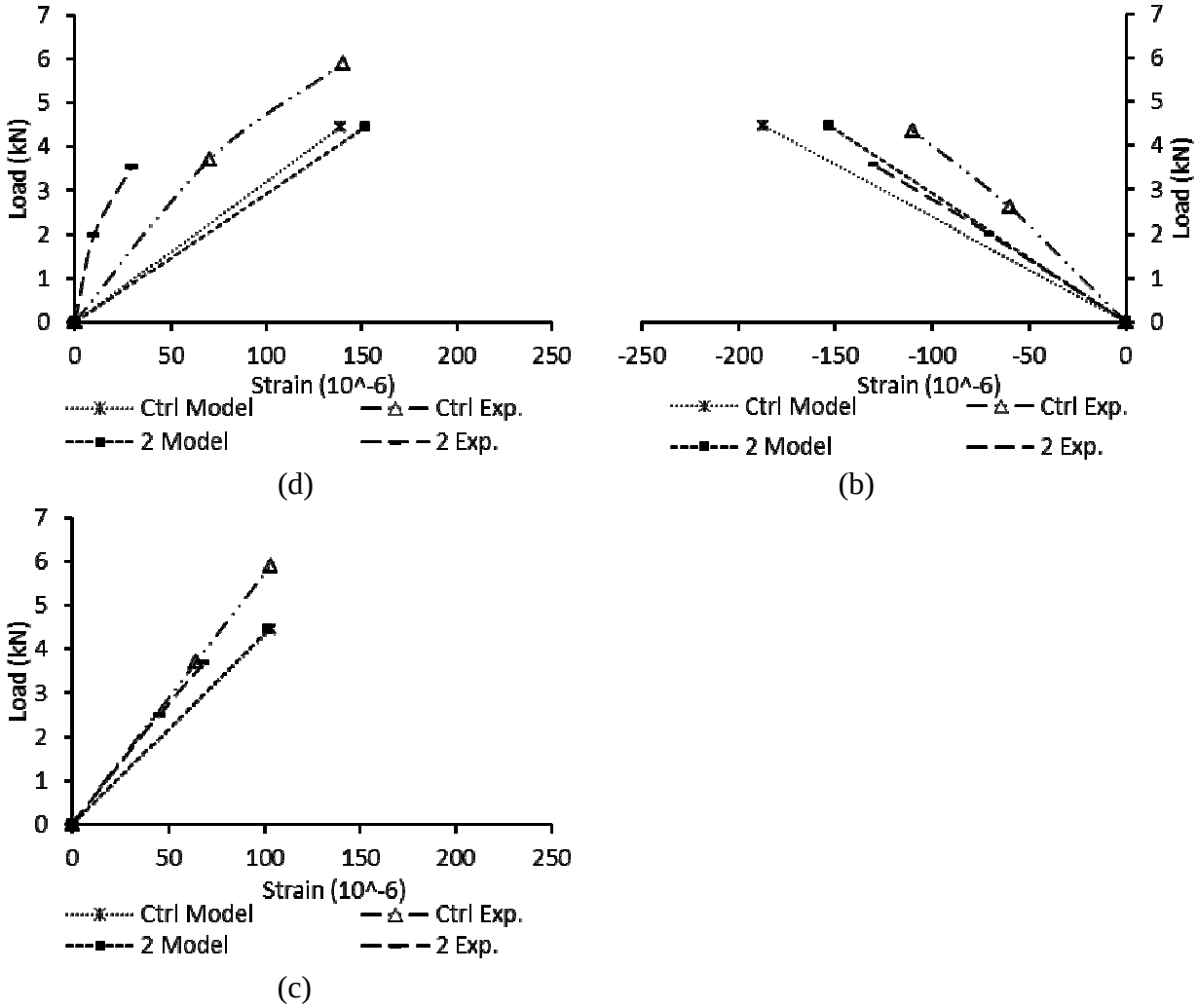

Fig. B.2 Strain response Specimen 2, Truss 1: (a) Top chord; (b) Bottom chord; (c) Web 1

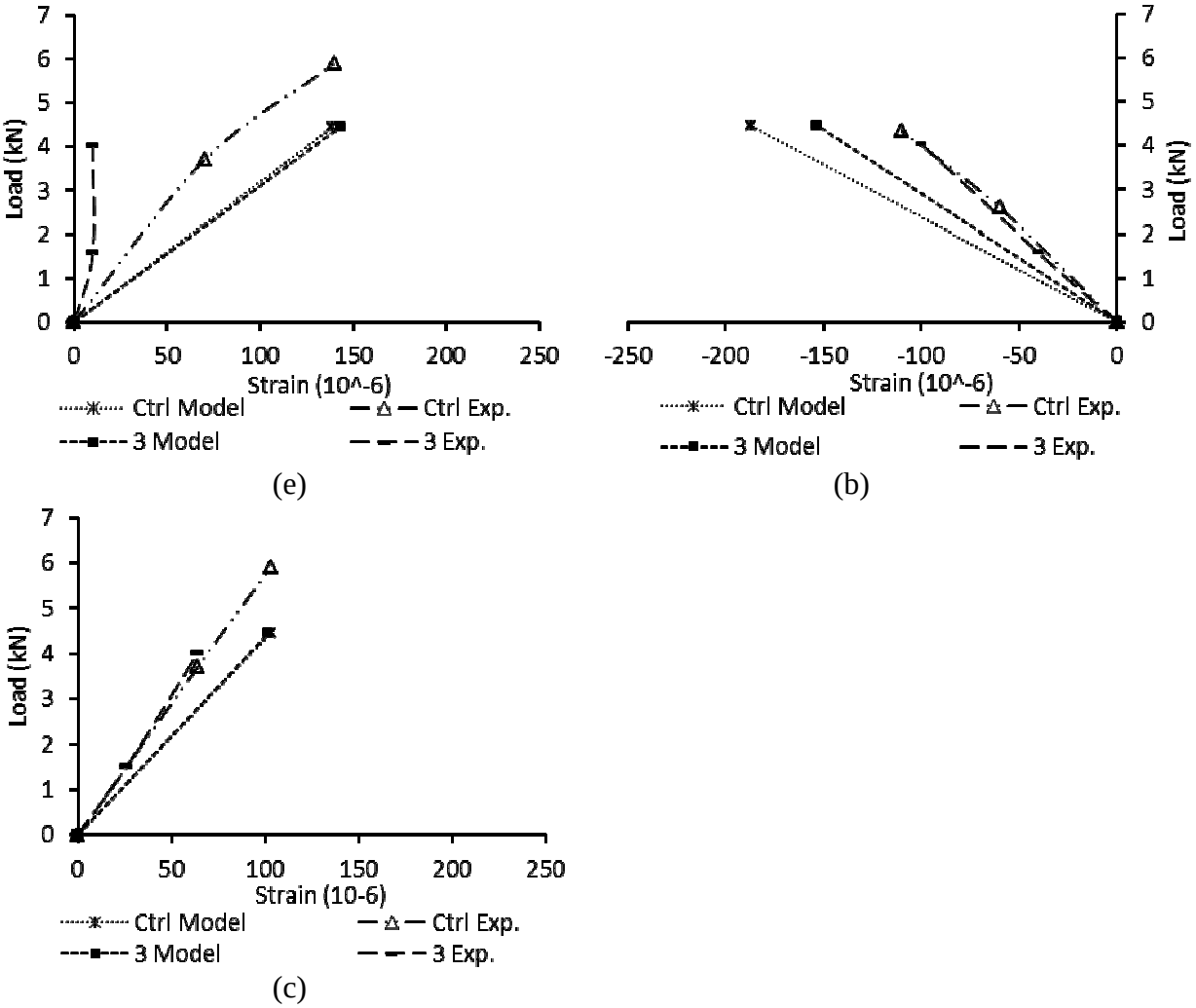

Fig. B.3 Strain response Specimen 3, Truss 1: (a) Top chord; (b) Bottom chord; (c) Web 1

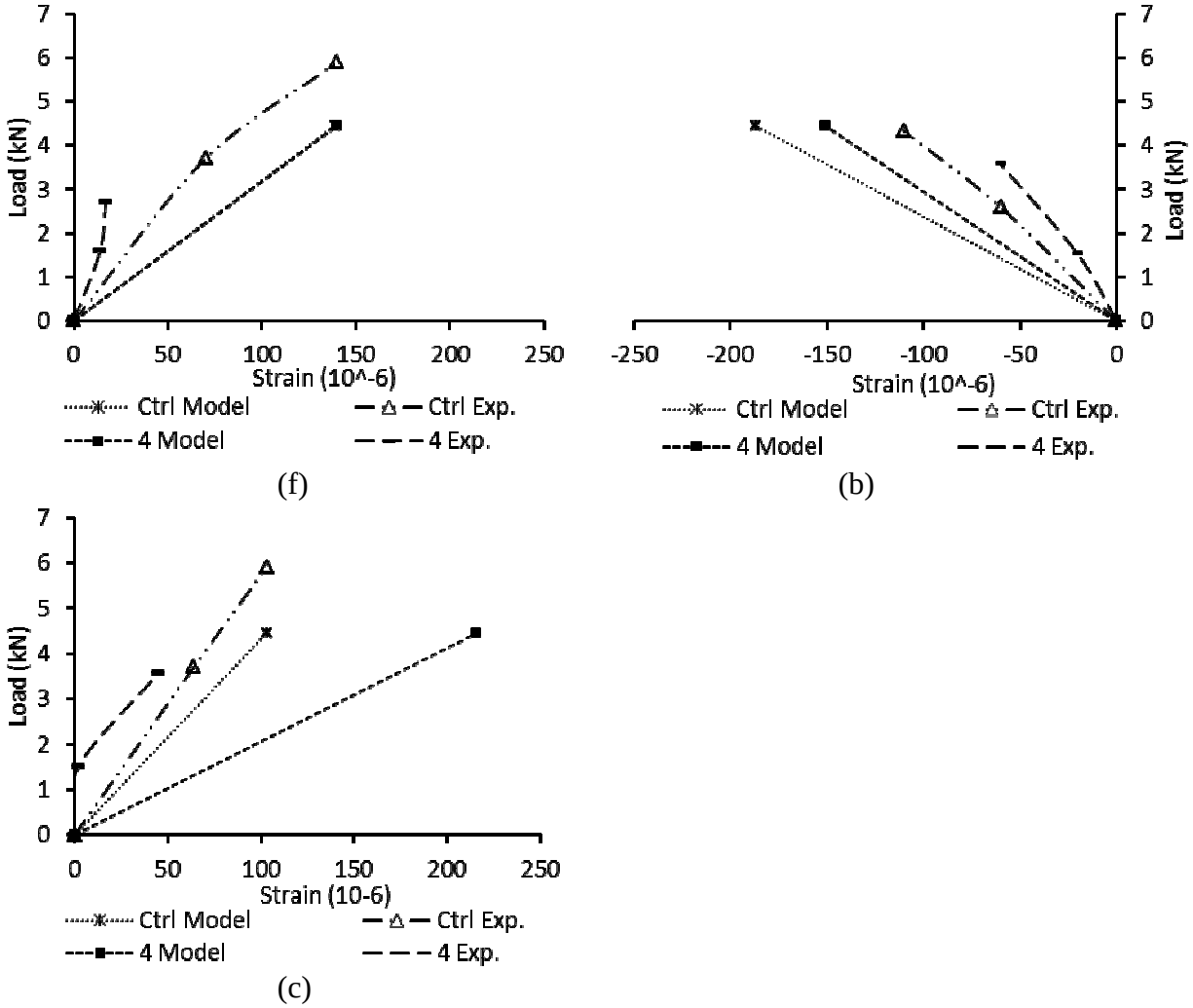

Fig. B.4 Strain response Specimen 4, Truss 1: (a) Top chord; (b) Bottom chord; (c) Web 1

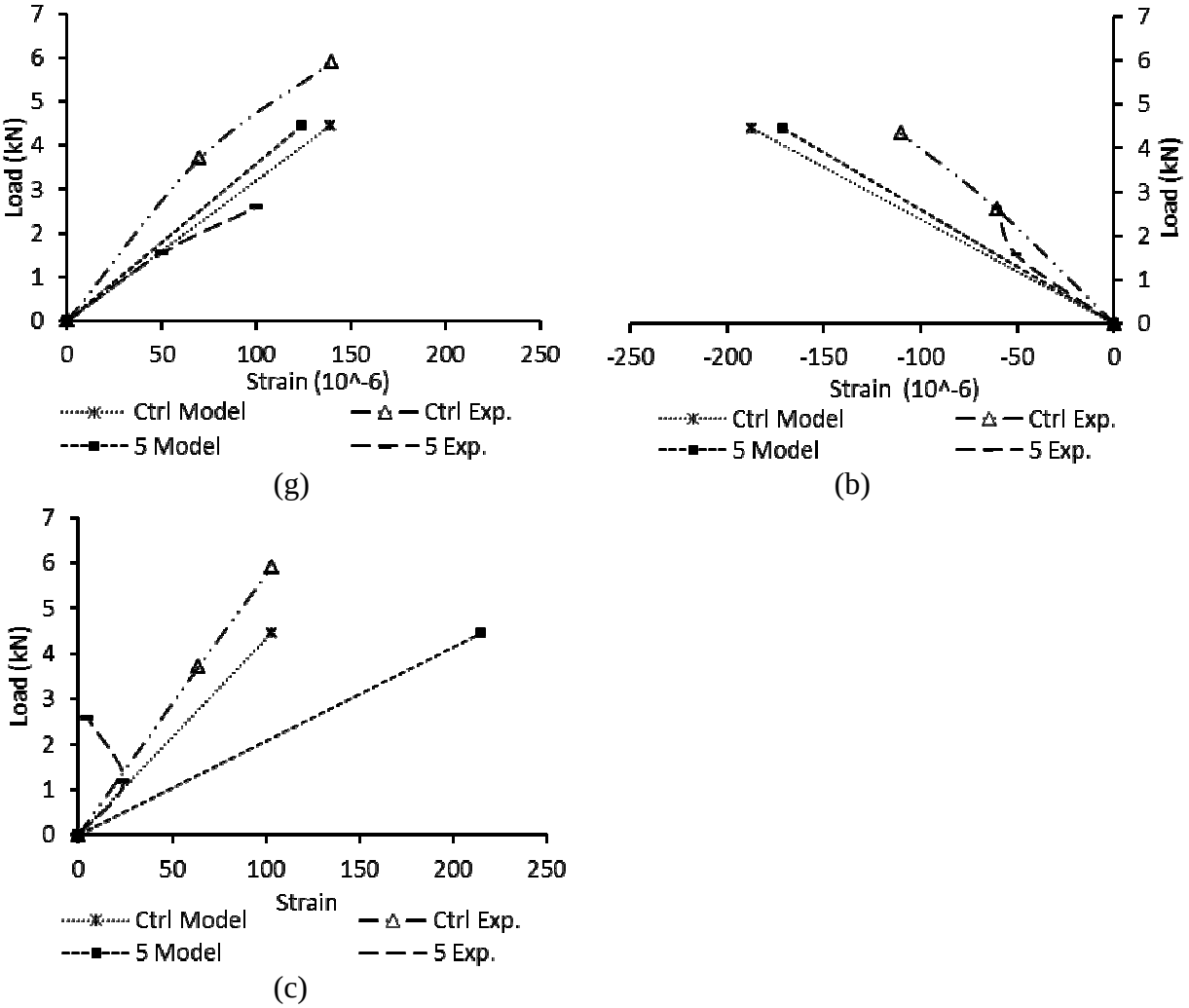

Fig. B.5 Strain response Specimen 5, Truss 1: (a) Top chord; (b) Bottom chord; (c) Web 1

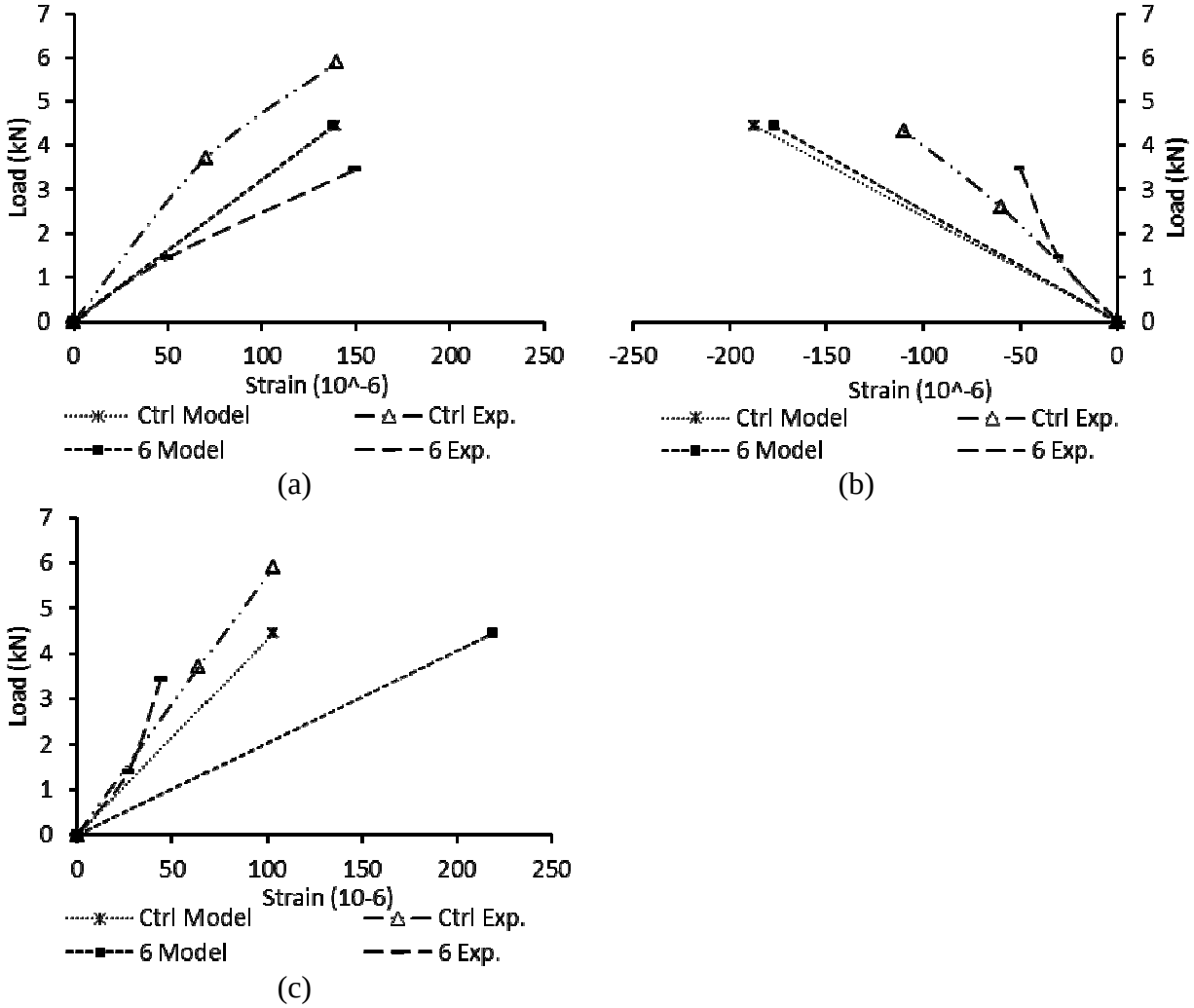

Fig. B.6 Strain response Specimen 6, Truss 1: (a) Top chord; (b) Bottom chord; (c) Web 1

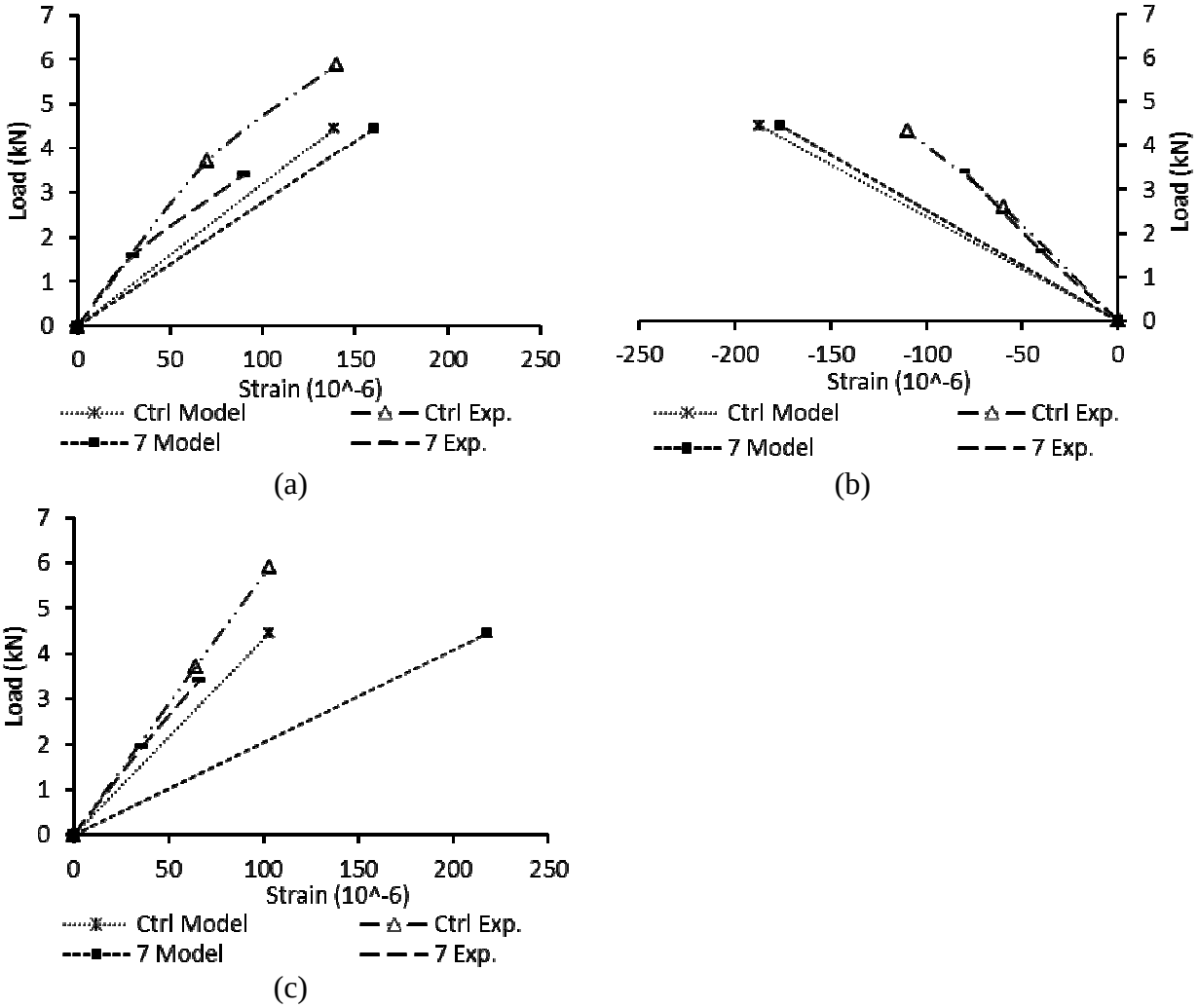

Fig. B.7 Strain response Specimen 7, Truss 1: (a) Top chord; (b) Bottom chord; (c) Web 1

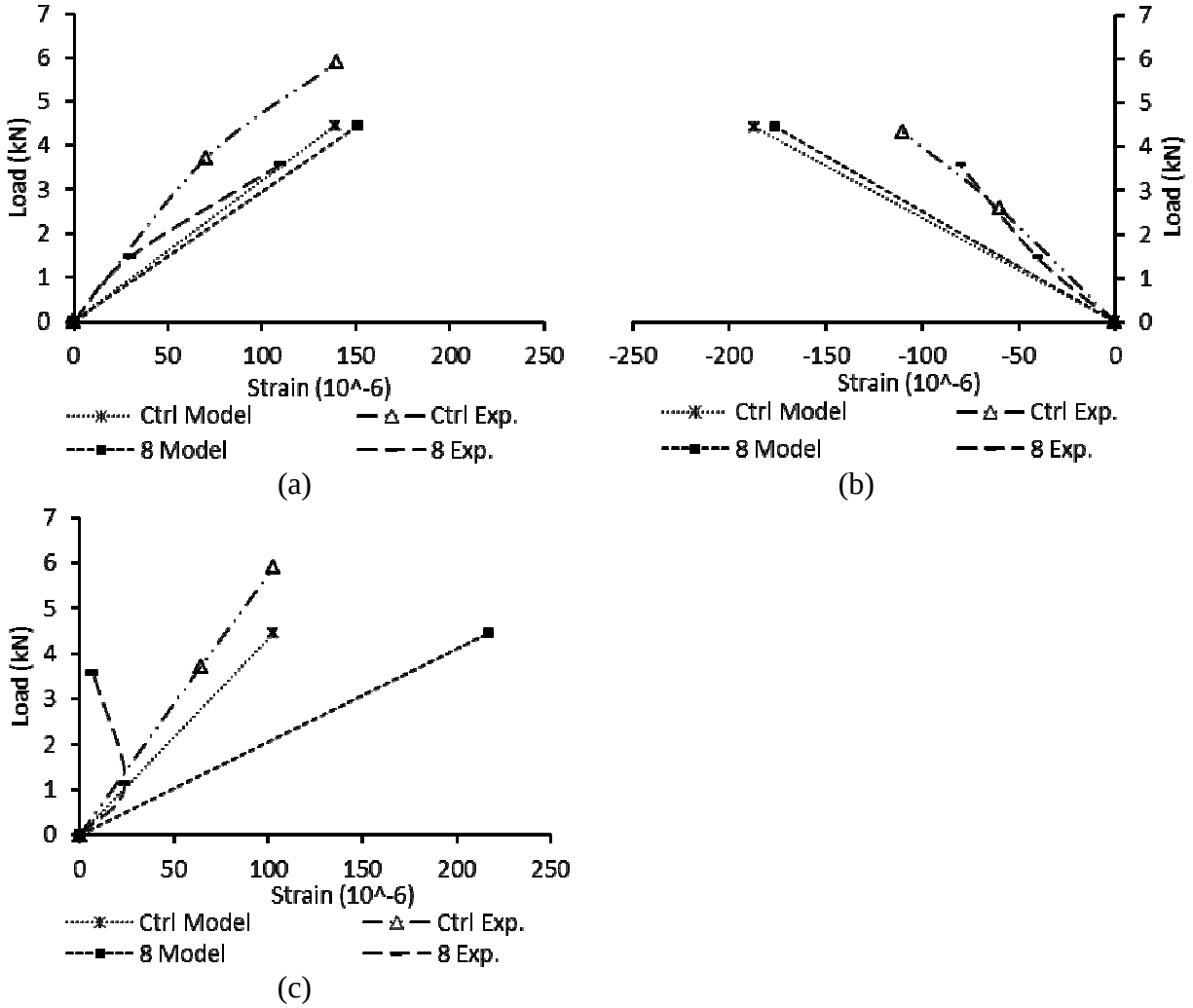

Fig. B.8 Strain response Specimen 8, Truss 1: (a) Top chord; (b) Bottom chord; (c) Web 1

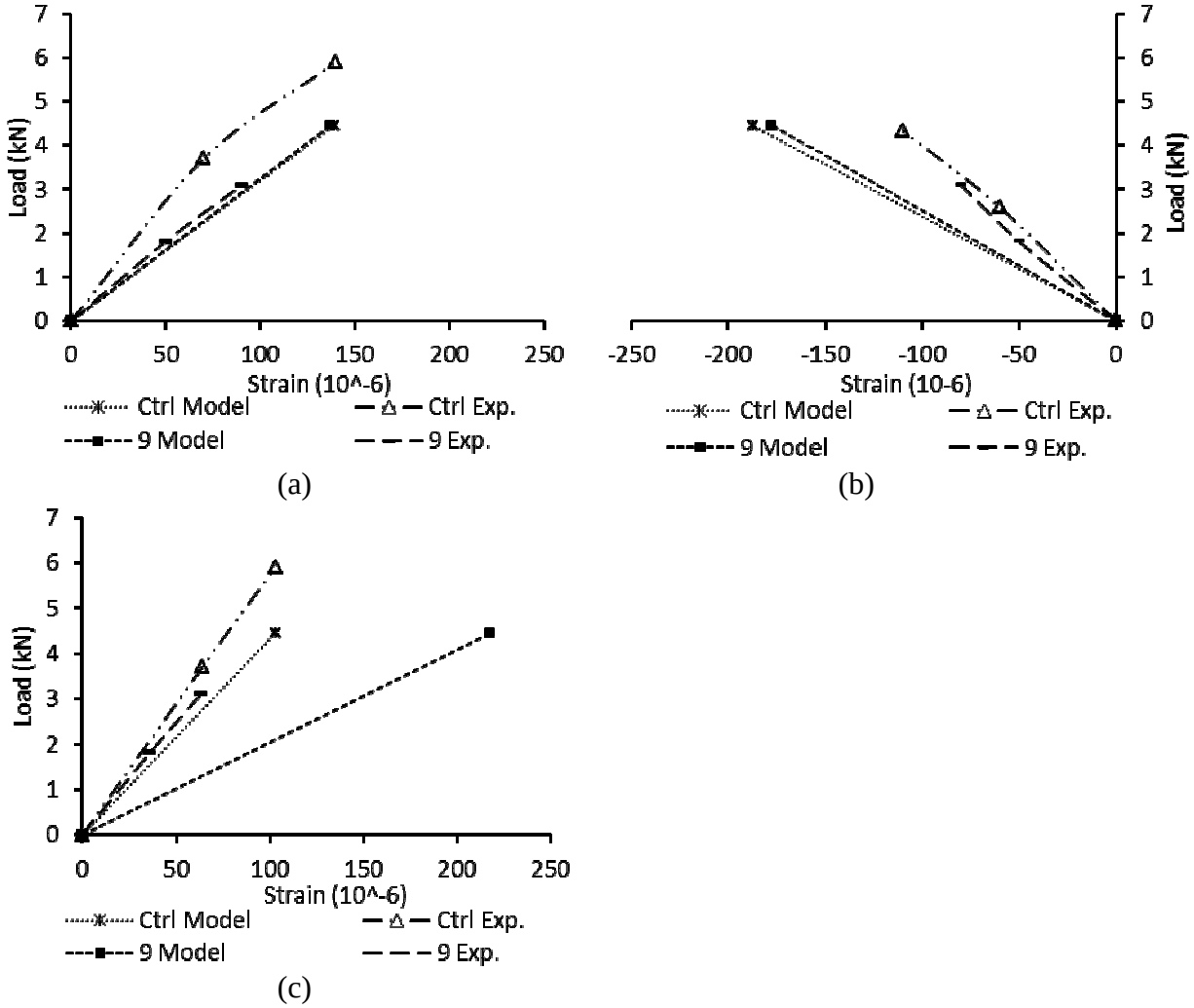

Fig. B.9 Strain response Specimen 9, Truss 1: (a) Top chord; (b) Bottom chord; (c) Web 1

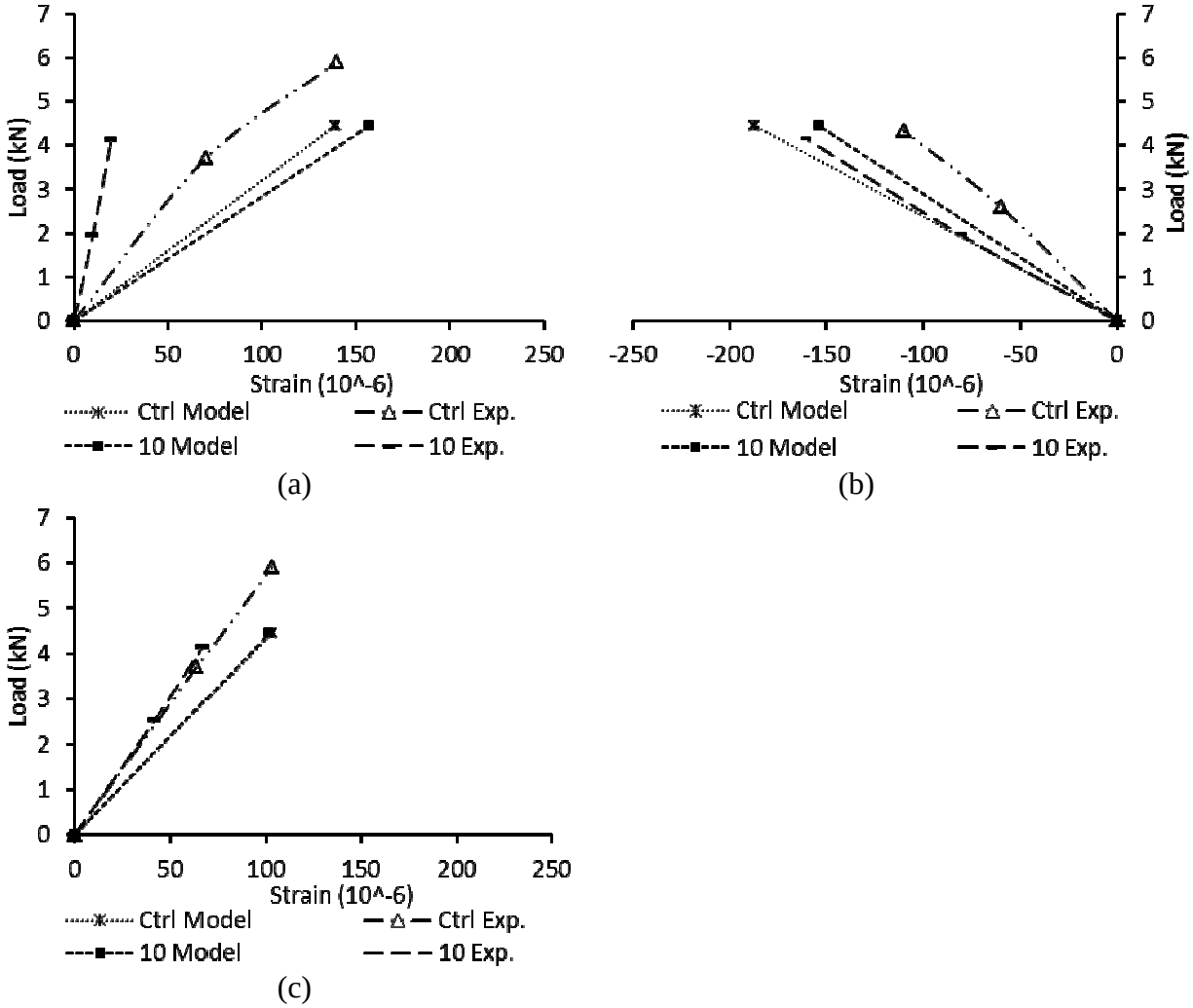

Fig. B.10 Strain response Specimen 10, Truss 1: (a) Top chord; (b) Bottom chord; (c) Web 1

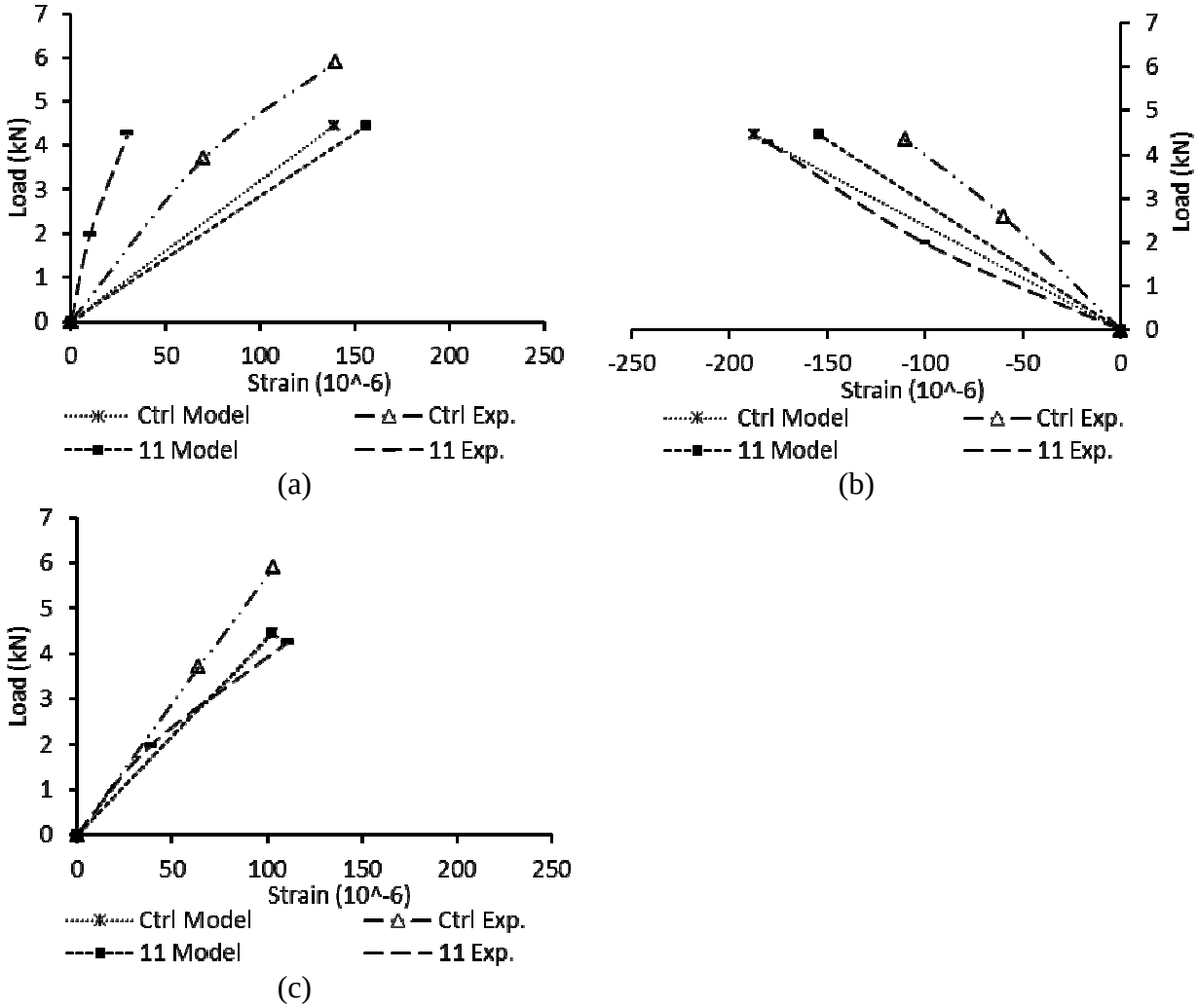

Fig. B.11 Strain response Specimen 11, Truss 1: (a) Top chord; (b) Bottom chord; (c) Web 1

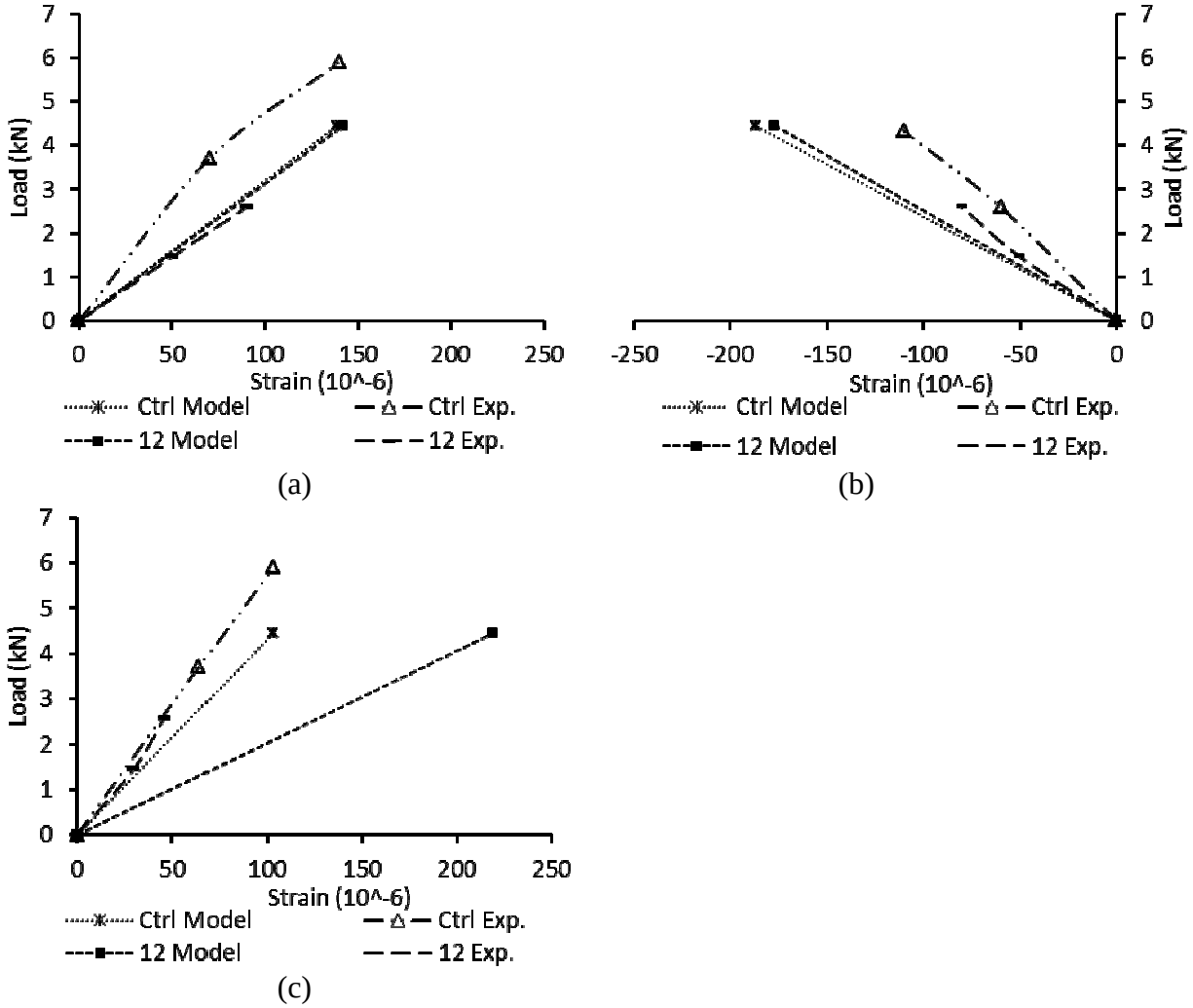

Fig. B.12 Strain response Specimen 12, Truss 1: (a) Top chord; (b) Bottom chord; (c) Web 1

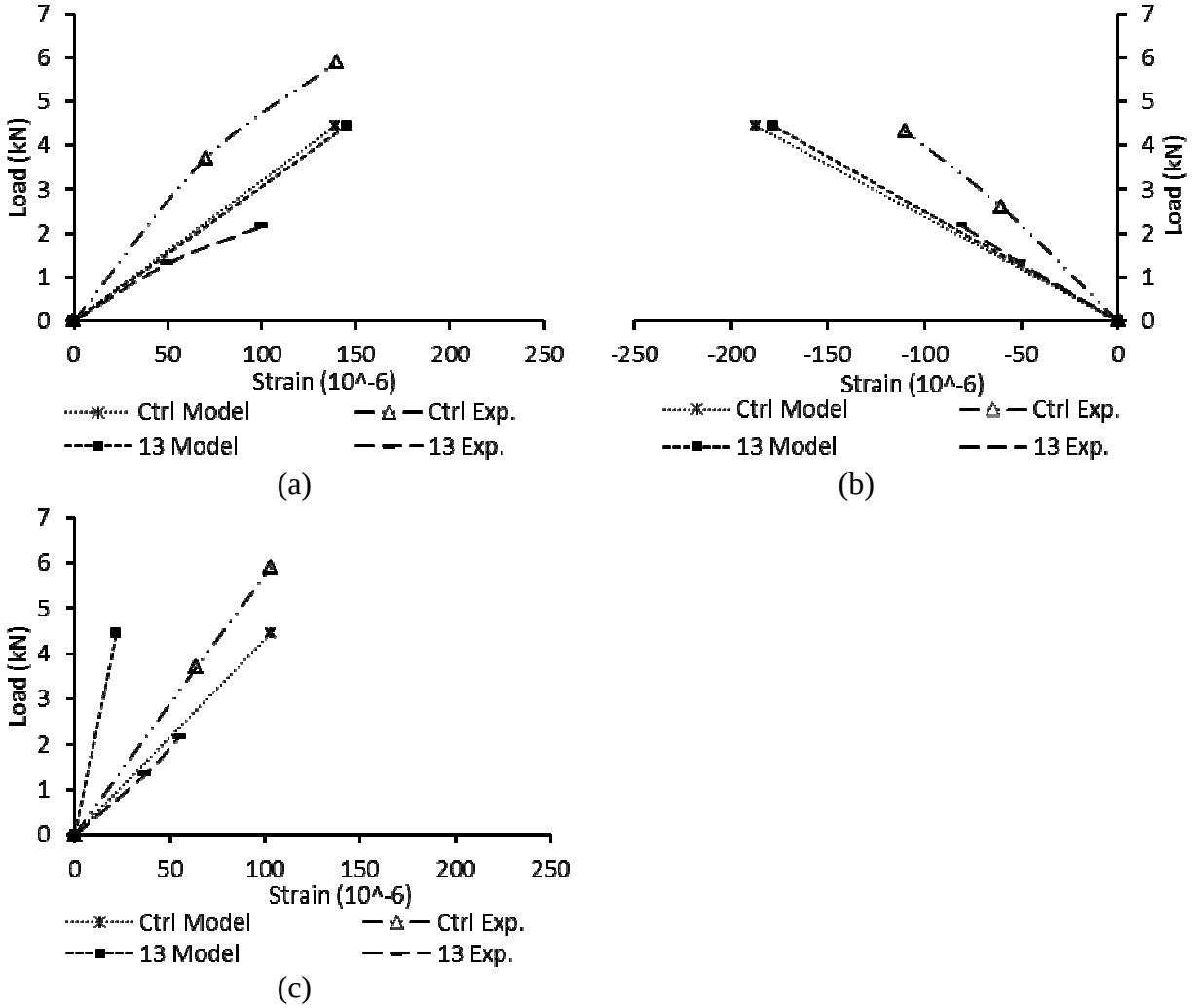

Fig. B.13 Strain response Specimen 13, Truss 1: (a) Top chord; (b) Bottom chord; (c) Web 1

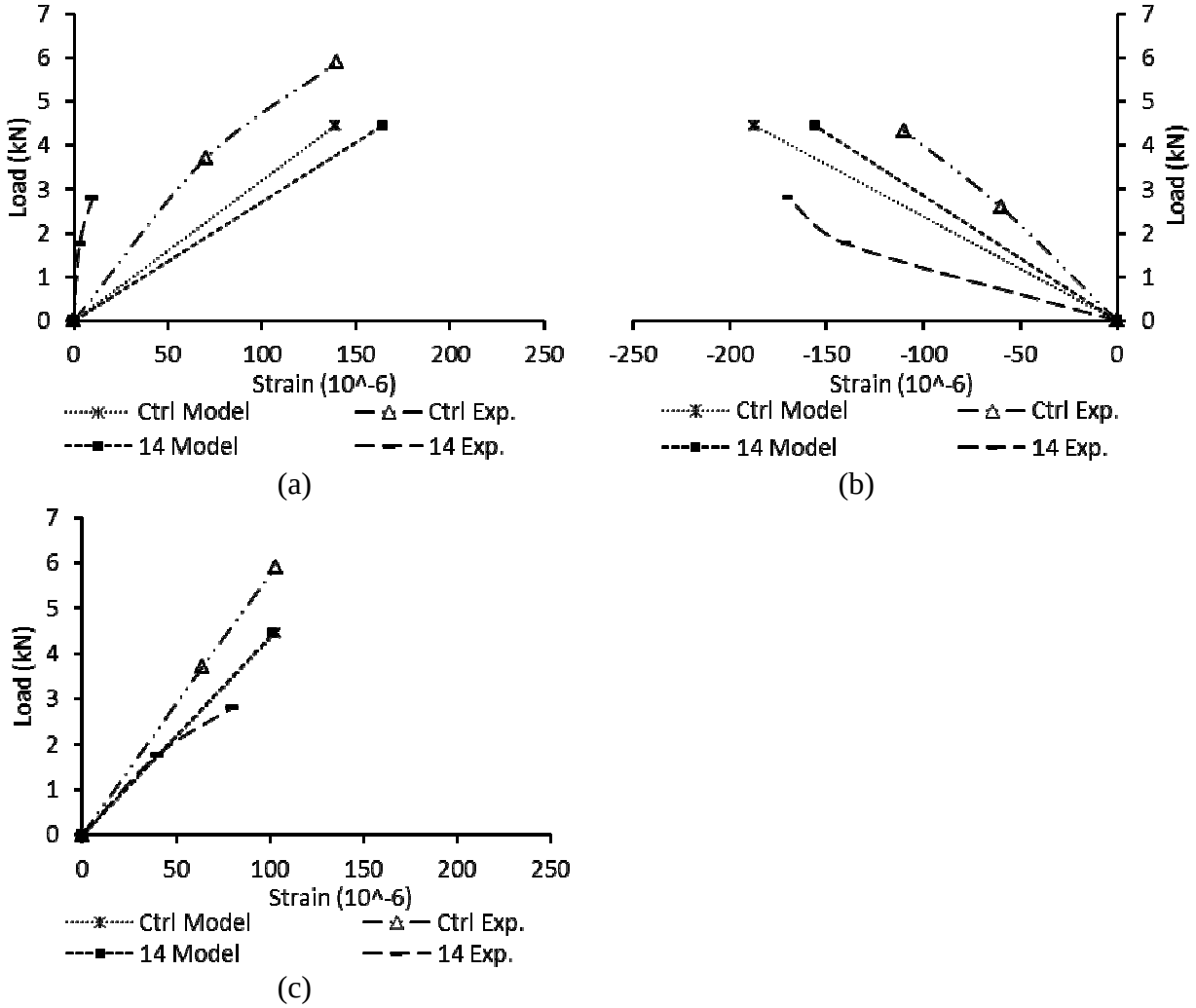

Fig. B.14 Strain response Specimen 14, Truss 1: (a) Top chord; (b) Bottom chord; (c) Web 1

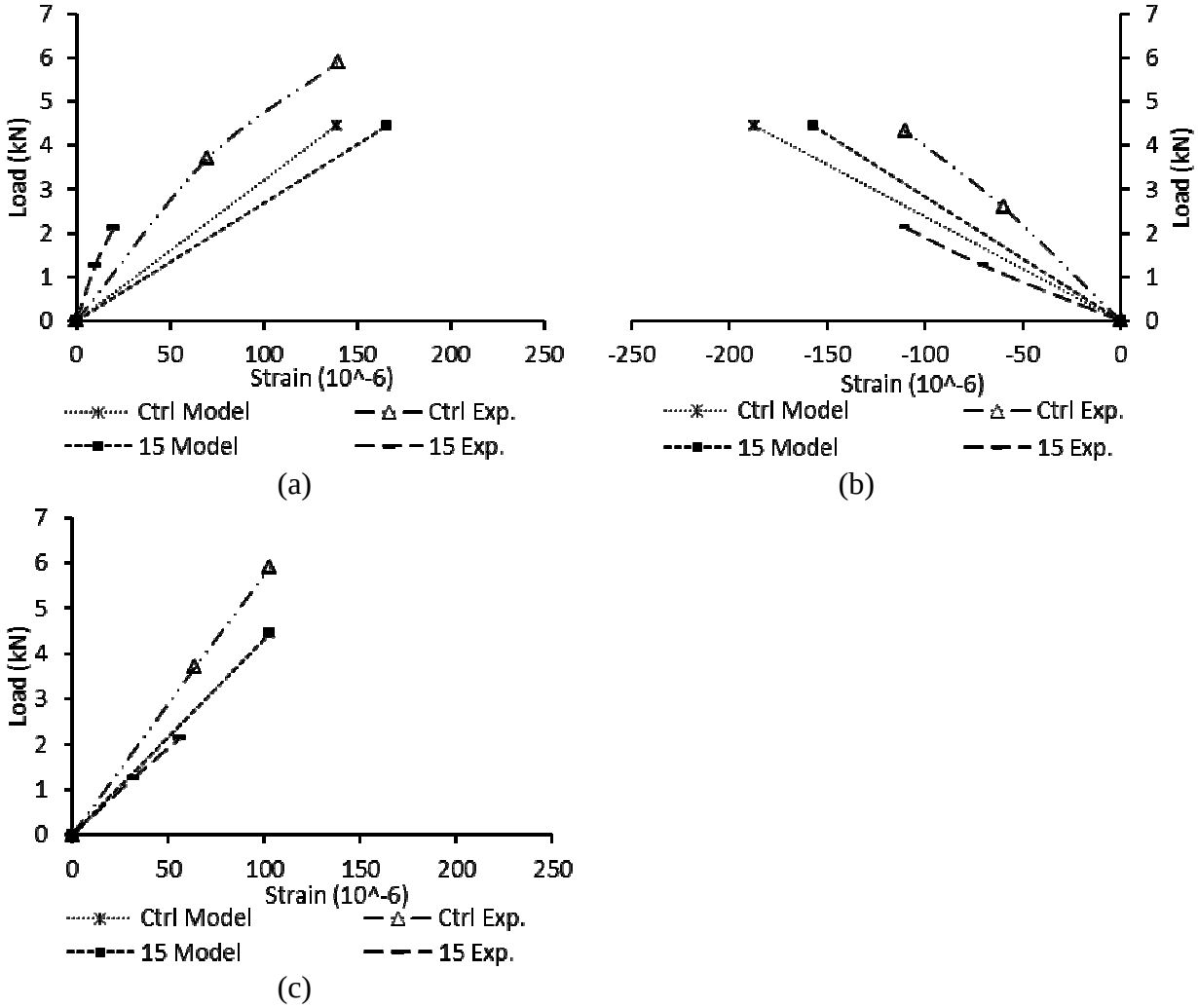

Fig. B.15 Strain response Specimen 15, Truss 1: (a) Top chord; (b) Bottom chord; (c) Web 1

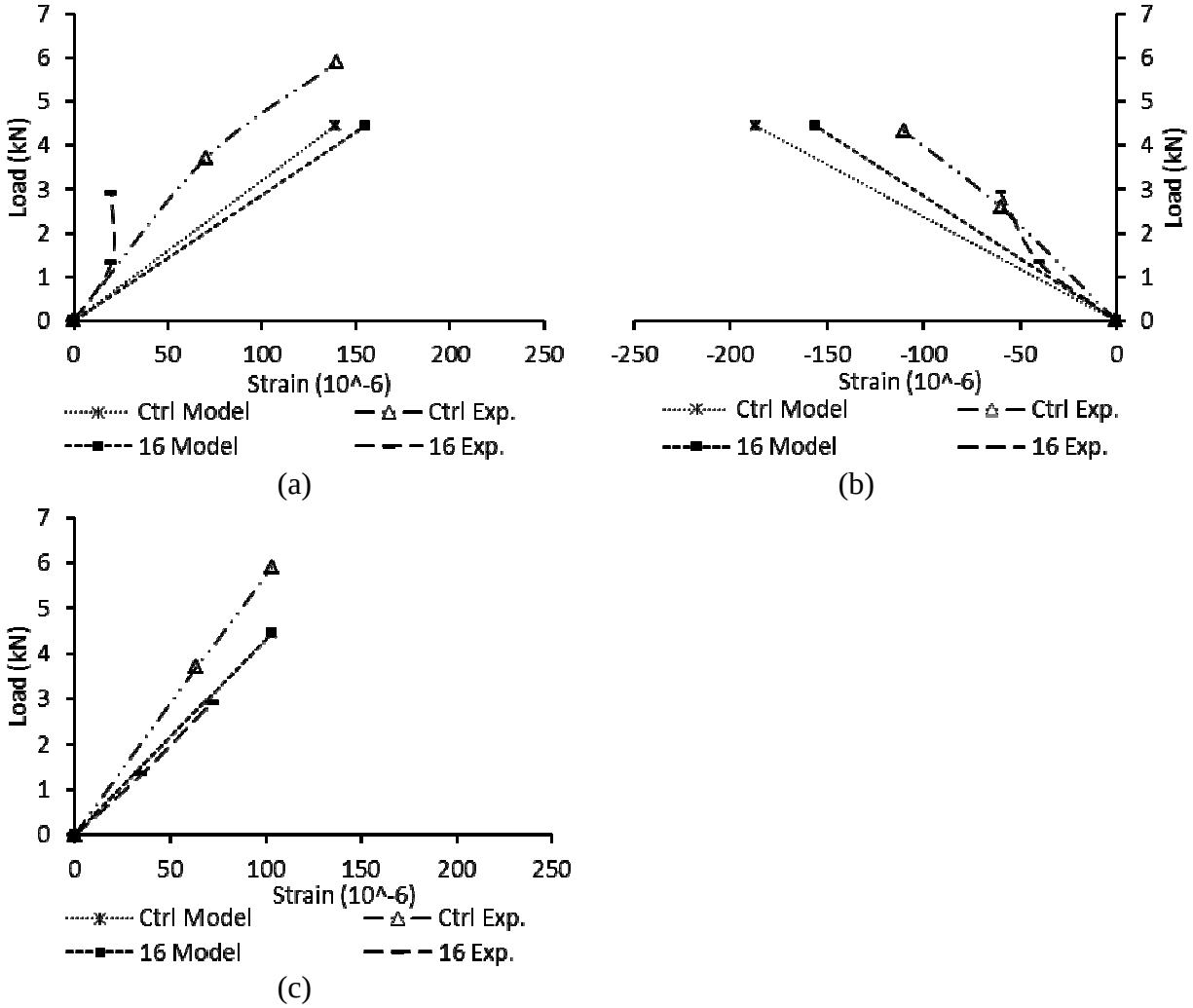

Fig. B.16 Strain response Specimen 16, Truss 1: (a) Top chord; (b) Bottom chord; (c) Web 1